The Dissertation Committee for Shinji Kenneth Strain Certifies that this is the approved version of the following dissertation:

A novel GC-MS/MS assay for the measurement of 2-hg enantiomers and the utility of 2-hg enantiomer levels as a biomarker for IDH mutant gliomas

Committee:

Mark R. Emmett, PhD

Jonathan Hommel, PhD

Celia Chao, MD

Melinda Moore, PhD

Morris Groves, MD, JD

A novel GC-MS/MS assay for the measurement of 2-hg enantiomers and the utility of 2-hg enantiomer levels as a biomarker for IDH mutant gliomas

by

Shinji Kenneth Strain, B.S.

Dissertation

Presented to the Faculty of the Graduate School of

The University of Texas Medical Branch

in Partial Fulfillment

of the Requirements

for the Degree of

Doctorate of Philosophy

The University of Texas Medical Branch

May 2019

Dedication

This dissertation is dedicated to my beautiful wife, my son, our future kids, and the patients and families who have fought and continue to fight battles with cancer. We are more than conquerors through him who loved us.

Acknowledgments

I would like to sincerely thank my mentor, Dr. Mark Emmett, for all of his support and guidance as teacher, leader, and friend. I have learned all I know of Mass Spectrometry from you and thoroughly enjoyed hearing your stories. To my clinical mentor, Dr. Kelly Olino, I wholeheartedly thank you for bringing out the best scientist within me and nourishing a fire to pursue academic excellence. I would also like to thank my lab members, Brooke and Anna for their friendship through the years.

To my committee members, Dr. Jonathan Hommel, Dr. Celia Chao, Dr. Melinda Moore, and Dr. Morris Groves, thank you for time, patience and invaluable critiques.

To the MD-PhD program, including Claiborne Fant, Chris Rhodes, Dr. Lawrence Sowers, Dr. Jose Barral, and Dr. Kristen Peek, I would not even be here unless you valued and invested yourselves into the building next generation of physician-scientist. I would also like to thank the Department of Neuroscience, Cell Biology and Anatomy as well as the Cell Biology Graduate Program for their continued support. Specifically, Aurora Galvan and Debra Moncrief in providing administrative support and Dr. Pomila Singh for her sustained advocacy for me as the program chair.

Thank you to my collaborators, Dr. Morris Groves and his staff at the Austin Brain Tumor Center (Texas Oncology), Dr. Jason Herring, Dr. Lawrence Sowers, Dr. Melinda Moore, and the UTMB Neurosurgery Dept for your altruistic support.

I owe a big thank you to the Shimadzu Corporation, The Head for the Cure Foundation, VUV Analytics, and the UTMB Institute for Translational Sciences (TL1 award) for their financial support in this project. The work presented herein would not have been at all possible without you.

To all my family, you gave me your unwavering love throughout my long years of education since I started my undergraduate schooling.

Finally, to wife and best friend. I love you. Thank you for being my biggest fan and loving me despite my shortcomings as a husband, son, brother, and father.

A novel GC-MS/MS assay for the measurement of 2-hg enantiomers and the utility of 2-hg enantiomer levels as a biomarker for IDH mutant gliomas.

Publication No._____

Shinji Kenneth Strain, Ph.D.

The University of Texas Medical Branch, 2019

Supervisor: Mark R. Emmett

The isocitrate dehydrogenase (IDH) gene has recently been identified to be mutated in gliomas, a malignant brain tumor. Mutant IDH (IDHmut) produces the oncometabolite, (R)-2-hydroxyglutarate (R-2-hg), resulting in a significant increase of intracellular concentrations above physiological levels. However, a lack of correlation between circulating 2-hg levels and IDH status has been observed. This is likely due to the lack of discrimination from the enantiomer of R-2-hg and (S)-2-hydroxyglutarate (S-2-hg). S-2-hg is also normally made in the body but can increase to levels comparable to R-2-hg during hypoxic and acidic conditions. Thus, it is important to differentiate between R-2-hg and S-2-hg to determine the utility of R-2-hg as a biomarker. Furthermore, the current mass spectrometry (MS) methods available for the separation and detection are lacking. Current assays use laborious methods that can result in interconversion of enantiomers during sample preparation, and since low-resolution mass spectrometry instruments have been utilized, incorrect characterization of 2-hg MS data has occurred.

A novel chiral gas chromatography-tandem mass spectrometry (GC-MS/MS) assay was developed which improves upon current methods. The assay utilizes a simplified ethyl

acetate extraction, separates 2-hg enantiomers using a chiral column which avoids racemization, and quantifies 2-hg enantiomers using stable-isotope dilution MS. Using 2-hg isotopologues, unique EI fragmentation pathways for both 2-hg and the 2-hg lactone have also been described resulting in the ability to simultaneously detect both 2-hg and 2-hg lactone enantiomers.

The assay was then validated and serum 2-hg levels from healthy patients were measured, establishing a new, comprehensive reference range for normal levels of each enantiomer. Differences in basal levels of 2-hg enantiomers were observed between races but not sex. Finally, serum levels of 2hg enantiomers were measured in patients with and without IDHmut gliomas. An increase in R-2hg levels was observed for a number of patients with growing IDHmut gliomas, however, not all patients with IDHmut gliomas had an increase in R-2-hg levels. Increased S-2-hg levels were also observed in patients who received prior chemotherapy/radiotherapy. Further work is needed to fully understand circulating 2-hg enantiomer biology, but the work presented herein takes a significant first step in providing the tools and framework for understanding the clinical utility of R-2-hg as a biomarker for IDHmut gliomas.

TABLE OF CONTENTS

List of Tables

List of Figures

List of Illustrations

List of Abbreviations

IDH	Isocitrate dehydrogenase
IDHmut	IDH mutant
IDHwt	IDH wild-type
2-hg	2-hydroxyglutarate
R-2-hg	(R)-2-hydroxyglutaric acid/(R)-2-hydroxyglutarate
S-2-hg	(S)-2-hydroxyglutaric acid/(S)-2-hydroxyglutarate
AML	Acute Myeloid Leukemia
HOT	Hydroxyacid-oxoacid transhydrogenase
2HGDH	2-hydroxyglutarate dehydrogenase
α-kg	alpha-ketoglutarate
2-OG	2-oxoglutarate
NADPH	Nicotine adenine dinucleotide phosphate oxidase
NADP+	Reduced form of NADPH
KDM	histone lysine demethylase
TET2	5-methylcytosine hydroxylase;
PHD2	prolyl hydroxylase domain-containing protein 2;
C-P4H	collagen prolyl 4-hydroxylases;
STAT1	Signal transducer and activator of transcription 1
NFAT	nuclear factor of activated T cells Effectors:
HIF-1α	Hypoxia-inducible factor;
5-mC	5-methylcytosine

5-hmC	5-hydroxymethylcytosine
CXCL9/10	C-X-C motif chemokine 9/10
GC-MS	Gas Chromatography-Mass Spectrometry
GC-MS/MS	Gas Chromatography-tandem Mass Spectrometry
LC-MS	Liquid Chromatography-Mass Spectrometry
LC-MS/MS	Liquid Chromatography-tandem Mass Spectrometry
CSP	Chiral Stationary Phase
DATAN	Diacetyl-L-tartaric anhydride
TSPC	N-(o-toluenesulfonyl)-L-phenylalanyl chloride
MRS	Magnetic Resonance Spectroscopy
R-5-OTFCA	(R)-5-oxo-2-tetrahydrofurancarboxylic acid
S-5-OTFCA	(S)-5-oxo-2-tetrahydrofurancarboxylic acid
EI-MS	Electron Ionization-Mass Spectrometry
MRM	Multiple Reaction Monitoring
VUV	Vacuum Ultra-Violet
U	uracil
T	thymine
C	cytosine
5-hmU	5-hydroxymethyluracil
5-hmC	5-hydroxymethylcytosine
5-FoU	5-fluoroUracil
5-FoC	5-FluoroCytosine
5caU	5-carboxyUracil

5-CaC	5-carboxycytosine
6-CaC	6-carboxycystosine
24-OH Chol	24(S)-hydroxycholesterol
25-OH Chol	25-hydroxycholesterol
27-OH Chol	27-hydroxycholesterol
Chol	cholesterol
Prego	pregnenolone
t-DHA	trans-Dehydroandrosterone
test	testosterone
(TMS)DAM	(Trimethylsilyl)diazomethane
MTBSTFA	N-tert-Butyldimethylsilyl-N-methyltrifluoroacetamide
TBDMCS	tert-Butyldimethylchlorosilane
BSTFA	*N*,*O*-Bis(trimethylsilyl)trifluoroacetamide
TMCS	trimethylchlorosilane
MCF	methyl chloroformate
$NaHCO_3$	Sodium Bicarbonates
$NaSO_4$	Sodium Sulfate
NaCl	Sodium Chloride
HCl	Hydrochloric acid
MeOH	Methanol
EA	Ethyl Acetate
PBS	Phosphate Buffered Saline
H_2O	Water

mM	millimolar
mL	milliliter
μM	micromolar
N	normal
QC	Quality Control
FDA	Food Drug Administration
IDL	Instrument Detection Limit
LLoQ	Lower Limit of Quantitation
RSD	Relative Standard Deviation
QQQ	Triple Quadrupole
EI	electron ionization
CI	chemical ionization
ESI	electrospray ionization
MALDI	Matrix-assisted laser desorption ionization
2-hg Ratio	R-2-hg:S-2-hg
B	Black
H	Hispanic
C	Caucasian
A	Astrocytoma
A/O	Anaplastic oligodendroglioma
GTR	gross total resection
STR	sub-total resection
XRT	radiation therapy

TMZ	temozolomide
CCNU	lomustine
TP	tumor progression
tx	treatment

Chapter 1: 2-hydroxyglutarate enantiomer biology and the current analytical methods used for its detection

IDH MUTATIONS AND CANCER: A RAPIDLY EMERGING ARCHETYPE OF ALTERED METABOLISM IN CANCER CELLS

The discovery that cancer cells undergo an altered cellular metabolism has recently been recognized as an emerging hallmark of cancer [1]. In 1924, Otto Warburg reported his novel findings that cancer cells preferentially undergo glycolysis over mitochondrial respiration in the presence of oxygen [2]. This has led to the hypothesis that the dysfunction of mitochondria, or more generally, dysfunction in cellular metabolism, is associated with tumorigenesis. Mutations in a metabolic gene essential to cellular respiration, isocitrate dehydrogenase (IDH), have been frequently identified in several deadly human cancers including low-grade gliomas (60-85%), acute myeloid leukemias (16%), intrahepatic cholangiocarcinomas (23%), and central chondrosarcomas (56%) [3]–[6]. Moreover, IDH mutations confer an enzymatic gain of function, resulting in the generation of the oncometabolite, (R)-2-hydroxyglutarate (R-2-hg), which has been strongly associated with tumorigenesis [7], [8]. The current understanding of the role of IDH mutations and R-2-hg for diagnostic and therapeutic implications is currently an active and ongoing area of investigation [9]. The prime focus of this dissertation will be in the detection of R-2-hg and its application as a biomarker for patients with IDH-mutant gliomas.

METABOLIC PATHWAYS IN IDH WILD-TYPE AND IDH MUTANT CELLS

IDH1/2 encode for two related enzymes involved in the decarboxylation of isocitrate to α-ketoglutarate (α-KG) (Figure 1.1A) [10]. IDH1 codes for a cytoplasmic enzyme and IDH2 codes for a mitochondrial enzyme, however, both convert NADP+ to NADPH in the synthesis of α-KG [11]. IDH3 is the IDH enzyme that plays a major role in

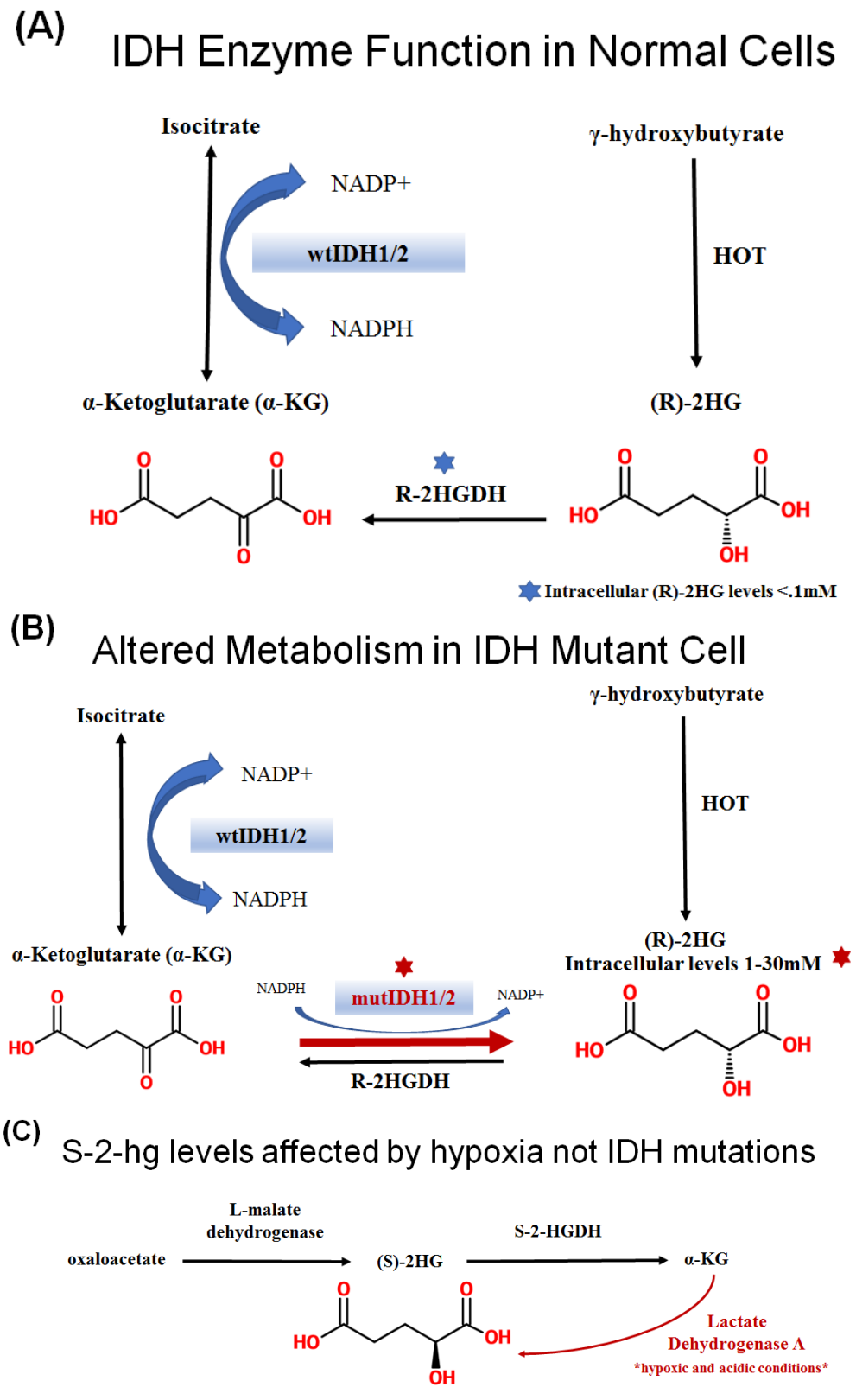

Figure 1.1. Metabolism of R-2-hg and S-2-hg in cells with and without IDH mutations

ATP production through the Krebs cycle but mutations of this enzyme are not observed and as such, it will not be further discussed. Besides the IDH mutant enzyme found in tumor cells, the enzyme hydoxyacid-oxoacid transhydrogenase (HOT) also produces R-2-hg [12]. However, R-2-hg in normal cells is metabolized back to α-KG by R-2-hg dehydrogenase (R-2HGDH), keeping basal physiological levels <0.1 mM intracellularly (Figure 1.1A) [11], [13]. Point mutations of IDH most commonly occur at the active site of the enzyme [7], [14]. The resulting point mutation decreases the binding affinity of the enzyme for isocitrate and instead increases the binding affinity of the mutant enzyme for NADPH. Subsequently, instead of carboxylation taking place in the reverse reaction, the carbonyl group on α-KG is reduced to a hydroxyl group, and the metabolite, R-2-hg, is produced (Figure 1.1B). Consequently, a shift in homeostasis follows between the regulatory enzymes of R-2-hg, resulting in an accumulation of R-2-hg in cancer cells heterozygous for IDH mutations (Figure 1.1B). R-2-hg is produced faster than it can be metabolized, leading to excess levels of R-2-hg in IDHmut cancer cells. Using mass spectrometry based-techniques, levels have been reported to increase intracellularly from 0.1 mM to 1 mM − 30 mM in IDH mutant tumor samples [11], [15]. Due to the significant increase in intracellular concentrations, the use of R-2-hg as a clinical biomarker of disease has garnered significant interest, especially with the recent development of targeted therapies towards the IDH mutant enzyme [9].

(S)-2-hydroxyglutarate (S-2-hg) is a stereoisomer of R-2-hg, specifically the left-handed enantiomer of 2-hydroxyglutarate. S-2-hg is normally produced by cells during the conversion of oxoacetate to (L)-malate by (L)-malate dehydrogenase and is similarly metabolized by S-2-hg dehydrogenase (S-2HGDH) to α-KG (Figure 1.1C) [16]. Both R- and S- 2-hg are produced during normal mitochondrial respiration and can be detected in blood and urine in healthy individuals [17]. However, the exact physiological role of these metabolites is not known. Mutations in IDH exclusively produce the right-handed enantiomer, R-2-hg, and not S-2-hg i.e. the natural synthesis of S-2-hg is not altered in an

IDH mutation [7], [18]. Since S-2-hg is regulated by different enzymes than R-2-hg the levels of each enantiomer can be significantly different. For instance, levels of S-2-hg are not altered by IDH mutations but are influenced by T-cell receptor activation, complex I inhibition, S-2-hg dehydrogenase (S-2HGDH) deficiencies, and most notably, hypoxia and low pH which have major implications in tumor biology [7], [19]–[22]. Under hypoxic conditions, the enzyme lactate dehydrogenase A (LDHA) is upregulated resulting in a subsequent increase in S-2-hg levels [22]. Naturally, metabolic acidosis can result from hypoxic conditions and prior work had demonstrated that a low pH can also induce LDHA to produce higher levels of S-2-hg [16], [23].

TUMORIGENESIS AND MICROENVIRONMENT MODULATION BY (R)-2-HYDROXYGLUTARATE

The increase in R-2-hg is not without consequence. Normal cells induced to express mutant IDH transform and demonstrate enhanced cellular proliferation and inhibition of differentiation [8], [24]–[26]. The mechanisms by which R-2-hg mediates tumorigenesis remains an active topic of investigation. It has been proposed that R-2-hg competitively inhibits 2-oxoglutarate-dependent dioxygenases, which may be due to the analogous structure of R-2-hg and 2-oxoglutarate (2-OG) [13]. There are numerous 2-OG dependent dioxygenases, and with almost 70 known, a multifactorial mechanism of tumor formation is likely [27], [28]. However, a few specific mechanisms have been proposed (Figure 1.2). The role of 2-OG-dependent oxygenases is to hydroxylate a specific target. For example, DNA, or a DNA-associated molecule, like histones, are among the most common targets. TET2 encodes a 2-OG dependent dioxygenase that converts 5-methylcytosine (5-mC) to 5-hydroxymethylcytosine (5-hmC) (Figure 1.2) [29]. Thus, in the absence of 2-OG, 5-mC remains methylated. R-2-hg also inhibits histone demethylases such as KDM2A and KDM5B, resulting in increased methylation of histones (Figure 1.2) [27], [29]. Therefore, R-2-hg can potentially increase histone methylation and DNA methylations,

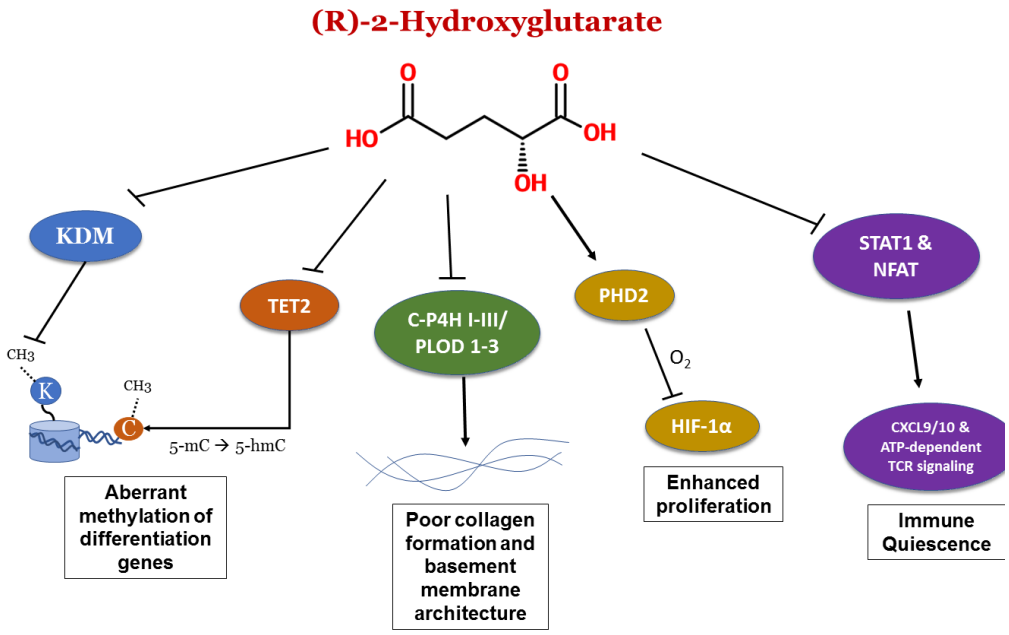

Figure 1.2. Molecular mechanisms of tumorigenesis in IDH mutants

wtIDH1/2 wild-type IDH1/2; **mutIDH1/2** mutant IDH1/2; **(R)-2-HGDH** (R)-2-hg dehydrogenase; α-Ketoglutarate-dependent dioxygenases: **KDM** histone lysine demethylase; **TET2** 5-methylcytosine hydroxylase; **PHD2** prolyl hydroxylase domain-containing protein 2; **C-P4H** collagen prolyl 4-hydroxylase; **STAT1** Signal transducer and activator of transcription 1, **NFAT** nuclear factor of activated T cells Effectors: **HIF-1*α*** Hypoxia-inducible factor; **5-mC** 5-methylcytosine, **5-hmC** 5-hydroxymethylcytosine **CXCL9/10** C-X-C motif chemokine 9/10

resulting in dysregulation of epigenetic modifications and gene expression, which may silence genes involved in cellular differentiation. Additionally, R-2-hg has been reported to inhibit prolyl 4-hydroxylases (CP4Hs) and procollagen-lysine, 2-oxoglutarate 5-dioxygenases I-III (PLOD I-III) enzymes [30]. Both enzymes play a role in collagen formation and maintenance of basement membrane integrity through hydroxylation of proline and lysine residues of collagen. Lastly, recent studies have shown that R-2-hg also results in a modulation of the immune cells of the tumor microenvironment (Figure 1.2). Entry of R-2-hg into tumor infiltrating T-cells results in the reduction of Signal Transducer and Activator of Transcription 1 (STAT1) levels and subsequent decrease production of C-X-C motif chemokine 9 and 10 (CXCL9 and 10) [31]. This consequently results in a

reduction in tumor infiltration by CD8+ T-cells. 2-hg can also inhibit Nuclear Factor of Activated T cells (NFAT) which inhibits ATP-dependent T cell receptor (TCR) activation and causes a decrease in T-cell activation and proliferation [31]. Lastly, R-2-hg can also cause genetic instability through disruption of DNA repair pathways (not shown in Figure 1.2) through inhibition of multiple repair enzymes, such as AlkB Homolog (ALKBH), among others [32]. In summary, R-2-hg has been shown to play a major role as an oncometabolite and only a broad overview was discussed herein. A full detailed review can be found elsewhere [11], [33]. Measuring R-2-hg levels would then allow investigators to not only potentially quantify tumor burden but also provide a prognostic indication since R-2-hg plays such an important role in tumor growth.

ANALYTICAL METHODS USED TO MEASURE 2-HG ENANTIOMERS

With the advent of sensitive mass spectrometry-based assays, accurate measurement of metabolites in clinical samples has become possible [47, 48]. However, since mass spectrometry measures the mass of a molecule, chiral molecules such as enantiomers require the use of special chromatography techniques before detection since the molecules have the same mass. Other considerations in the development of an assay to measure enantiomers from a biological sample must go through the proper evaluation of steps, as shown in Illustration 1.1. Each methodology at a given step has its advantages and disadvantages and improper utilization of a given method can lead to sample loss or a significant loss in sensitivity. Extraction of 2-hg is commonly performed through the use of a low-temperature organic-aqueous solvent mixture. Typically, an 80:20 mixture of MeOH and H_2O at dry ice temperatures (-80°C) is mixed with the sample to immediately quench cellular metabolic processes followed by an incubation period from 15 min. to overnight at -80°C [16], [34]. The sample is then centrifuged, and the supernatant is taken for analysis.

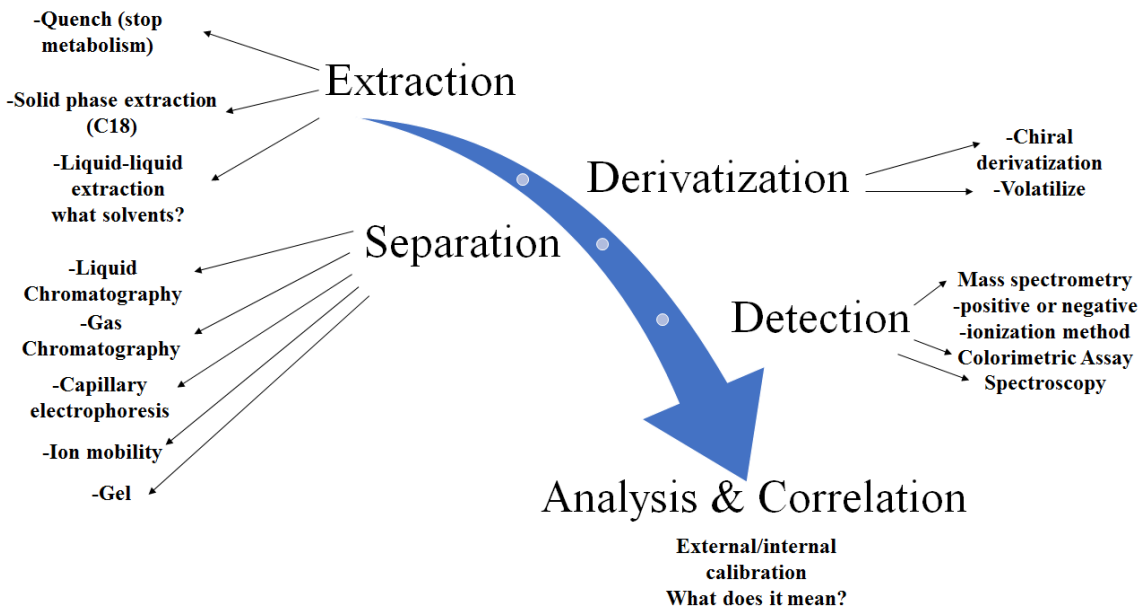

Illustration 1.1. Analytical process for measurement of metabolites from a biological sample.

This methodology is often preferred as it is simple, not selective for one class of metabolites, and is compatible with Liquid Chromatography-tandem Mass Spectrometry (LC-MS/MS)-based methods. However, the method requires the use of dry-ice temperatures and because it is not selective, can result in a multitude of metabolites which can cause issues with chromatography, derivatization efficiency, and ion suppression during MS analysis. Another common method uses a liquid-liquid solvent extraction technique where a phase separation into organic (often ethyl acetate) and aqueous layers are utilized to separate compounds of interest. The procedure requires a few more steps as compared to the MeOH-based protocol, but the solvent-solvent extraction is more selective for organic acids (such as 2-hg) since the solvent-solvent solution is acidified and saturated with NaCl, forcing organic acids into the non-polar ethyl acetate layer. Since organic acids are favored, this limits the class of metabolites harvested for analysis and minimizes the amount of superfluous metabolites injected onto the analytical column. Another less common method utilizes solid phase extraction to extract 2-hg enantiomers which can be

a simple and quick methodology, but it requires the use of expensive SPE cartridges and a vacuum manifold to rapidly extract samples [35].

Gas chromatography (GC) and liquid chromatography (LC) are the most common methods used to separate metabolites. However, as mentioned previously, R-2-hg and S-2-hg are enantiomers, meaning they are stereoisomers that are mirror images of each other (Figure 1.3). By definition, stereoisomers have the same atom connectivity but a different spatial arrangement, whereas constitutional isomers are molecules with different atom connectivity but same chemical composition [46]. This distinction is important since standard reverse phase columns cannot separate enantiomers prior to MS analysis and chiral chromatography techniques must be utilized to separate enantiomers.

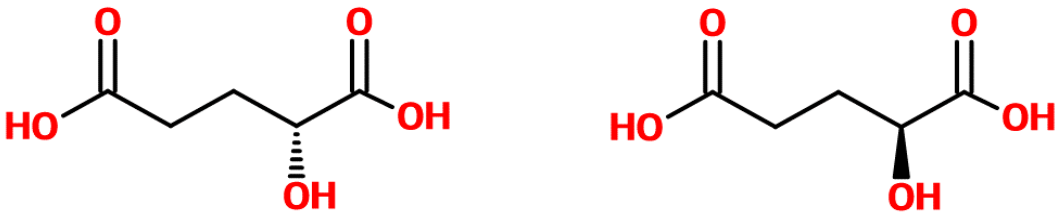

(R)-2-hydroxyglutarate – (R)-2-hg
D-2-hydroxyglutarate – D-2-hg

(S)-2-hydroxyglutarate – (S)-2-hg
L-2-hydroxyglutarate – L-2-hg

Figure 1.3. Structures of R-2-hg and S-2-hg

In general, chiral chromatography utilizes the specific configuration of an isomer to separate one compound from another. 2-hg is a dicarboxylic acid with a hydroxyl group at the alpha or 2nd carbon (Figure 1.3). The configuration of the asymmetric carbon differentiates between the R- form (or the D- form using D/L notation) and the S- (L-) form; this specific stereocenter is used as the basis of separation of the enantiomers.

Methods used to separate and detect 2-hg enantiomers were initially developed to detect levels in the urine of patients with inborn errors of metabolism by means of chiral derivatization [36]–[38]. Diastereomers of 2-hg were created by derivatization with (R)-(—)-2-butanol, separated over an achiral gas chromatography (GC) column and detected

by mass spectrometry (MS). Separation and detection were sufficient to detect large increases of either enantiomer in urine, and a recent study has used this method to detect levels of 2-hg enantiomers in patients with IDH-mutant (IDHmut) AML with success [15]. Though (R)-(—)-2-butanol derivatization allows for separation of 2-hg from biological fluids, the method results in significant racemization (5-7%) and requires multiple steps to complete the derivatization procedure. Thus, it is not suitable for applications that require accurate and sensitive methodologies, such as the detection of changes in serum 2-hg enantiomer levels from a brain tumor with a complex blood-brain tumor barrier. Furthermore, the aforementioned GC-MS assays utilized only a low-resolution single quadrupole (MS) instrument. In order to increase specificity, reduce background, and eliminate any potential interference from co-eluting compounds, the use of tandem mass spectrometry (MS/MS) is needed (Illustration 1.2).

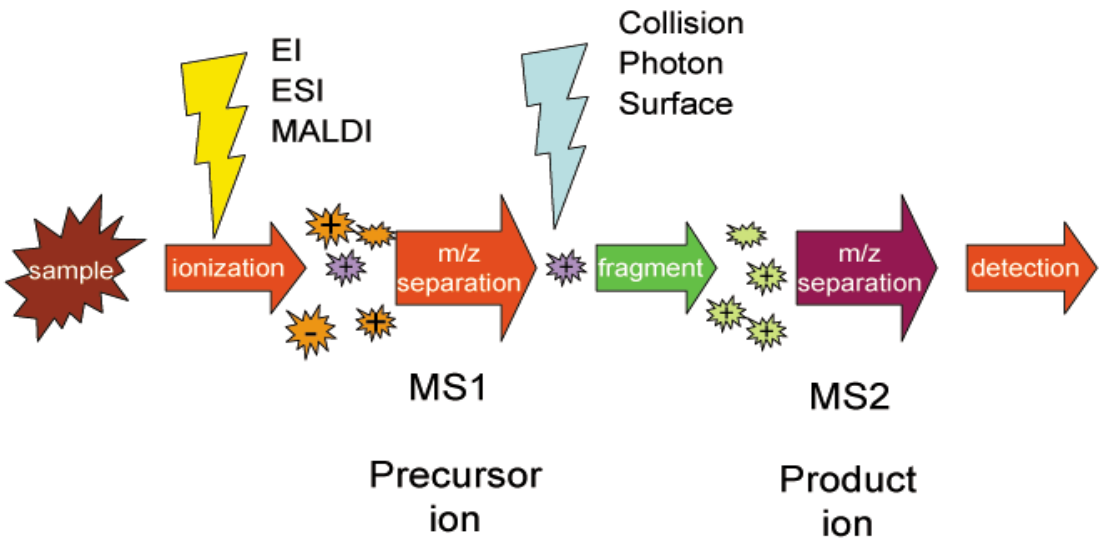

Illustration 1.2. Schematic of tandem mass spectrometry. Image was copied from commons.Wikimedia.org under the GNU Free Documentation License and the Creative Commons Attribution-Share Alike 3.0 Unported License. Author: K. Murray

Tandem mass spectrometry provides the necessary specificity as it detects a fragment (product ion) of a fragment (precursor ion). The way in which molecules fragment is

typically unique to each molecule and can be reconstructed to provide the structure and chemical composition of a given compound. To date, MS/MS methods for detection of 2-hg have been coupled with LC but not GC.

Other chiral derivatization methods have since been developed for use in Liquid Chromatography-tandem Mass Spectrometry (LC-MS/MS) where Diacetyl-L-tartaric anhydride (DATAN) or N-(o-toluenesulfonyl)-L-phenylalanyl chloride (TSPC) is the derivatization agent [39], [40]. Derivatization with DATAN has gained the most traction due to the lower chance of racemization and its lower cost as compared to (R)-(−)-2-butanol [34], [41], [42]. Though DATAN has been used in methods for measurement of 2-hg enantiomers from bodily fluids, it requires evaporation of all water before derivatization, the use of heat during derivatization, and drying and re-suspension post-derivatization. Chiral derivatization with TSPC reported improved sensitivities over tartaric acid-based procedures, but the derivatization protocol requires the use of hazardous pyridine and significantly lengthens the retention times from 4-8 minutes to 21-23 minutes. No racemization data was reported for the TSPC-based derivatization assay, so the extent of racemization is unclear for this method. Although LC-MS/MS assays are increasing in use to study cellular metabolites, the overall methodology from extraction, derivatization, separation, and detection for 2-hg enantiomers can be laborious and thus difficult to implement for clinical assays.

2-hg enantiomers can also be separated using a chiral column which avoids the use of any chiral derivatization and its associated drawbacks. Chiral columns contain a chiral stationary phase (CSP) which has a higher affinity for one enantiomer over the other. LC columns include the glycopeptide CHIROBIOTIC R column (Sigma) and quinidine/quinine-based columns [43]–[45]. Both LC columns are commercially available but are costly and the latter has not been validated for use with MS to measure 2-hg enantiomers. Chiral separation using GC columns is a mature method and as a result, a variety of robust CSPs exists [46]. β-cyclodextrin is a common CSP and has been

previously utilized to separate and detect 2-hg enantiomers in the urine by GC-MS [47], [48]. The methodology is simple to implement and depending upon the GC settings, it can separate enantiomers with a retention time of fewer than 15 minutes. Similar to LC chiral columns, GC chiral columns have historically been costly as compared to chiral derivatization methods and consequently not widely used. However, because commercial chiral columns have become widely available across multiple vendors, the price of chiral GC columns are comparable to standard achiral reverse phase LC columns. Therefore, chiral GC columns are now amenable for use in a wide variety of applications including clinical assays [46].

Non-Mass Spectrometry-based assays for the detection of 2-hg enantiomers

A non-mass spectrometry-based assay has also been developed and is commercially available, but the enzymatic assay is not widely utilized due to expense, inability to detect both enantiomers simultaneously, lack of serum sensitivity and the indirect measurement outcome. The assay uses a fluorometric reporting system to report levels of R-2-hg from cells and serum [49]. However, the assay does not report levels of S-2-hg and the reported sensitivities for serum is only 2.77 μM, which is insufficient to measure basal levels of enantiomers (as detailed in chapter 4). The fluorometric assay does have some advantages though. Overall, the assay is less complex as compared to GC and LC-MS-based assays since it does not require the use of mass spectrometry or chromatography instrumentation, making it less expensive overall. The assay is also quicker as compared to MS-based methods. However, given the sensitivity of the assay, a fluorometric-based assay for the detection of 2-hg enantiomers would be insufficient for high sensitivity applications, such as the measurement of 2-hg enantiomer levels from patients with IDHmut brain tumors.

Another assay that detects 2-hg is Magnetic Resonance Spectroscopy (MRS) that detects the metabolite *in vivo*. MRS is a non-invasive technique analogous to nuclear magnetic resonance spectroscopy as it specifically looks for the specific 2-hg signal from

the tumor. Though much work has been done showing detection of 2-hg from brain tumors using MRS [50]–[52], the method suffers from lack of sensitivity and operator interpretation. The complexity needed to employ the post-processing alone is a major barrier as well. Lastly, the method does not distinguish between enantiomers and as such, *in vivo* accurate measurement of R-2-hg is unlikely.

To date, other such assays to separate and detect 2-hg enantiomers from serum do not exist. MS-based methods are most common and due to the necessity of separating enantiomeric compounds in a complex biological matrix, MS-based methods are needed. In an attempt to create a cheaper and quicker alternative to MS-based methods, a novel method using GC-Vacuum Ultra-Violet (VUV) spectroscopy was also developed. The results of the GC-VUV assay are discussed in chapter 3.

2-hg can also exist as lactones and must be considered during separation

Each enantiomer can also readily undergo cyclization to its lactone, R-2-hg to (R)-5-oxo-2-tetrahydrofurancarboxylic acid (R-5-OTFCA) (Figure 1.4A) and S-2-hg to (S)-5-oxo-2-tetrahydrofurancarboxylic acid (S-5-OTFCA) (Figure 1.4B). 2-hg lactones have been reported to preferentially form under acidic conditions [53], however, mechanisms of hydrolysis of lactones have been reported under acidic [54], alkaline [55], and neutral conditions [55]. This suggests that preference for the cyclic or acyclic conformations could vary between sample type and other variables, such as salt concentration, could also play a major role in the cyclization of the 2-hg.

The favorability of a linear molecule to undergo ring formation is often dictated by the stereochemistry of the transition state as dictated by Baldwin's rules [56]. Three factors are considered in Baldwin's rules. First is the number of atoms in the formed ring. Any ring greater than or equal to three can occur. The second rule describes the position of broken bond when cyclization occurs. The broken bond can occur outside of the newly formed ring (exo), or inside the ring (endo). Thirdly, the hybridization, such as sp^3

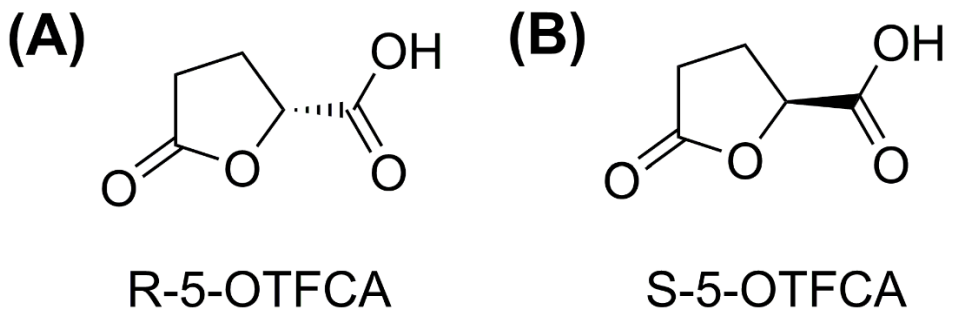

Figure 1.4. Structures of 2-hg lactone from the R enantiomer (A) and the S enantiomer (B)

(tetrahedral), sp^2 (trigonal), or sp (diagonal) at the site of the ring closure matters. Baldwin's rules are used to predict favorability for a number of hypothetical ring structures but in general, the following guidelines hold: exo formations are favored for tetrahedral and trigonal targets and endo formation is favored for diagonal formations. The formation of the 2-hg lactone is an exo trigonal cyclization that forms a five-membered ring which is a favored process (Figure 1.5).

As shown in the mechanism of lactone formation, a water loss occurs demonstrating that cyclization must occur prior to any derivatization for analysis. If the sample was modified for analysis, such as creating a methyl ester to volatilize the metabolite, the formed methyl ester would prevent cyclization as it is a poor leaving group as compared to a hydroxyl group i.e. MeOH loss is not favored but a water loss is.

Accordingly, one study using chiral GC-MS reported that the dominant compound detected in the urine or serum is the lactone [47]. Other assays, however, have reported detection of both species by separation in retention time, while others did not address the lactone whatsoever [38], [48], [57]–[60]. Additionally, the specific 2-hg lactone enantiomer was not reported, and it is unclear if clear separation of all four compounds was achieved. An assay specifically targeted to detect each species separately is needed.

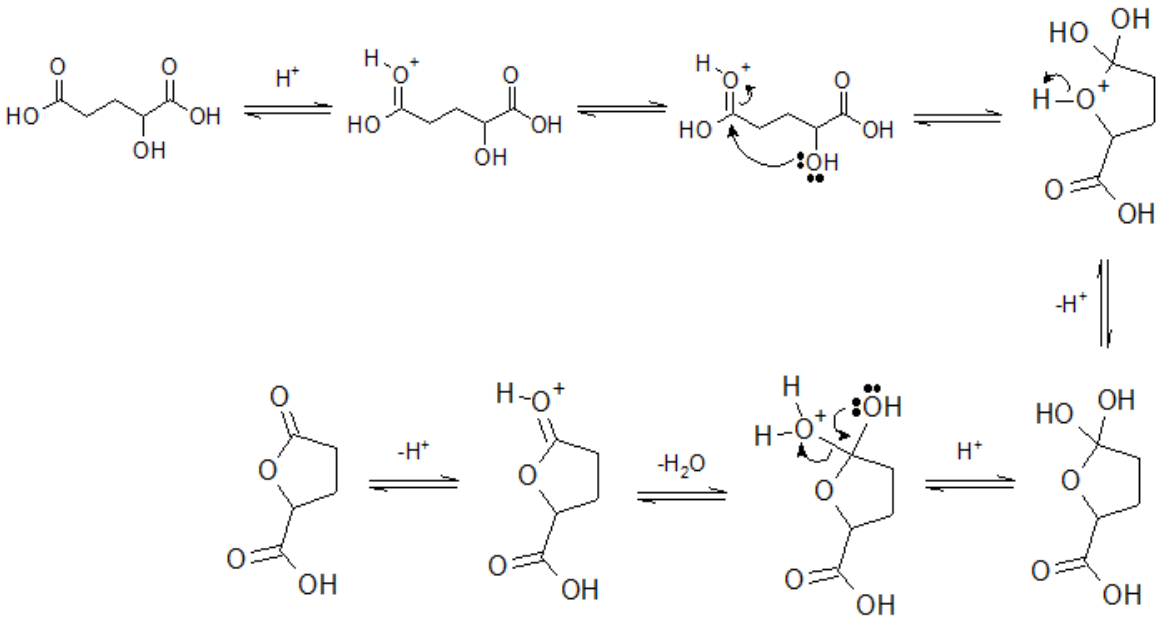

Figure 1.5. Mechanism of 2-hg lactone formation under acidic conditions

SUMMARY

R-2-hg is an important oncometabolite that has the potential to be a viable biomarker for the management of patients with IDH mutant cancers. Although methods have been developed to separate and detect 2-hg enantiomers, current methodologies are lacking either due to the use of chiral derivatization (which leads to racemization), laborious sample preparation (due to redundant extraction steps) or the lack of specificity (through the use of low-resolution quadrupole mass spectrometry instruments). The following chapters address the current problems through the development and validation of a robust, sensitive, and specific chiral gas chromatography-tandem mass spectrometry (GC-MS/MS) assay that can be used in clinical chemistry laboratories (chapter 2). An alternative method using GC-VUV was also built in an attempt to create an even cheaper and quicker alternative to MS-based methods for 2-hg enantiomer separation and detection (chapter 3). The GC-MS/MS assay was then used to measure 2-hg enantiomers from

healthy donors to understand the normal range of 2-hg enantiomers in serum (chapter 4). Lastly, the results of an ongoing study measuring 2-hg enantiomers from patients with IDHmut gliomas are discussed (chapter 5). The dissertation is ended with concluding remarks and future works (chapter 6).

Chapter 2: Development of a clinical assay to measure 2-hg enantiomers

Parts of this chapter, which include select paragraphs, figures, and tables, are a copy or an adaptation of Strain S. et al. RCM. 2019. doi: 10.1002/rcm.8485. [61] *and Strain S. et al. 2020. doi: 10.1016/j.clinms.2019.11.002* [62].

INTRODUCTION

The overall aim of this chapter is to describe the development of a Gas Chromatography-tandem Mass Spectrometry assay (GC-MS/MS) for the separation and detection of 2-hg enantiomers.

First, an optimal derivatization procedure for the volatilization of 2-hg was determined using 2-hg standards. Then, EI fragmentation structures of derivatized 2-hg were predicted and utilized to develop an assay to simultaneously separate and detect both the 2-hg enantiomers and its lactone. The structure and molecular formula of each 2-hg fragment were predicted by comparing the EI-MS spectra of 2-hg to two different stable isotope compounds. This led to a different interpretation of a major peak and for the first time, the mechanism of EI fragmentation of 2-hg which showed that the major fragments were the result of secondary fragmentation. EI-MS spectra of 2-hg lactones were also obtained and a fragment unique to the linear 2-hg compound was discovered. EI fragmentation results were subsequently verified by product ion analysis. An assay using chiral gas chromatography and multiple reaction monitoring (MRM) was then built to distinguish between each 2-hg enantiomer and their corresponding lactones by triple quadrupole (QqQ) MS. Our data showed that the dominant compound in both the urine and serum, as measured by our assay, is the acylic 2-hg compound though the lactone is present and varies in amount from sample to sample.

The second aim of this chapter focuses on the optimization and the validation of the developed GC-MS/MS assay. A modified ethyl acetate-based extraction was used to extract 2-hg to demonstrate that the assay can be adapted for efficient sample preparation

as it applies to clinical laboratories. Validation was performed according to current guidelines published by the Food and Drug Administration (FDA) for bioanalytical assays and according to current standard methods utilized for stable-isotope dilution MS assays [63], [64].

MATERIALS AND METHODS

Chemicals and Reagents

D-α-Hydroxyglutaric acid disodium salt (≥98%), L-α-Hydroxyglutaric acid disodium salt (≥98%), and (R)-(−)-5-Oxo-2-tetrahydrofurancarboxylic acid (98%) standards were purchased from Millipore Sigma (St. Louis, MO). (S)-(+)-5-Oxo-2-tetrahydrofurancarboxylic acid was purchased from VWR (Randor, PA). Deuterated 2-hg, Disodium (RS)-2-Hydroxy-1,5-pentanedioate-2,3,3-d3,OD (≥95%), was purchased from CDN Isotopes (Pointe-Claire, Québec) and DL-2-hydroxyglutaric acid disodium salt (^{13}C5, 99%) was purchased from Cambridge Isotopes (Wobum, MA). GC-MS grade ethyl acetate, hydrochloric acid solution (6.0N), and sodium chloride (NaCl, ≥99%) were purchased from Millipore Sigma (St. Louis, MO). (Trimethylsilyl)diazomethane ((TMS)DAM) solution (2.0M) in Hexanes from ACROS chemical or Millipore Sigma was used for esterification (Waltham, MA). N-tert-Butyldimethylsilyl-N-methyltrifluoroacetamide (MTBSTFA) with 1% tert-Butyldimethylchlorosilane (t-BDMCS) and *N*,*O*-Bis(trimethylsilyl)trifluoroacetamide (BSTFA) with 1% trimethylchlorosilane (TMCS) were purchased from ThermoFisher Scientific (Waltham, MA). LC-MS grade methanol, LC-MS grade H_2O, LC-MS grade acetonitrile, and LC-MS chloroform were obtained from J.T. Baker (Phillipsburg, NJ). Pyridine and methyl chloroformate were obtained from Millipore Sigma (St. Louis, MO). $NaHCO_3$ and $NaSO_4$ were obtained from Fisher Scientific (Waltham, MA).

Preparation of 2-hg standards for GC-MS and GC-MS/MS

1 mg of powder was weighed out for each compound and dissolved in H_2O accordingly to make 1 mM stock solutions. The amount of water used to create 1 mM solutions was modified to account for purity, sodium salts, and racemic mixtures. Stock solutions were aliquoted and stored at -80°C. Ten microliters of a stock solution or a 100 µM solution were pipetted into an autosampler glass vial and dried in a vacuum concentrator for derivatization.

Biological Samples

Serum samples acquired from 10 individual healthy donors were obtained from Innovative Research (Novi, MI, USA). After thawing, each serum sample was aliquoted and stored at -80°C. Urine samples were taken from an ongoing, IRB-approved study at The Austin Brain Tumor Center (Texas Oncology, Austin, TX). The study obtained urine samples from IDHmut and IDHwt patients with and without active disease. Eleven urine samples from individuals without active disease, but previously had IDHwt tumors, were used in this study.

Serum Extraction

To a 1.5 mL microcentrifuge tube was added 250 µL of serum and 3 µL of 100 µM deuterated 2-hg as an internal standard. Ten microliters of 6 N HCl was then added followed by NaCl to saturation. The solution was vortexed for 30 sec. One milliliter of ethyl acetate was subsequently added to the tube and vortexed for another 30 sec. The sample was then centrifuged for 5 min at 4000xg and 900 µL of the top organic layer was then pipetted into a 2 mL wine glass vial. For lactone experiments, a second extraction with another 1 mL of ethyl acetate was performed and the organic layers were combined and dried in a vacuum concentrator.

Urine Extraction

To a 1.5 mL microcentrifuge tube was added 100 µL of urine and 12 µL of 100 µM deuterated 2-hg as an internal standard. Ten microliters of 6 N HCl was then added followed by NaCl to saturation. One milliliter of ethyl acetate was subsequently added to the tube and vortexed for another 30 sec. The sample was then centrifuged for 5 min at 4000xg and 900 µL of the top organic layer was then pipetted into a 2 mL wine glass vial and dried in a vacuum concentrator.

Silylation Derivatization

To each dried sample was added 100 µL of Acetonitrile and MTBSTFA + 1% TBDMCS (1:1) to form tert-butyl silyl derivatives and in separate vials, 100 µL of Acetonitrile and BSTFA + 1% TMCS (1:1) to form trimethylsilyl derivatives. The samples were then crimp sealed and heated at 60°C for 30 min. The samples were then allowed to cool and injected for analysis.

Esterification Derivatization

(TMS)DAM derivatization was performed by adding 100 µL of MeOH and 20 µL of (TMS)DAM to a glass vial containing a dried sample. The vial was then capped with a crimp seal and shaken for 30 min at room temperature (25°C). After incubation, the solution was injected directly into the GC-MS instrument. Optimization of derivatization conditions was achieved by examining the yield at 30 minutes, 60 minutes, and 90 minutes at room temperature. Temperature was also varied from RT to 50°C to 75°C at a constant time of 30 minutes.

For MCF derivatization, to a dried sample in a glass vial was added 90 µL of 4 N NaOH, 333 µL of MeOH, and 67 µL of pyridine. The solution was then vortexed for 5 seconds and 80 µL of MCF was added and the mixture was vortexed for 60 seconds. Next, 400 µL of cold chloroform was added and the mixture was vortexed for 10 seconds. Four microliters of 50 mM $NaHCO_3$ was then added (solution was made prior) and the solution

was mixed for 10 seconds after which a phase separation ensued. Using a glass Pasteur pipette, the lower chloroform layer was transferred into a glass tube where $NaSO_4$ was added to wick any transferred aqueous solution. The chloroform layer was then used directly for analysis.

GC-MS and GC-MS/MS

Compounds were detected using a TQ-8050 Gas-Chromatography Triple Quadrupole Mass Spectrometer (Shimadzu, Kyoto, Japan) equipped with a CP-Chirasil-Dex CB, 0.25mm x 25m x 25µm column (Agilent, Santa Clara, CA). The chiral capillary column has a chiral stationary phase composed of β-cyclodextrin bonded to dimethylpolysiloxane. After derivatization, 1 µL microliter of sample was injected into the GC splitless inlet (set at 220°C) with an initial oven temperature of 80°C. After sampling for one minute at 80°C, the oven was ramped at 4°C/min to 180°C and held for 4 minutes. The total run time of each sample was 30 min. Helium was used as the carrier gas with a column flow of 1.5 mL/min at the constant linear velocity setting. The following MS parameters were used for all modalities: the ion source temperature and the interface temperature were set at 200°C, ionization energy at 70 eV, and the solvent cut time at 4 min.

Fragmentation Patterns by GC-MS

Fragmentation patterns of 2-hg, 2-hg lactone, and the stable isotopes of 2-hg were determined by electron ionization in Q3 scan mode from 20-200 *m/z* using an event time of 0.500 sec.

Product ion analysis

Product ions were obtained by setting the precursor ions at 85 *m/z* and 117 *m/z* for 2-hg and the 2-hg lactone. Ions were scanned from 20-200 *m/z* at a scan speed of 666 (event

time of 0.3 sec) at the high-resolution setting. Collision energies for each compound were set at 13.00 V for the 85 *m/z* fragment and 15.00 V for the 117 *m/z* fragment.

Optimization of collision energies for MRM

Collision energies for each MRM transition were optimized by observing the transition signal intensity for a range of collision energies set from 3 to 30 V.

Detection of endogenous 2-hg enantiomers in serum & urine by MRM

Detection of endogenous 2-hg enantiomers was performed by multiple reaction monitoring. Two transitions, 85.00 *m/z* > 29.00 *m/z* and 117.00 *m/z* > 85.00 *m/z* with collision energies of 13.00 V and 6.00 V, respectively, were used to monitor 2-hg using an event time of 0.04 sec. Collision energies were selected to provide the optimal MRM transition signal.

Linearity and Limits of Detection

Serial 1:10 dilutions of 1mM and 0.5 mM to 0.1 µM and 0.5 µM, respectively, were used to test linearity. Ten microliters of each sample were used for analysis and prepared for GC-MS/MS analysis as described below. Each data point was normalized to 10 µL of a 10 µM solution of deuterated 2-hg. Limits of detection were reported using two metrics. The instrument detection limit (IDL) and Lower Limit of Quantitation (LLoQ) were determined by injecting 8 technical replicates of the 1 µM solution, from three separate dilutions on three separate days. IDL is determined by the following equation *t*RSD*concentration/100*, where t is the 99% confidence level for n-1 degree freedom and RSD, is the relative standard deviation (RSD). The lower limit of quantitation (LLOQ) is also a common metric of limit of detection and is defined as the amount injected onto the column that has an RSD ≤ 20%.

Quality Controls, Accuracy, Precision

Ten microliters of four different QCs at 3 µM (Low QC), 8 µM (Mid-Low QC), 40 µM (Mid QC), 90 µM (High QC), plus LLoQ, were used to assess accuracy and precision of the assay. Accuracy and precision were assessed over three separate dilutions where each dilution had three technical replicates run for three aliquots of each QC. Each new dilution was run on one day and used to analyze intra-assay variability between the three aliquots and technical replicates of each aliquot. Inter-assay variability compared accuracy and precision across all three separate dilutions. Inter-assay precision of the extraction method was measured by calculating the RSD of three biological replicates of each serum sample as measured on three different days.

Selectivity & Specificity, Recovery, Carry-over and Stability

Selectivity & specificity were demonstrated by measuring for 2-hg enantiomers signals from the extraction of 5 blank extraction (no serum) samples, 5 PBS samples, and 5 vials with only derivatization reagents. Recovery was assessed by comparing serum samples spiked with deuterated 2-hg before and after extraction where 10 µL of three concentrations, 3 µM, 30 µM and 90 µM in a total of 15 different serum samples were used (five each). Carryover was assessed by measuring 2-hg enantiomer levels after injecting a blank solvent, such as ethyl acetate or acetonitrile, between experiments analyzing QC and serum samples. Lastly, stability was assessed by comparing the change in concentration (by percent difference) after 24 hrs. in the autosampler, 4 hrs. on the bench top, and 4 freeze-thaw cycles (5 separate serum samples per experiment).

RESULTS AND DISCUSSION

Optimization of separation of 2-hg enantiomers by chiral chromatography

In order to separate 2-hg enantiomers, a chiral column with β-cyclodextrin as the chiral stationary phase (CSP) was chosen to separate 2-hg enantiomers. The specific column was selected as it is one of the most common CSPs used for chiral gas chromatography, and it has been used previously to separate urine 2-hg enantiomers [36]–[38]. Though a common chiral GC column has been established for separation of enantiomers, a wide variety of derivatization agents can be used to volatilize 2-hg. Four derivatization agents were selected based upon feasibility in cost, derivatization schema, and chemical product created (Figure 2.1).

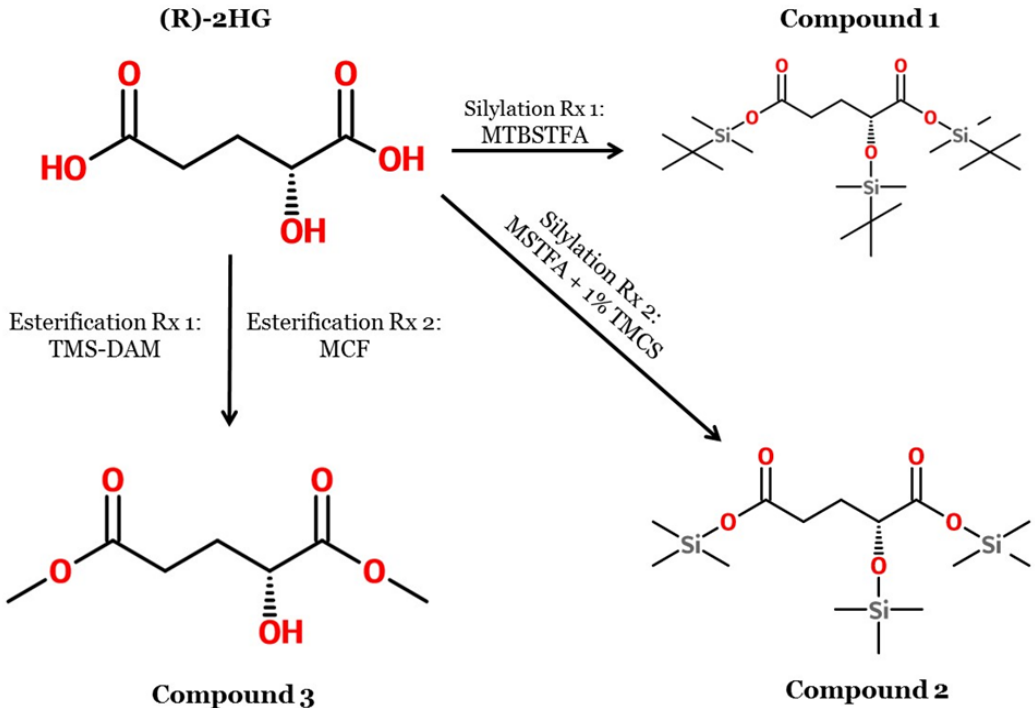

Figure 2.1. Four derivatization schemes used for the optimization of enantiomer separation

Silylation Rx 1 and 2 add different silyl groups to each functional group, while esterification Rx 1 and 2 add only methyl groups to the carboxylic acids. Although the end result of esterification Rx 1 and 2 are the same, the procedure with each agent (TMS-DAM and MCF) are significantly different (detailed in methods). Separation using silylation Rx 1 is shown in Figure 2.2A. Each 2-hg enantiomer standard was injected and overlaid. No clear separation in retention time (67.2 min) was observed between the R-2-hg and S-2-hg. It is likely that the tert-butyl silyl groups are too bulky for the chiral resin to bind to and create any difference in separation between the two enantiomers. As expected, the EI fragmentation patterns of each enantiomer were identical (Figure 2.3A). The MS data also

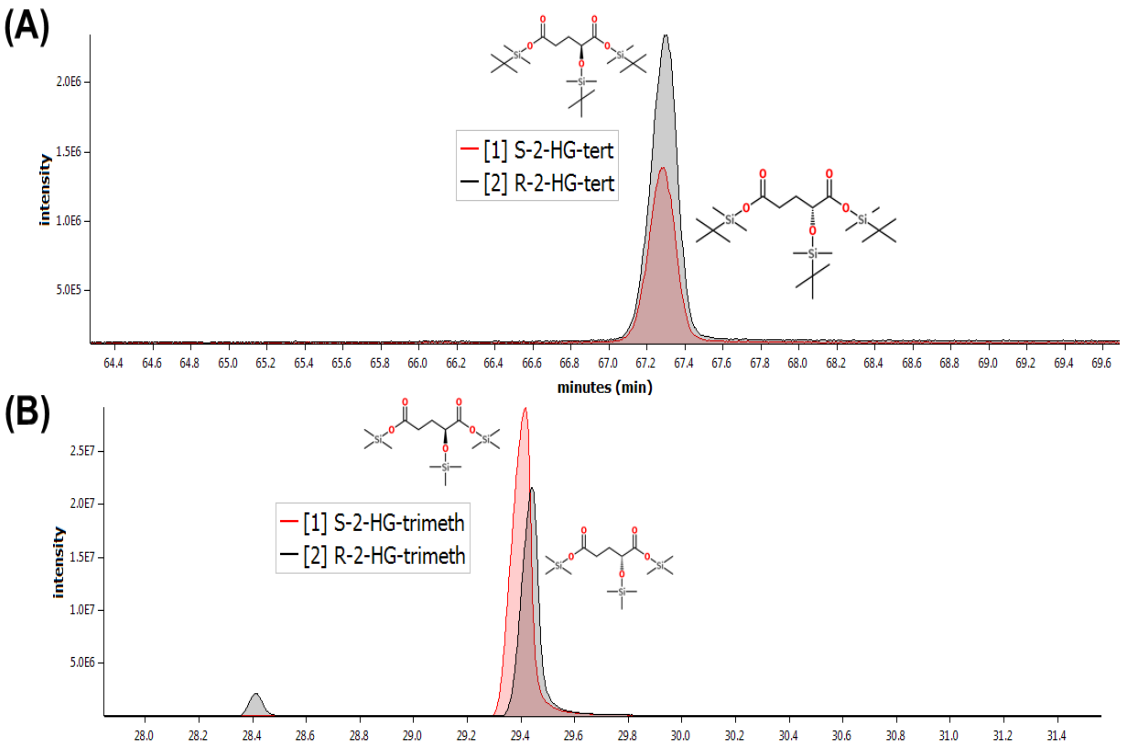

Figure 2.2. Retention time for tert-butyl derivatives (Silylation Rx 1) and trimethylsilyl derivatives (Silylation Rx 2) for each enantiomer.

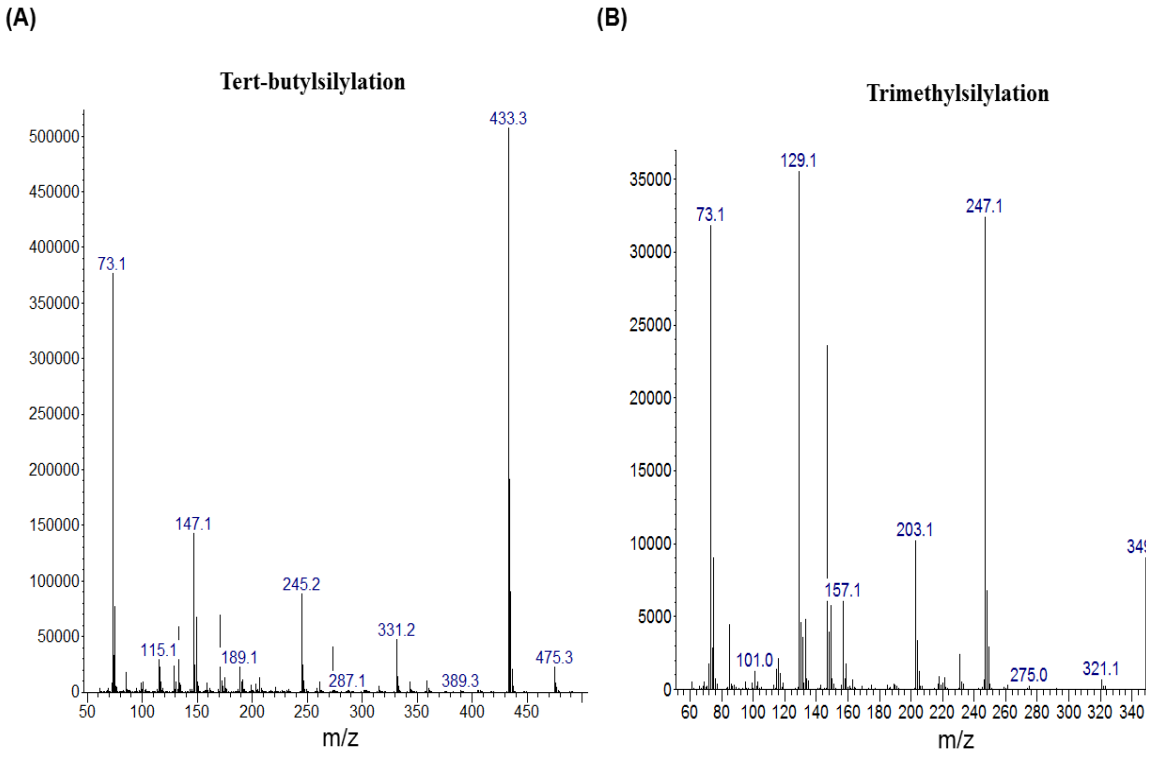

Figure 2.3. Electron ionization fragmentation of tertbutyl derivatives (A) and trimethylsilylation derivatives (B). Only fragmentation from one enantiomer is shown since the fragmentation of each enantiomer is identical

confirms that the right derivative was produced since the characteristic loss of 57 (tert-butyl group) to an m/z of 433.1 occurred from the 490.3 Da parent. Derivatives with only a trimethylsilyl group added (Silylation Rx 2) are less bulky compared to the tert-butyl silyl groups but only a slight difference was observed in the separation of enantiomers at roughly 29.40 min (Figure 2.2B). Again, the EI fragmentation patterns of each enantiomer were identical (Figure 2.3B). The characteristic loss of 15 m/z for this derivative was observed at 349.1 m/z where the parent compound has a monoisotopic mass at 364.1 Da.

Esterification reactions produced derivatives that were baseline-separable on the chiral column (Figure 2.4A). Both reactions also produced the fragmentation pattern as shown in Figure 2.4B. Each esterification reaction procedure produced comparable results

in regard to signal-to-noise and efficiency. However, even though the MCF derivatization procedure (as outlined in the methods section) does not require an incubation period, it is significantly more laborious and requires the use of hazardous materials such as chloroform and pyridine. Therefore, derivatization with the (TMS)DAM reagent was selected as the reagent of choice for the volatilization of 2-hg metabolites for the rest of the work presented herein.

Derivatization conditions, such as time (Figure 2.5A) and temperature (Figure 2.5B), can also be varied to further increase derivatization signal for serum extracts. Influence of time and temperature were investigated using sera extracts to account for the abundance of other metabolites extracted from sera with 2-hg. Time had a modest effect on derivatization at 60 minutes but drastically increased signal at 90 minutes. Increases in temperature also correlated to an increase in signal. Given that 30 minutes at room temperature provided sufficient signal to noise and that the goal of the assay was to be as efficient as possible, no heat or extended time was used for the rest of the experiments presented herein. In summary, derivatization with (TMS)DAM is advantageous as it does not require heat and only small quantities of reagent are needed to produce a significant methyl ester product. Furthermore, the chiral center is not modified during (TMS)DAM derivatization (Figure 2.6), avoiding the racemization that occurs with chiral derivatization reagents such as DATAN and (R)-(—)-2-butanol.

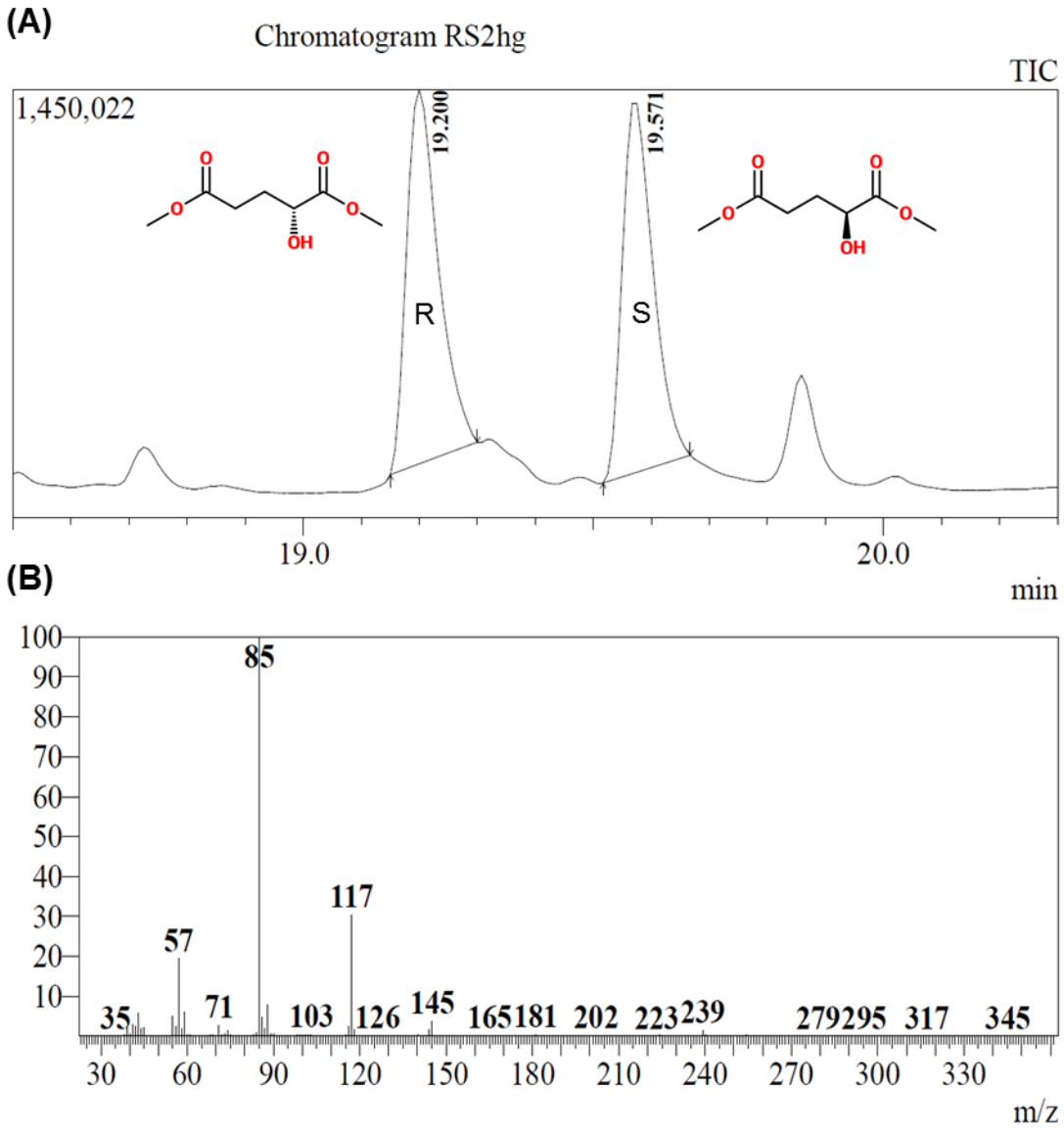

Figure 2.4. Separation of products from esterification reaction 1 & 2 (A) and the resulting EI fragmentation pattern (B). The products from each reaction were identical, as expected.

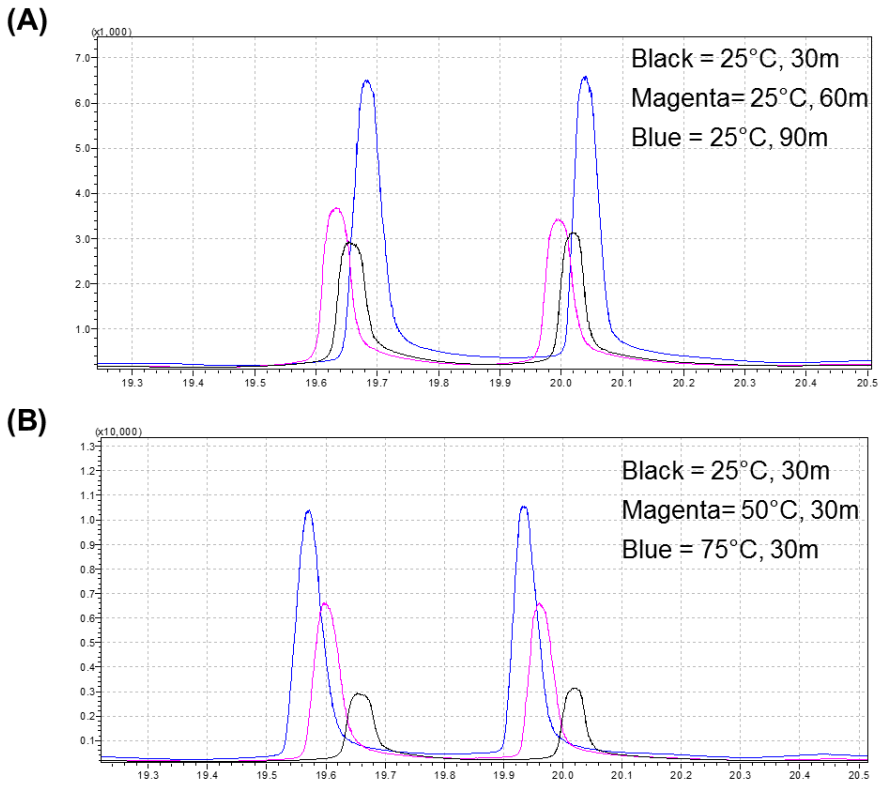

Figure 2.5. 2-hg enantiomer signal from varying derivatization time (A) and temp. (B)

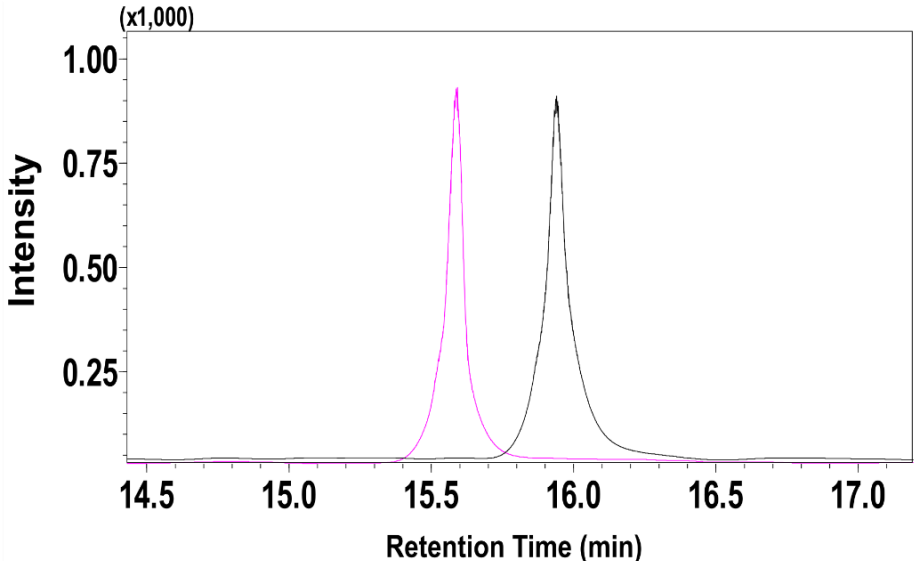

Figure 2.6. A superimposed chromatogram of separate runs of derivatized R-2-hg (magenta) and S-2-hg (black) standards demonstrating the absence of racemization.

Differentiation of 2-hydroxyglutarate enantiomers and its lactones by GC-MS/MS

EI FRAGMENTATION PATTERNS OF 2-HG, STABLE ISOTOPE LABELED 2-HG, AND 2-HG LACTONE

EI mass spectra of 2-hg and 2-hg labeled with either deuterium or ^{13}C were obtained by GC-MS (Figure 2.7A-2.7C). The EI spectrum of 2-hg has dominant peaks at 117, 85, 57, and 29 *m/z*, with 85 *m/z* shown as the base peak. Mass spectra of labeled compounds displayed an identical fragmentation pattern with major peaks at 120, 88, 60, and 32 *m/z* for the deuterated 2-hg compound and 121, 89, 60, and 31 *m/z* for the ^{13}C-labeled compound. Peaks at 85, 57, and 29 *m/z* were also observed for the 2-hg lactone, but the 117 *m/z* fragment was noticeably absent suggesting that the 117 fragment is unique to the linear 2-hg compound (Figure 2.8). Using the fragments obtained from each EI spectra, the molecular formulae and structures of the unlabeled 2-hg fragments were then determined by the comparison of isotopologue fragments (Table 2.1).

Compound	**M+· (*m/z*)**	**Major EI Fragment 1 (*m/z*)**	**Major EI Fragment 2 (*m/z*)**	**Major EI fragment 3 (*m/z*)**	**Major EI Fragment 4 (*m/z*)**
2-hg	176	117	85 (BP)	57	29
Deuterated 2-hg	179	120	88 (BP)	60	32
^{13}C-labeled 2-hg	181	121	89 (BP)	60	31
2-hg lactone	144	--	85 (BP)	57	29

Table 2.1. Isotopologue m/z peaks from EI of 2-hg, labeled 2-hg compounds, and the lactone of 2-hg. Base Peak (BP).

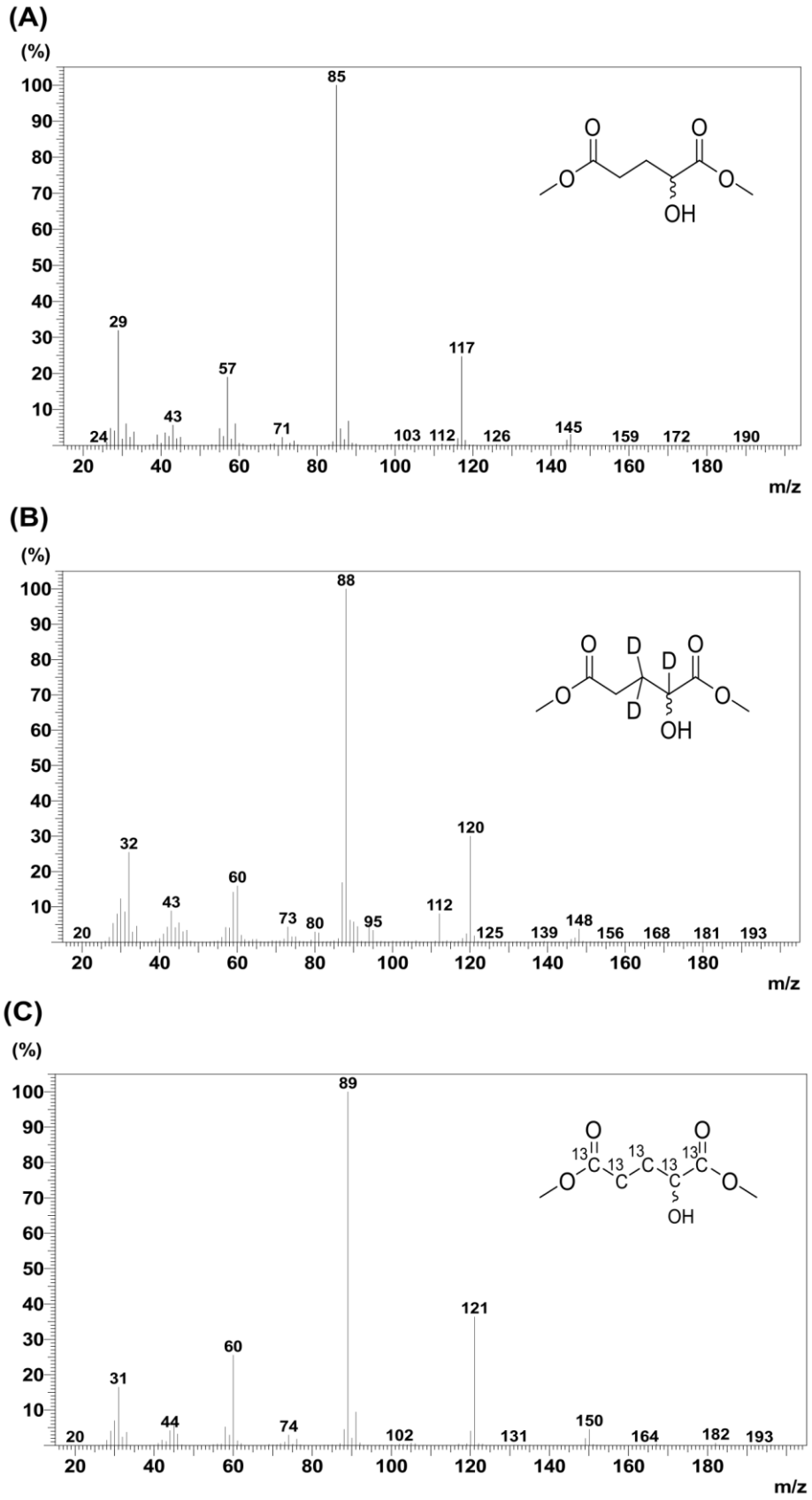

Figure 2.7. EI-MS spectra of 2-hg (A), Deuterated 2-hg (B), 13C-labeled 2-hg (C)

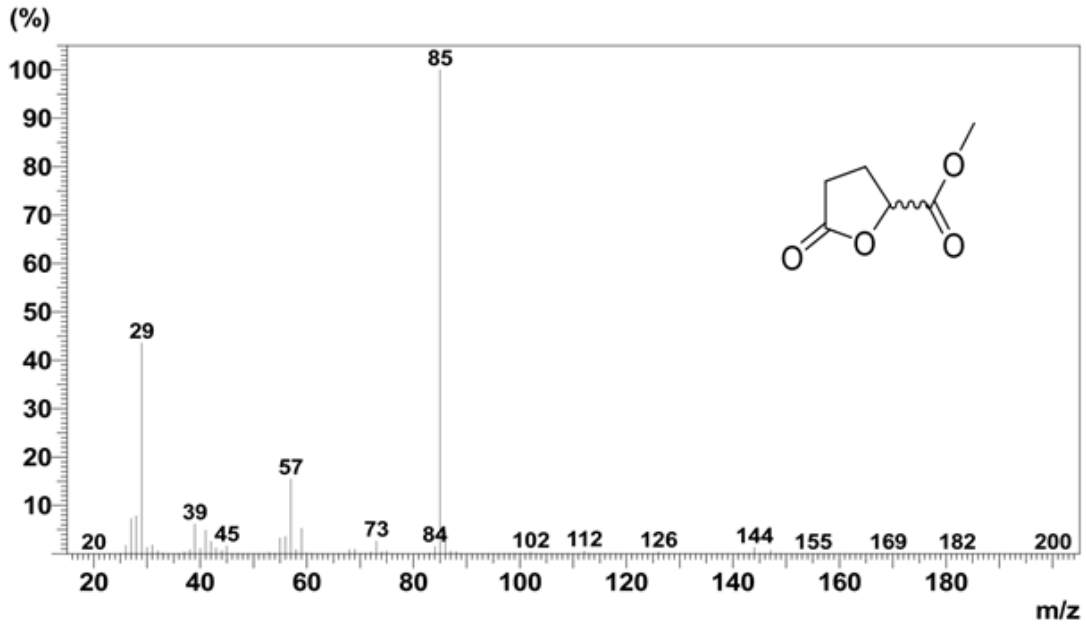

Figure 2.8. EI-MS spectra of 2-hg lactone

117 m/z fragment

A fragment at M^+-59 indicates a loss of a methyl ester group ($COOCH_3$) by inductive cleavage. This observation was confirmed by the peak shifts observed in the labeled 2-hg compounds. The deuterated 2-hg compound had a peak at 120 *m/z* (a shift of 3 *m/z*), indicating that the 3 inner carbons with deuterium atoms were still intact. The ^{13}C-labeled 2-hg compound fragmented to 121 *m/z* (a shift of 4 *m/z*), indicating that one of the two carbons lost was unlabeled. Since only the methyl groups added by derivatization contained unlabeled carbons, the fragment lost was indeed one of the two methyl ester functional groups. The specific methyl ester lost was dictated by the species that formed after fragmentation. As shown in Figure 2.9, the ester adjacent to the chiral hydroxyl group forms a secondary carbocation, ion ***a***, and is favored over fragmentation of the opposite ester since a primary carbocation, ion ***a'***, transpires [65]. The 117 *m/z* fragment then has the molecular formula $C_5H_9O_3$ and has the proposed structure designated by ion ***a***. Isotopologue fragment structures for the deuterated and ^{13}C-labeled 2-hg compounds are shown in Figure 2.10 and Figure 2.11, respectively.

85 m/z fragment

The 85 *m/z* peak corresponds to a molecular formula of $C_4H_5O_2$ (-$C_3H_7O_3$, -91 *m/z*) as the deuterated 2-hg compound had a 3 *m/z* shift to 88 *m/z* and the ^{13}C-labeled 2-hg compound, a 4 *m/z* shift to 89 *m/z*, indicating that the remaining methyl ester was lost. A loss of a carbon other than the methyl ester would result in a different shift in *m/z*. The structure of a $C_4H_5O_2$ 2-hg fragment was previously thought to be a cyclic fragment (ion ***b'***) since the lactone form was thought to be the dominant form of 2-hg (Figure 2.9) [47], [48]. However, given that the lactone does not have a 117 *m/z* fragment (Figure 2.8), a different, linear structure is likely. As represented by ion ***b***, we propose then that the 85 *m/z* fragment was the result of methanol elimination from ion ***a*** (Figure 2.9). Ion ***b*** then is

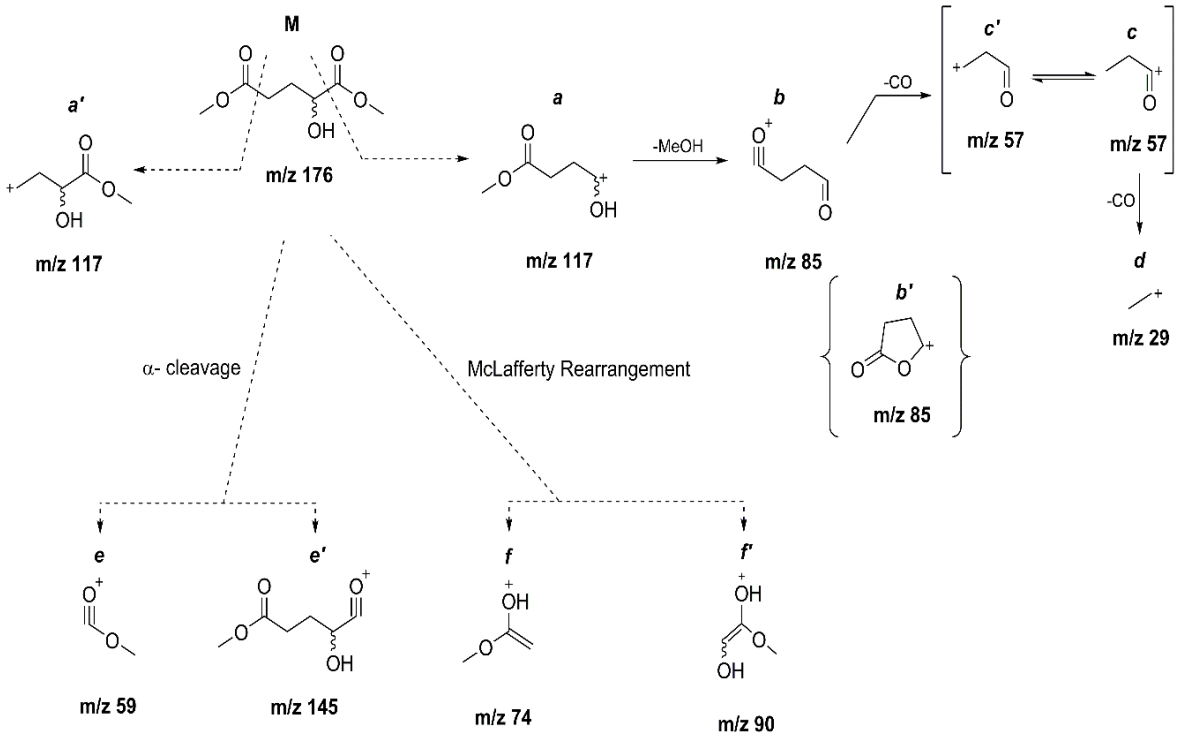

Figure 2.9. Ion structures of derivatized 2-hg after electron ionization. Both observed and theoretical structures are shown with an ion label above and the m/z below.

a 4-carbon chain with an aldehyde on one end, and a carbon-oxygen (C-O) triple bond on the other end.

57 m/z fragment

The deuterated 2-hg compound still had a 3 *m/z* shift to 60 *m/z* but the ^{13}C-labeled compound lost a second labeled carbon resulting in a compound with three labeled ^{13}C carbons at 60 *m/z*. Given that the 85 *m/z* fragment was the result of secondary fragmentation, the 57 *m/z* fragment follows from the subsequent loss of one of the carbon-oxygen bonds of ion ***b*** to ion ***c'*** (Figure 2.9). Since the aldehyde carbon is deuterated and no deuterated carbons were lost, the C-O triple bond was most likely lost resulting in the structure shown in ion ***c'***. However, following fragmentation, a hydride shift likely occurred to form ion ***c*** since the rearrangement results in a secondary carbocation and a fragment with the molecular formula of C_2H_5, the significance of which is explained below for the 29 *m/z* fragment.

29 m/z fragment

Further secondary fragmentation of 57 *m/z* results in the loss of the aldehyde C-O bond to give a 29 *m/z* fragment with the molecular formula C_2H_5 as indicated by ion ***d*** (Figure 2.9). A shift of 3 *m/z* and 2 *m/z* was observed for both the deuterated and the ^{13}C-labeled 2-hg compound, respectively, indicating the loss of one deuterated carbon and three ^{13}C-labeled carbons. Therefore, C_2H_5 is confirmed to be the only possible molecular formula possible since the other possible molecular formula, COH, would only have a shift of 1 *m/z* to 30 *m/z* for both the deuterated and the ^{13}C-labeled compounds. A hypothetical COH fragment could occur if a hydride shift of ion ***c*** did not occur prior to the aldehyde fragmentation.

Additional EI fragments

Other expected EI fragments for dimethyl esters were either low in abundance or not observed at all (Figure 2.9). Alpha cleavage products, 59 *m/z* (ion ***e***) and 145 *m/z* (ion

e'), are fragments commonly observed in EI fragmentation of esters but were either not observed or only minor products of the acyclic 2-hg compound. Additionally, McLafferty rearrangement products, which are significant EI fragments for compounds with an ester and a γ-hydrogen, were not observed [66]. Figure 2.9 shows the absent McLafferty fragment structures at 74 *m/z* (ion ***f***) and a 90 *m/z* (ion ***f'***). Finally, the precursor ion (M+·) was also low in abundance for the lactone at 1.55% (144 *m/z*) but was not detected at all for the acylic compound (176 *m/z*), which is common for EI fragmentation of methyl esters [66].

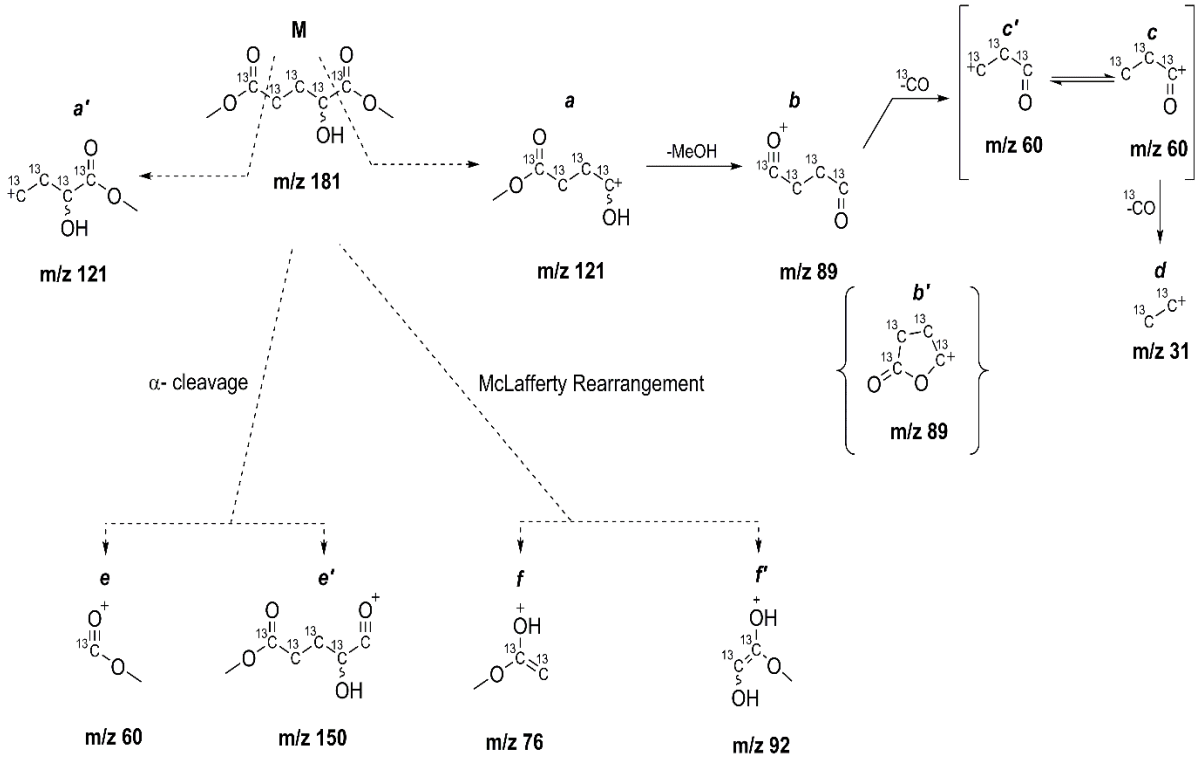

Figure 2.10. Ion structures of derivatized deuterated 2-hg (A) and 13C-labeled 2-hg (B) after electron ionization. Both observed and theoretical structures are shown with an ion label corresponding to that given for the unlabeled fragments shown in Figure 2.9.

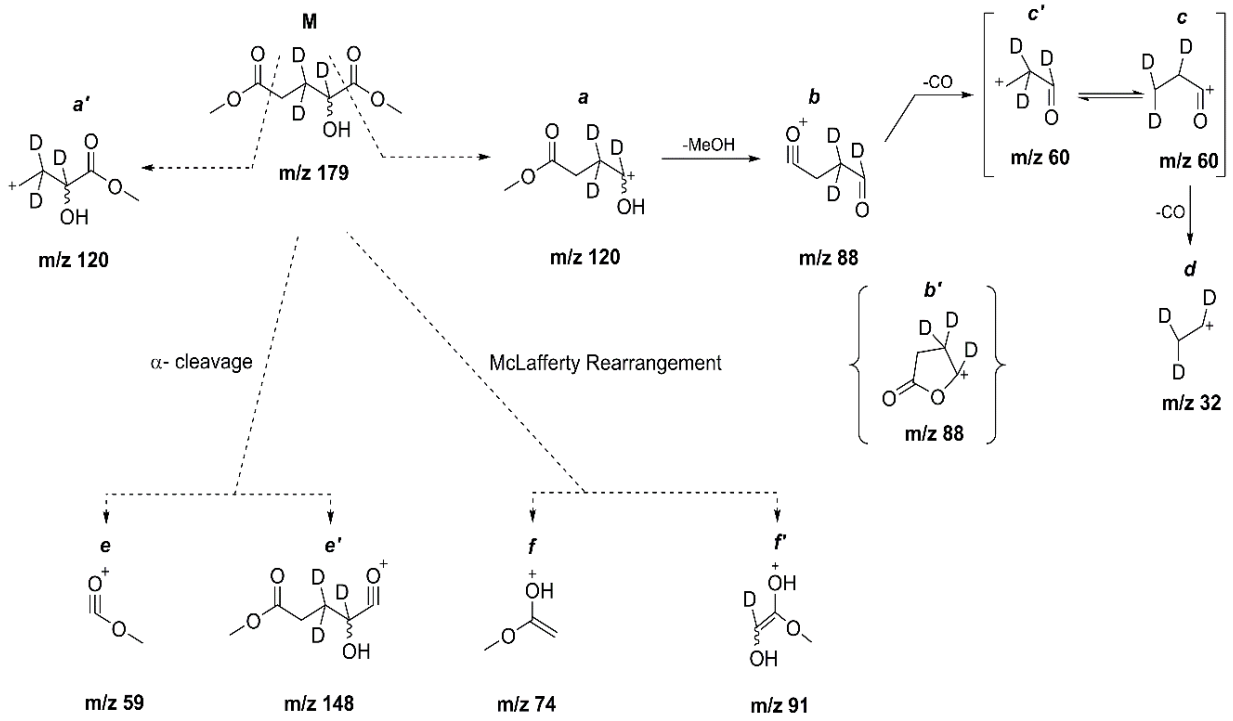

Figure 2.11. Ion structures of derivatized deuterated 2-hg (A) and 13C-labeled 2-hg (B) after electron ionization. Both observed and theoretical structures are shown with an ion label corresponding to that given for the unlabeled fragments shown in Figure 2.9.

VERIFICATION OF 2-HG FRAGMENTATION BY MS/MS

Product ion analysis of the 85 *m/z* and 117 *m/z* fragments were obtained to verify that the majority of the fragments observed were due to secondary fragmentation. Indeed, the major product ions of 85 *m/z* were 57 and 29 *m/z*, while 117 *m/z* fragmented to 85, 57 and 29 *m/z* (Figure 2.12A-2.12B). Thus, only the 117 *m/z* is a direct result of EI fragmentation while 85, 57, and 29 *m/z* are secondary fragments.

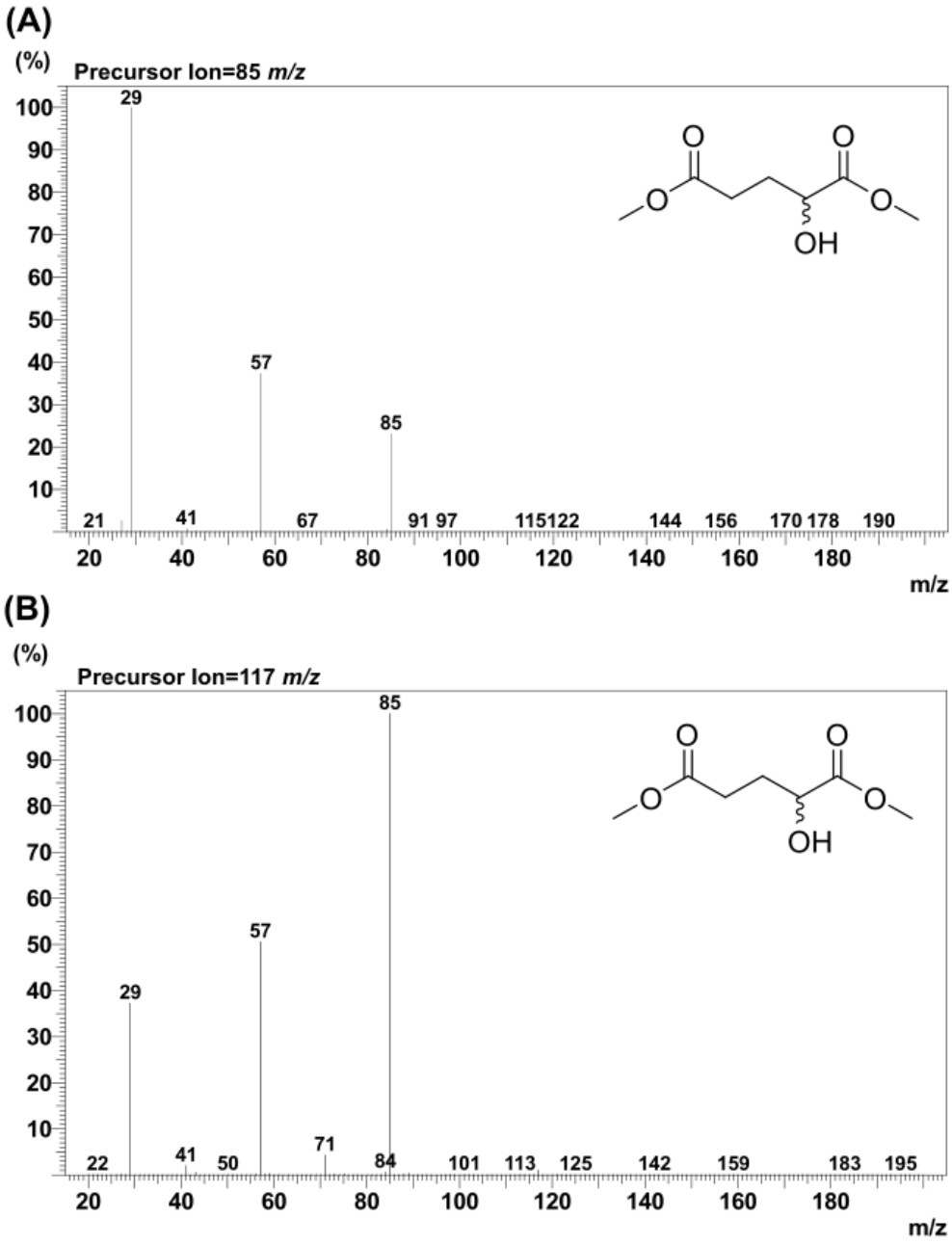

Figure 2.12. Product ion scan of derivatized 2-hg with the precursor ion set at 85 m/z (A) and 117 m/z (B).

The same experiment was repeated for the 2-hg lactone, confirming that 117 *m/z* was not a major fragment of the 2-hg lactone and that 85, 57, and 29 *m/z* were shared fragments with the acyclic compound (Figure 2.13A-2.13B). Some studies advocate for the use of high-resolution GC-MS, such as GCTOFMS/GCOrbitrap, to have unambiguous identification of fragments [67]–[69]. Though imperative with larger and more complex molecules, the extra resolution would not provide any additional data given that the typical fragments observed and expected for 2-hg methyl esters did not result in fragments close in *m/z*, nor would the analysis benefit from the determination of mass defect differences.

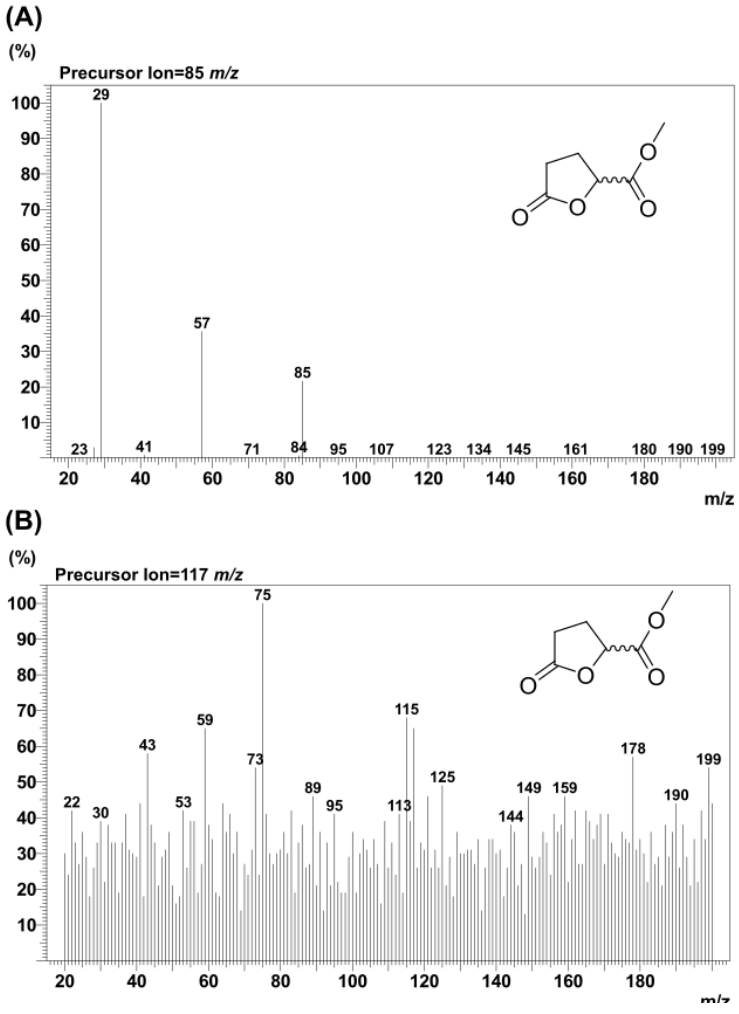

Figure 2.13. Product ion scan of derivatized 2-hg with the precursor ion set at 85 m/z (A) and 117 m/z (B).

DIFFERENCES IN THE FRAGMENTATION MECHANISM OF 2-HG AND 2-HG LACTONE

To explain the similarities and differences in EI fragmentation between 2-hg and its lactone, we propose the following EI fragmentation mechanisms. The dimethyl ester of 2-hg initially loses one methyl ester group by induction cleavage followed immediately by methanol elimination to form ion ***b*** (Figure 2.14). The lactone characteristically loses its only methyl ester, also to $C_4O_2H_5$ 85 *m/z*, but in a cyclic configuration as shown by ion ***b'*** (Figure 2.14). There is no feasible EI fragmentation mechanism that can result in a 117 *m/z* fragment from the 2-hg lactone. The cyclic 85 *m/z* fragment has a resonant structure with the positive charge on the oxygen heteroatom (ion ***b''***) that can subsequently break into a linear $C_4O_2H_5$ compound, analogous to ion ***b***. The resulting acyclic $C_4O_2H_5$, 85 *m/z* compound then fragments into 57 and 29 *m/z* as explained previously.

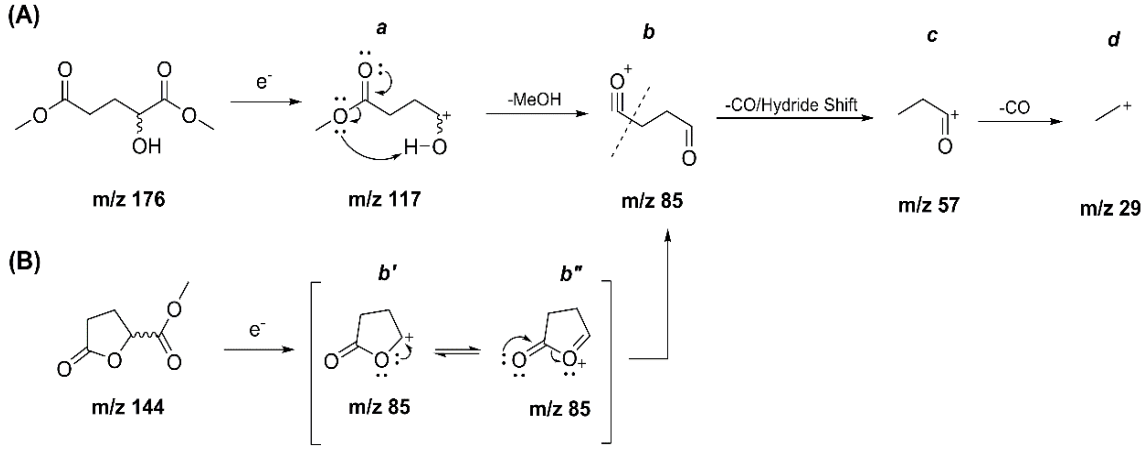

Figure 2.14. Similarities and differences in the EI fragmentation mechanism of 2-hg and its lactone, 5-OTFCA. The lactone has a cyclic structure at 85 m/z which can also undergo secondary fragmentation in the same pathway as the acyclic 2-hg compound.

DETECTION OF 2-HG ENANTIOMERS AND THEIR CORRESPONDING LACTONES IN SERUM & URINE

A prior study using a β-cyclodextrin capillary GC column reported that an unspecified lactone enantiomer eluted prior to the elution of the linear 2-hg enantiomers [38], [48], [57]. Using (R) & (S)-5-OTFCA standards, we have observed that (S)-5-OTFCA elutes at 15.85 min, prior to the 2-hg enantiomers at 16.42 min (R-2-hg) and 16.75 min (S-2-hg) (Figure 2.15). However, (R)-5-OTFCA elutes at 16.45 min and is not resolved from the R-2-hg peak. The minor/shoulder peak in the lactone samples at 15.95 min is superfluous and does not have any fragment ions of 2-hg or the 2-hg lactone (Figure 2.16). Thus, given the co-elution and the similarity in EI fragmentation of R-2-hg and its enantiomer, prior studies aiming to detect R-2-hg in serum and urine could have had confounding results.

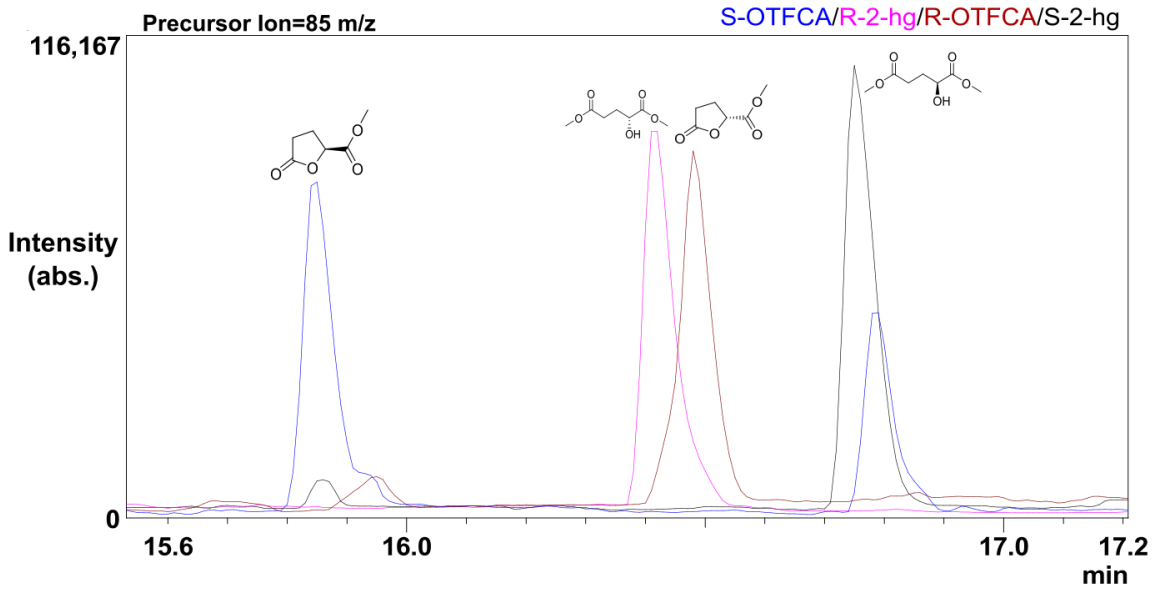

Figure 2.15. Overlay chromatogram of both acyclic and cyclic 2-hg enantiomers showing the separation of each set of enantiomers. The chromatogram was obtained by product ion scans using 85 m/z as the precursor ion. R-2-hg and R-OTFCA significantly overlap demonstrating that an ion unique to the acylic compound must be monitored.

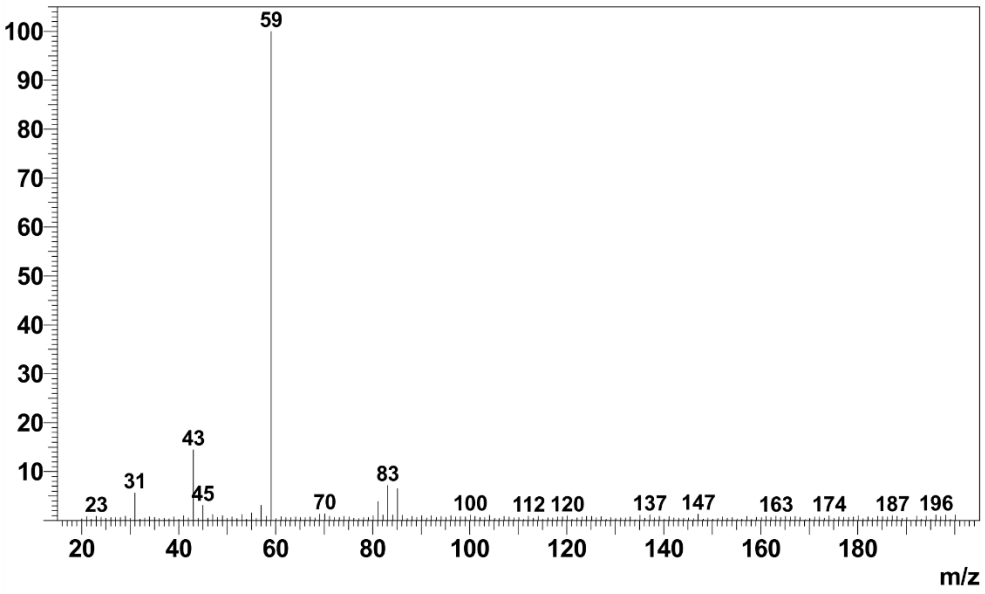

Figure 2.16. Product ion analysis of 15.95 min peak from Figure 2.15. Fragments ions indicate that this peak is a separate compound that elutes next to the S-2-hg lactone.

In order to circumvent the above problem, an MRM method was built to detect and differentiate 2-hg and its lactone based upon the unique 117 *m/z* fragment found only in the linear 2-hg compound. The MRM transition 117 *m/z* > 85 *m/z* was used to detect the linear dimethyl ester forms of 2-hg, and a second MRM transition 85 *m/z* > 29 *m/z* (not unique to the dimethyl ester) was used as a qualifier transition to verify true detection of 2-hg. The MRM method collision energies were optimized by monitoring transition signal for each transition as a function of the collision energy (3 to 30 V). The results of the optimization are shown in Figure 2.17. Other potential transitions (85 *m/z* > 57 *m/z*) and (117 *m/z* > 29 *m/z*) were also plotted as other potential transitions to monitor. The secondary transitions did not produce as strong signal (when not-normalized) as the 117 *m/z* > 85 *m/z* and 85 *m/z* > 29 *m/z* transitions and were therefore not used. The optimal collision energy for the 117 *m/z* > 85 *m/z* transition and 85 *m/z* > 29 *m/z* was found to be 13 V and 6 V, respectively, for each enantiomer (Figure 2.17).

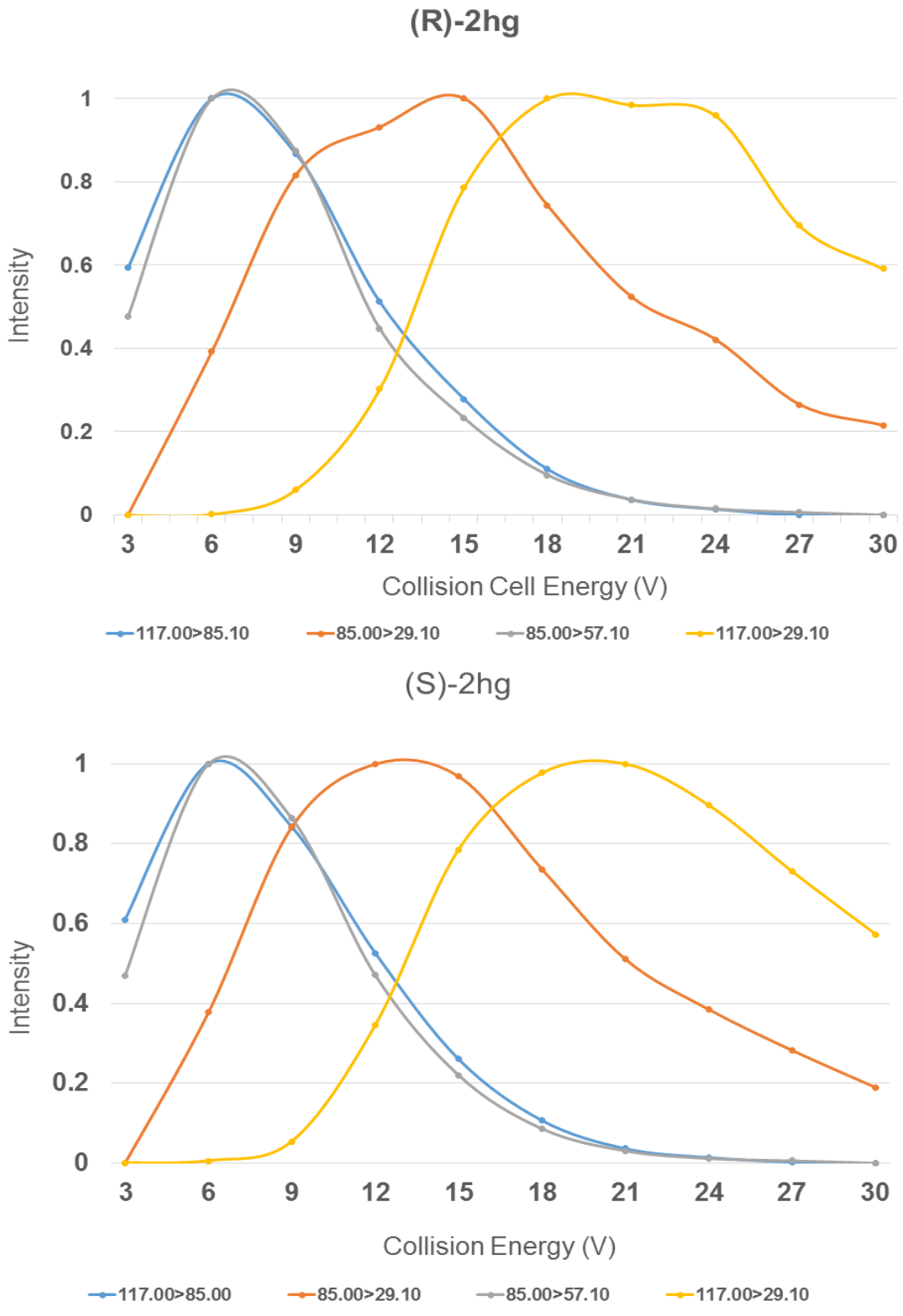

Figure 2.17 Collision energy optimization for each MRM transition

The MRM method was then used to detect 2-hg enantiomers in serum (Figure 2.18A) and urine (Figure 2.18B). Separation of detection of basal levels of 2-hg enantiomers was achieved in both biological fluids with a signal-to-noise ratio greater than 20:1. The range of 2-hg enantiomer lactones varied in abundance according to the sample type, with the urine having the most notable difference in lactone peaks between urine samples. A urine sample with high levels of lactone showed that the S-2-hg lactone was confirmed to be the lactone that eluted prior to the acylic 2-hg enantiomers and the R-2-hg lactone, though separate from S-2-hg lactone peak, overlapped with the linear R-2-hg molecule in the 85 > 29 *m/z* MRM analysis (Figure 2.19). The serum sample shown in Figure 2.18A demonstrates a blood sample with higher lactone peaks as compared to the rest of the serum samples analyzed.

The amount of 2-hg lactone present within each sample was quantified as follows. S-2-hg lactone was measured according to a percent ratio of the peak areas of the lactone to the linear molecule. Pure measurement of the R-2-hg lactone cannot be achieved since it co-elutes with the linear R-2-hg molecule. However, the percent differences in the ratio of R-2-hg:S-2-hg for the two MRM transitions can be used as a surrogate marker for the amount of R-2-hg lactone present since that specific lactone accounts for the majority of any observed differences in peak areas between the two transitions. The calculated levels of 2-hg enantiomer levels for the serum and urine samples are summarized in Table 2.2. S-2-hg lactone ranged from 2-26% with an average ratio of approximately 12% in serum, and from 3-20% in urine with an average of 7%. The R-2-hg lactone, as measured by the percent difference, ranged from 8-46% for serum and 13-150% for urine indicating that the R-2-hg lactone was indeed present even when it was not as obvious as shown in Figure 2.19. Altogether, though the major compounds detected in the majority of samples are the linear 2-hg enantiomers, the lactone is non-negligible in a number of samples. Thus, only

the 117 > 85 transition can reliably be used in an assay to quantitate the amount of linear 2-hg molecule present within a biological sample.

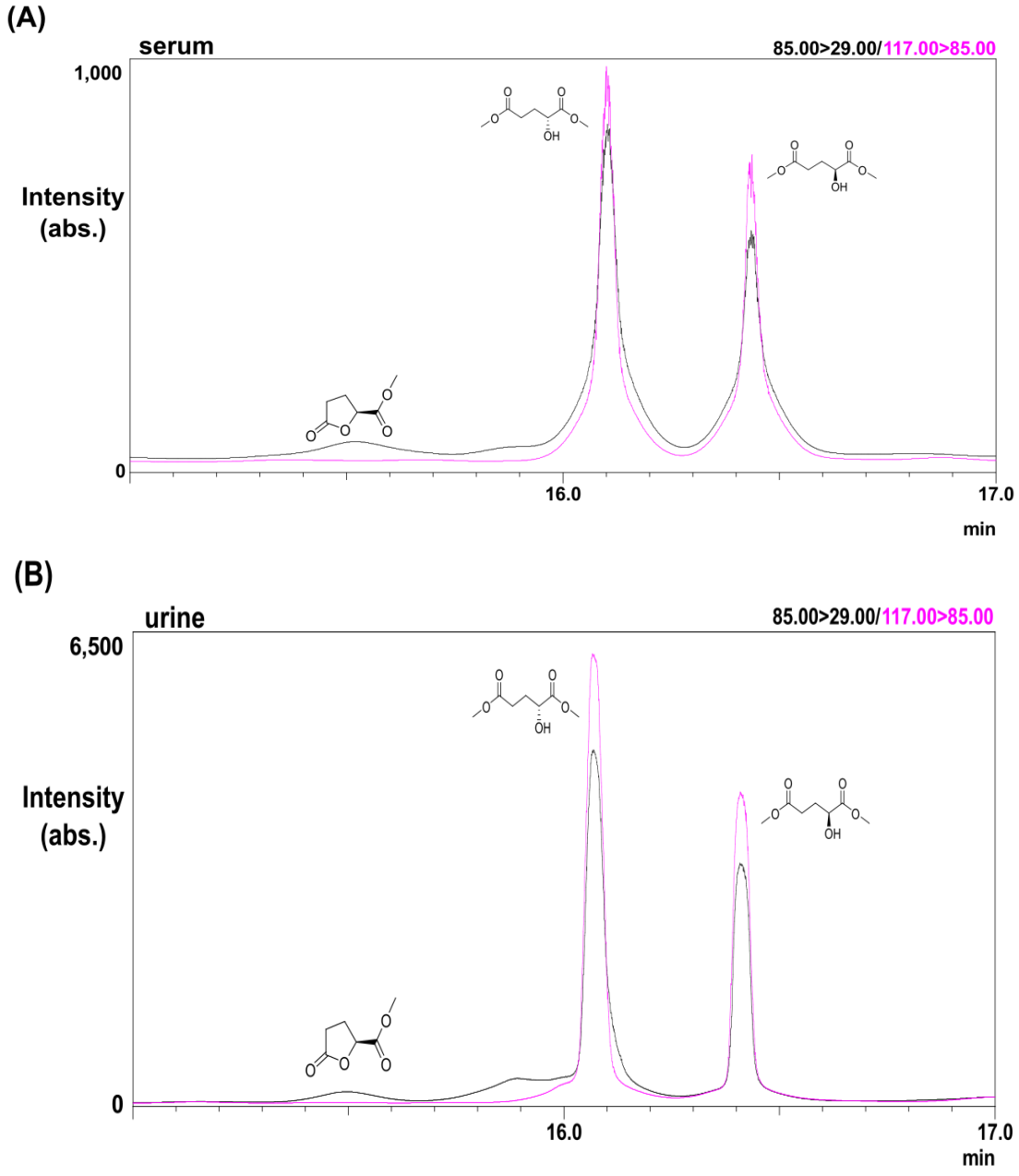

Figure 2.18. A representative chromatogram demonstrating the separation and detection of 2-hg enantiomers from serum (A) and urine (B).

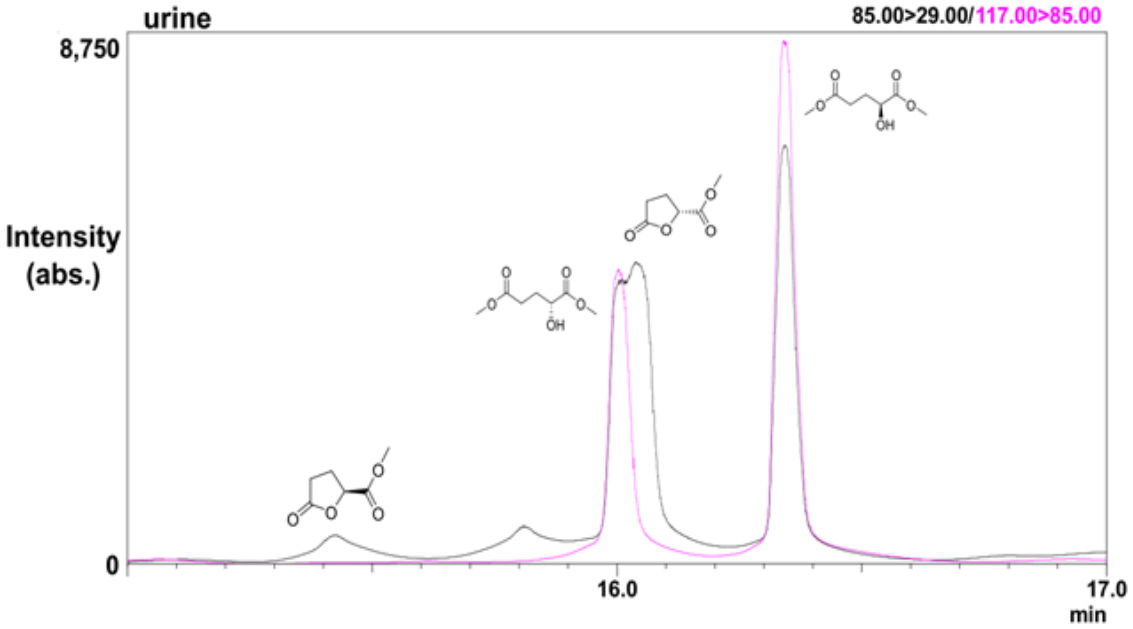

Figure 2.19. A second urine sample with a large R-2-hg lactone peak and a significant S-2-hg lactone peak is also shown

Biological Sample	R-2-hg Surrogate Marker: % Difference of 2-hg enantiomer ratios between MRM transitions	% Peak Area Ratio Lactone S-2-hg:Linear S-2-hg
Serum	8-46	2-26
Urine	13-150	3-20

Table 2.2. 2-hg lactone enantiomers detected in biological samples

Assay enhancements through the simplifying of extraction procedure

To examine whether the extraction procedure can be simplified to increase throughput, the ethyl acetate extraction protocol was modified from previous methods that were utilized for extraction of organic acids from urine [70]–[72]. The method was optimized by reducing the organic solvent volume and by eliminating an incubation step and a second solvent-solvent extraction step. Prior studies using an ethyl acetate based-

extraction method utilized ethyl acetate (EA) volumes up to 5 mL [70], [72]. The volume was reduced to 1 mL, allowing the extraction to be carried out in one glass vial, while also keeping a sufficient sample to organic solvent volume ratio (1:4). The assay was further optimized by eliminating an incubation step between the collection of the extraction layer and the subsequent centrifugation step, eliminating a drying step with sodium sulfate, and removing a second 5 mL EA re-extraction step. Repeated solvent-solvent extraction with a second 5 mL of ethyl acetate did slightly improve yield (data not shown), but the signal-to-noise from only one ethyl acetate extraction step was sufficient. Additionally, our method is advantageous over extractions using 80% MeOH at low temperatures (-80°C) by drastically reducing incubation periods. Methods using 80% MeOH can require incubation times of 6-8 hrs and also requires access to dry ice temperatures. Results of this method are shown in Figure 2.20. The signal-to-noise was sufficient and demonstrated the feasibility of reducing the extraction procedure. Overall, our method significantly improves sample preparation by reducing the number of steps and the total extraction time.

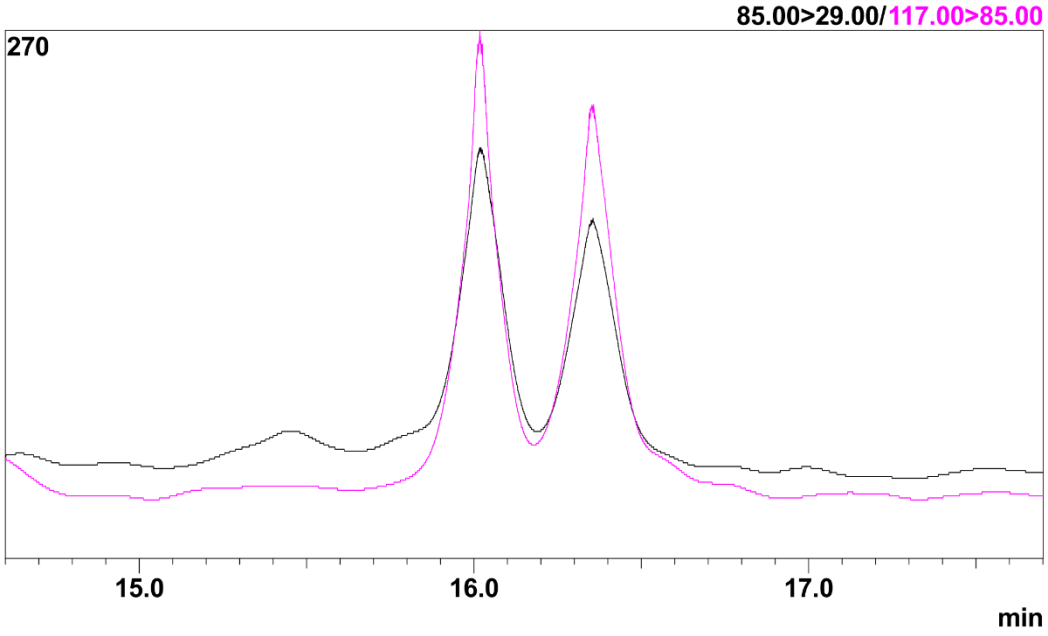

Figure 2.20. 2-hg signal using modified extraction procedure

Assay Validation

The results of the method validation are summarized in Table 2.3. A linear instrument response was observed from 35.7 fmol to 14.3 pmol injected on to the column. The assay demonstrated a high sensitivity with an IDL of 16.3 fmol for R-2-hg, 19.7 fmol for S-2-hg and a LLOQ of 71.4 fmol for both enantiomers. This is an improved sensitivity over DATAN-based LC-MS/MS methods and comparable to the method using TSPC. According to the Federal Drug Administration (FDA) guidelines for Bioanalytical Method Validation, the target accuracy for each QC sample must be within 15% with a precision ≤ 15% CV and within 20% and 20% CV at the LLoQ level [63]. All measurements of precision and accuracy for the assay fell well within the recommended target values. Intra-assay values for accuracy and precision are shown using a range as observed over the three separate days. The average inter-assay variability for all serum samples was observed to be 9.8% for R-2-hg and 10.0% for S-2-hg.

Each injection of a blank extraction, PBS, or derivatization solution resulted in no measurable signal above background for either 2-hg enantiomer. The ideal test of selectivity, specificity, and matrix effects involve a sample with and without the metabolites of interest, but to our knowledge, no serum sample exists that is void of 2-hg enantiomers. As expected by utilizing a simplified extraction protocol, the recovery was not 100% and ranged from 15.6 – 23.0% for R-2-hg and 11.1 – 21.2% for S-2-hg. However, the signal-to-noise as demonstrated in Figure 2.20 and the sensitivity and precision as shown in Table 2.3, is sufficient to counterbalance what is lost in the recovery. Additionally, FDA guidelines do not necessitate 100% recovery, only consistency and reproducible results, which the serum precision data support. Lastly, the serum samples were shown to be stable in the autosampler after 24 hrs. (1.6 ± 1.3 & 1.2 ± 0.7 %-difference) and at room temperature for up to 4 hours (6.4 ± 5.0 & 5.3 ± 5.2 %-difference) for each

enantiomer. However, four freeze-thaw cycles consistently and drastically reduced the amount of 2-hg measured by 35.8 to 40.4%.

	R-2-hg	**S-2-hg**
Linear Dynamic Range (fmol – pmol)	35.7 – 14.3	35.7 – 14.3
Limits of Detection (fmol)		
IDL	16.3	19.7
LLoQ	71.4	71.4
Accuracy (% Error)		
Intra-assay		
High QC	2.2 – 3.2	2.4 – 3.4
Mid QC	1.1 – 7.0	3.0 – 3.5
Mid-Low QC	4.2 – 5.9	3.8 – 5.7
Low QC	6.2 – 9.1	3.1 – 8.3
LLoQ	9.0 – 13.2	8.7 – 11.1
Inter-assay		
High QC	2.7	3.0
Mid QC	4.3	3.2
Mid-Low QC	5.0	4.9
Low QC	7.3	5.2
LLoQ	10.9	9.8
Precision (CV %)		
Intra-assay		
High QC	1.9 – 2.6	1.6 – 4.0
Mid QC	1.3 – 3.6	2.7 – 4.2
Mid-Low QC	2.8 – 4.1	0.7 – 2.9
Low QC	4.7 – 5.8	1.6 – 4.1
LLoQ	7.7 – 9.6	7.3 – 11.1
Inter-assay		
High QC	2.3	3.0
Mid QC	2.6	3.3
Mid-Low QC	3.4	2.0
Low QC	5.2	3.2
LLoQ	8.8	9.7
Serum	9.8	10.0
Selectivity/Specificity		
PBS/Blank Extraction/Derivatization Solution	No signal	No signal
Recovery (%)		
High QC	15.6 ± 6.9	11.1 ± 6.8
Mid QC	18.9 ± 3.8	17.1 ± 4.6
Low QC	23.0 ± 1.9	21.2 ± 1.2
Stability (% Difference)		
24-hour autosampler	1.6 ± 1.3	1.2 ± 0.7
4-hour at Room Temp.	6.4 ± 5.0	5.3 ± 5.2
Freeze-Thaw x 4	35.8 ± 5.7	40.4 ± 9.3

Table 2.3. GC-MS/MS Validation

CONCLUSIONS

A GC-MS/MS assay to separate and detect 2-hg enantiomers in serum and urine was developed. The extraction, derivatization, and detection parameters were optimized to improve efficiency while simultaneously eliminating racemization and maintaining a sufficient signal-to-noise ratio. The assay was also shown to be robust and reproducible and was demonstrated to be more sensitive than the commonly used DATAN LC-MS/MS assay. Furthermore, the GC-MS/MS can differentiate between 2-hg lactone enantiomers while also separating the acyclic 2-hg enantiomers. This was accomplished by fully describing the unique EI fragmentation pathways for both 2-hg and the 2-hg lactone.

Chapter 3: Gas Chromatography-Vacuum Ultra-Violet (VUV) Spectroscopy of 2-hg enantiomers

INTRODUCTION

Disadvantages of MS for quantification

Although MS-based methods for detection of 2-hg have proven useful, there are several major disadvantages of using this technique. First, mass-to-charge (m/z) peaks acquired on a mass spectrometer show relative intensities between ions of a sample. To quantify a peak, an internal heavy-isotope standard must be used. For example, to quantify R-2-hg in a biological sample, a deuterium-labeled standard of R-2-hg of known concentration must be spiked into the sample during sample preparation, prior to MS analysis. The intensity of the measured heavy 2-hg can then be compared to the endogenous levels of 2-hg within the sample to determine the concentration of endogenous 2-hg. This is called stable isotope dilution mass spectrometry. In order to quantify every analyte of interest, a heavy isotope internal standard must be purchased or, if not available, synthesized de novo for every compound of interest. Secondly, to measure an analyte by mass spectrometry, it must be ionized before detection. Ionization methods in mass spectrometry is an extensive topic discussed elsewhere [73]. Briefly, for GC-MS, a molecule is fragmented via electron ionization (EI) or chemical ionization (CI), and the resulting fragmentation pattern can be used to uniquely identify a molecule. In LC-MS, a sample in solution is exposed to a voltage (electrospray ionization, ESI), or hit with a laser after embedded in a matrix (matrix-assisted laser desorption ionization, MALDI). Different molecules are more susceptible to different ionization methods, and with the added need to analyze both positive and negative ions, an inherent variability can exist from sample to sample when using MS-based methods [73]. A method, such as VUV spectroscopy

(described below) that avoids the pitfalls of MS-based methods would greatly improve the tools available for analytical chemistry of biological samples, such as 2-hg.

Vacuum Ultraviolet (VUV) Spectroscopy

Vacuum ultraviolet (VUV) spectroscopy is based upon the property that chemical compounds absorb strongly within the VUV range, 115-185nm [74]. Historically, VUV absorption spectra have been acquired using synchrotrons, which are large particle accelerators that emit circularly polarized light in the VUV range as they are accelerated and bent [75]. Recently, a detector (VUV Analytics, Austin, TX) has been designed to detect absorption of photons emitted from a deuterium lamp within the VUV range [74]. Instead of requiring a >$100 million synchrotron facility, this technology allows tabletop acquisition of VUV spectra. VUV photons have a higher energy than UV photons and are able to be absorbed by the sigma (σ) and pi (π) bonds which produce a unique absorption spectrum [74].

As shown in Figure 3.1, compounds from a GC are transferred to the VUV flow cell where optical lenses and a charge couple device detect light transmitted through the analytes of interest to collect an absorption spectrum. There are several major advantages of the VUV detector as compared to an MS detector. First, each absorption spectrum is unique to each compound and can serve as a fingerprint to identify a compound. Isomers also absorb VUV light and produce unique VUV absorption spectra that can be used to distinguish one isomer from another. Therefore, isomeric compounds which are invisible to conventional mass spectrometry methods can be distinguished using VUV spectroscopy. As demonstrated in Figure 3.2, 1-naphthol has a unique absorption spectrum as compared to 2-naphthol, demonstrating that a VUV detector can be used to distinguish between constitutional isomers. Secondly, heavy isotope internal standards are not needed to quantify a compound. Quantitation for the VUV detector is based upon the beer-lambert law which states that the absorption is directly proportional to the concentration of the

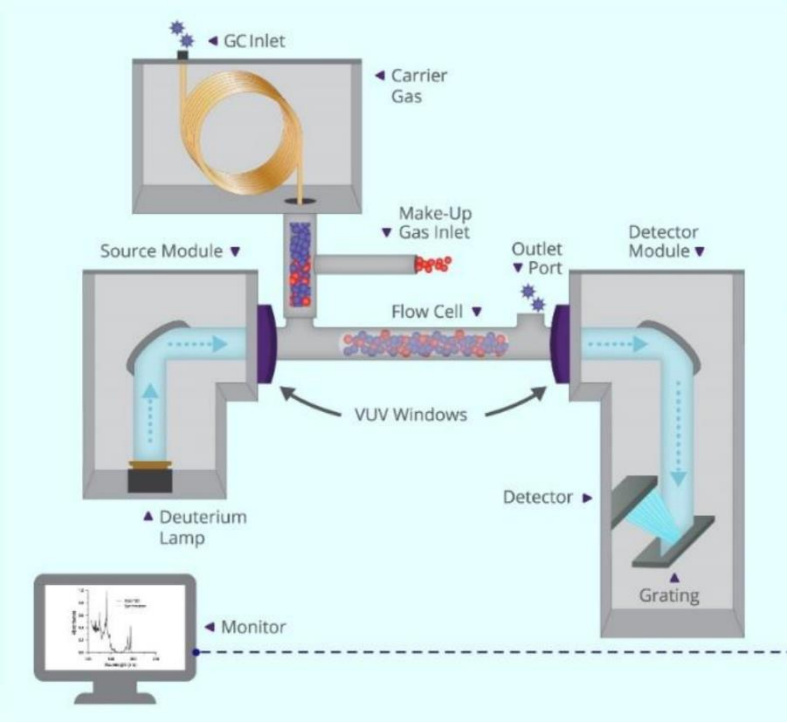

Figure 3.1. GC-VUV schematic. Image was copied from commons.wikimedia.org under the Creative Commons Attribution-Share Alike 4.0 International license. Author: Patfacts

absorbing species [76]. A compound, at various concentrations, can then be used to obtain a standard response curve. As a result, quantitation can be performed using the shape of the absorption spectrum and the area of the chromatography elution peak. Lastly, VUV does not require the use of ionization. This is advantageous as some molecules are inherently difficult to ionize, including 2-hg [40]. Furthermore, since VUV detection is a non-destructive, mass-sensitive detector, the residence time within the flow cell can be easily adjusted to maximize signal. VUV limits of detection are comparable to some mass spectrometry modes (such as selected ion monitoring MS) with sensitivities reported as ~10-200 picograms for compounds like benzene, nicotine, and methanol [74]. However, GC-MS can be more sensitive, depending upon the application. Another disadvantage of this method is that every analyte requires a standard reference spectrum that must be entered into the reference library. Without a reference spectrum, a compound cannot be

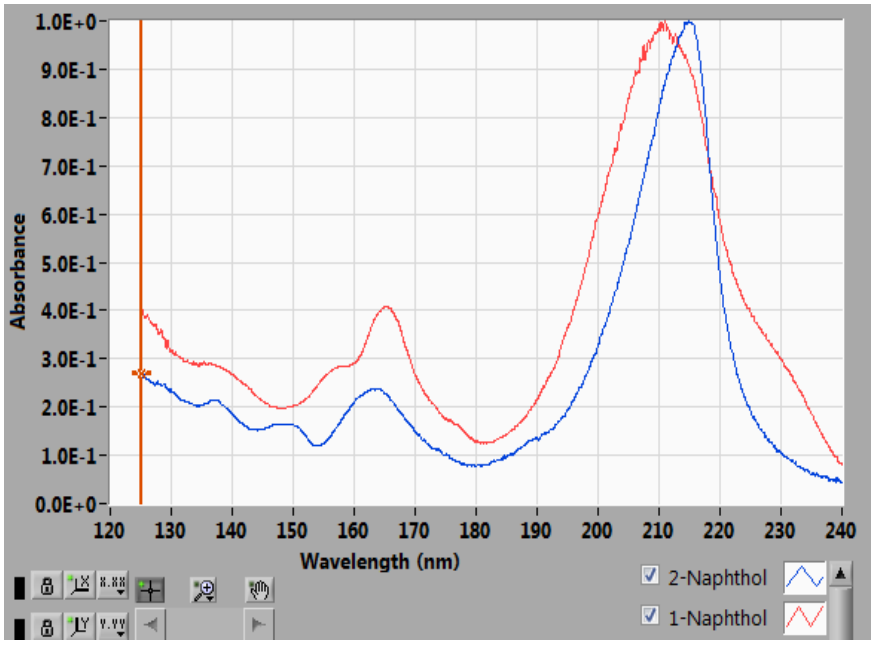

Figure 3.2. Difference in absorption spectra of 1-Naphthol and 2-Naphthol. Spectra were taken from publicly available spectra in the library of VUV data viewer software

identified, and de-convolution of co-eluting compounds is not possible. The use of VUV in a complex biological sample has yet to be demonstrated. However, published studies have shown that the utility of a VUV detector is extensive.

Our preliminary data (Figure 3.3), along with published work on pesticides [57], fatty acid methyl esters [58], and diesel fuels [59, 60], has collectively shown the ability to distinguish isomers within the VUV range. Co-eluting compounds can also be differentiated by taking the resulting absorption spectrum and deconvoluting the spectrum using an established library of known compounds. The ability to distinguish co-eluting isobaric compounds without the use of any chiral derivatives, or chiral columns, provides a complementary analysis of organic metabolites like 2-hg.

METHODS

Chemicals and Reagents

24(S)-hydroxycholesterol (24-OH Chol), 25-hydroxycholesterol (25-OH Chol), and 27-hydroxycholesterol (27-OH Chol), cholesterol (chol), pregnenolone (preg), trans-Dehydroandrosterone (t-DHA), and testosterone (test) were purchased from Avanti Lipids (Alabaster, AL). 1mM stock solutions of Uracil (U), thymine (T), cytosine (C), 5-hydroxymethyluracil (5hmU), 5-hydroxymethylcytosine (5-hmC), 5-fluorouracil (5-FoU), 5-FluoroCytosine (5-FoC), 5-carboxyUracil (5caU), 5-carboxycytosine (5caC), 6-carboxycytosine (6-caC) and the 15-Nitrogen labeled counterparts were a gift from The Lawrence Sowers lab at UTMB (Galveston, TX). LC-MS grade acetonitrile was obtained from J.T. Baker (Phillipsburg, NJ).

Standard preparation

1 mg of powder was weighed out for each cholesterol compound and dissolved in MeOH accordingly to make 1 mM stock solutions. Stock solutions were aliquoted and stored at -80°C. Ten microliters of a stock solution or a 100 μM solution were pipetted into an autosampler glass vial and dried in a vacuum concentrator for derivatization.

Silylation Derivatization

To each dried sample was added 100 μL of Acetonitrile and MTBSTFA + 1% TBDMCS (1:1) to form tert-butyl silyl derivatives and in separate vials. The samples were then crimp sealed and heated at 60°C for 30 min. The samples were then allowed to cool and injected for analysis.

GC-VUV

A VGA-100 VUV detector (VUV Analytics, Inc, Austin TX) coupled to a Shimadzu GC-2010 gas chromatograph (Shimadzu Scientific Instruments Inc, Columbia MD) was used to collect spectra. Both the transfer line and flow cell temperatures were set at 275°C and the nitrogen make-up gas was optimized for signal averaging at 0.2 psi and 0.1 psi for analysis of steroids and DNA metabolites, respectively. The detector integration time was set at 11ms. A (30 m x 0.25 mmID x 0.25 μm) SH-Rtx-5ms column (Restek) was used with the GC carrier gas (helium) set at a constant flow rate of 2 mL/s. 0.5 μL of each sample

was manually injected. Inlet temperature temperature was set at 280°C with a split ratio of 500:1.

Analysis

Eluted peaks were integrated using VUV Model & Analyze software and the VUV Data Viewer software.

RESULTS AND DISCUSSION

GC-VUV Analysis of Cholesterols & Nucleobases

The separation of cholesterol compounds is shown in Figure 3.3, demonstrating the similarity in chromatograms obtained by GC-VUV methods with GC-MS methods. The absorption spectra of two neurosteroid compounds, specifically 24(S)-hydroxycholesterol and 25-hydroxycholesterol (all structural isomers with chemical composition of $C_{27}H_{46}O_2$ and monoisotopic mass of 402.350 Da)

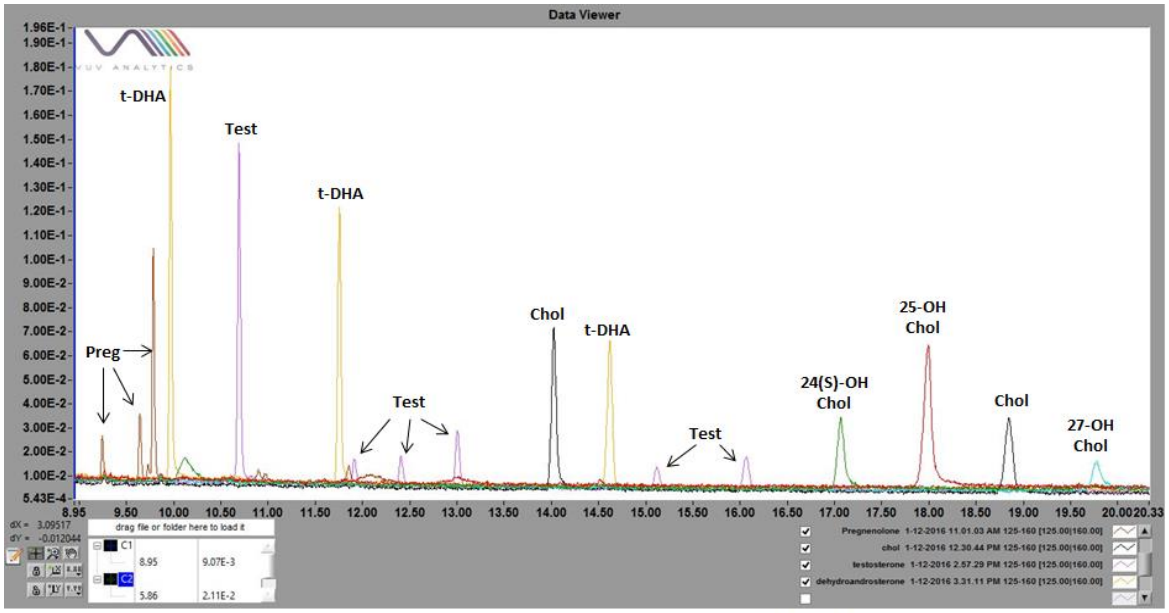

Preg=Pregnenolone; t-DHA= *trans*-Dehydroandrosterone; Test= Testosterone; Chol= Cholesterol; 24(S)-OH Chol= 24(S)-hydroxycholesterol, 25-OH Chol= 25-hydroxycholesterol; 27-OH Chol= 27-hydroxycholesterol

Figure 3.3. Separation and detection of a multitude of cholesterol compounds by GC-VUV

demonstrate the capability of the GC-VUV instrument to further differentiate differences between the isomers by spectroscopic means (Figure 3.4). There is a key noticeable difference in absorption spectra between 24- and 25- hydroxycholesterol in the lower wavelength regions (125nm-165nm).

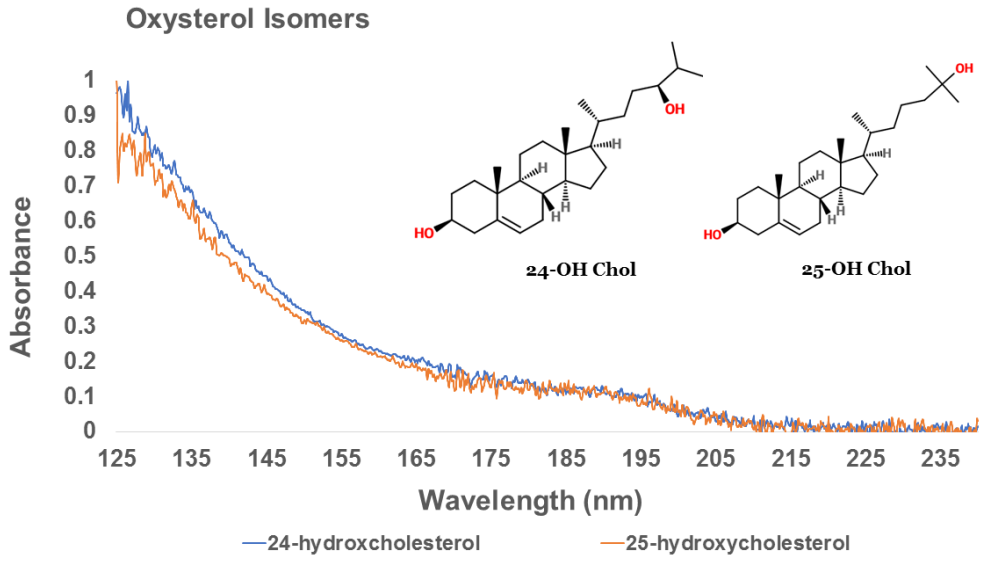

Figure 3.4 VUV spectra for 24-OH cholesterol and 25-OH cholesterol

GC-VUV can also other separate and detect other classes of compounds, such as nucleobases which are of interest for understanding DNA damage repair (Figure 3.5) The advantage of this methodology is demonstrated by the culmination of its ability to distinguish between two co-eluting compounds of the same mass, 6-carboxyuracil (orotic acid) and 5-carboxyuracil. These compounds are positional isomers and have distinct VUV spectra, especially between 155nm-205nm (Figure 3.6A). As expected, these compounds are indistinguishable by GC-MS and elute under one peak (Figure 3.6B). However, using the unique spectral fingerprint of each compound, the resultant spectrum (purple) can be deconvoluted as the superposition (red) of 6-CaU (green) and 5-CaU (blue) (Figure 3.6B).

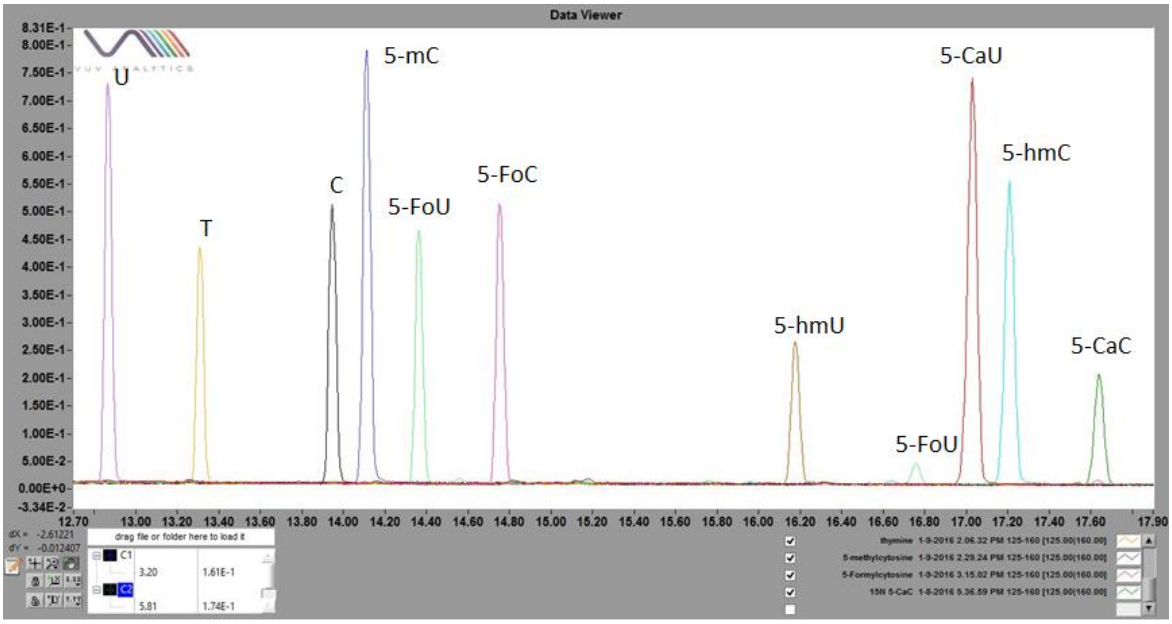

U=uracil; T=thymine; C=cytosine; 5-mC= 5-methylcytosine; 5-formyluracil; 5-formylcytosine; 5-hmU=5-hydroxymethyluracil; 5-CaU= 5-carboxyuracil; 5-hmC= 5-hydroxymethylcytosine; 5-CaC= 5-carboxycytosine

Figure 3.5. Chromatogram demonstrating separation of a number of nucleobases.

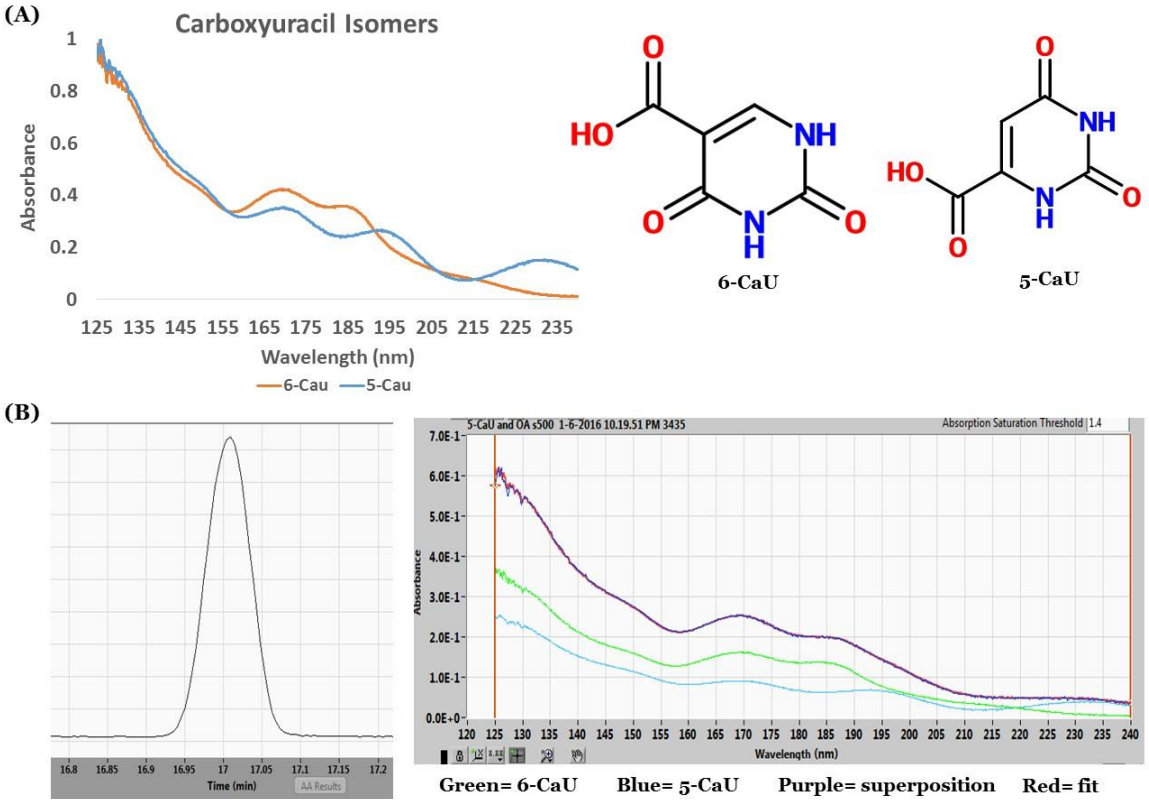

Figure 3.6 VUV spectra of 6-CaU and 5-CaU (A) and the deconvolution of the co-eluting compounds (B)

GC-VUV analysis of 2-hg enantiomers

VUV spectra of 2-hg enantiomers were then obtained to determine whether co-eluting 2-hg enantiomer could also be separated by GC-VUV (Figure 3.7). The resulting spectra overlap and have no distinguishing regions of difference.

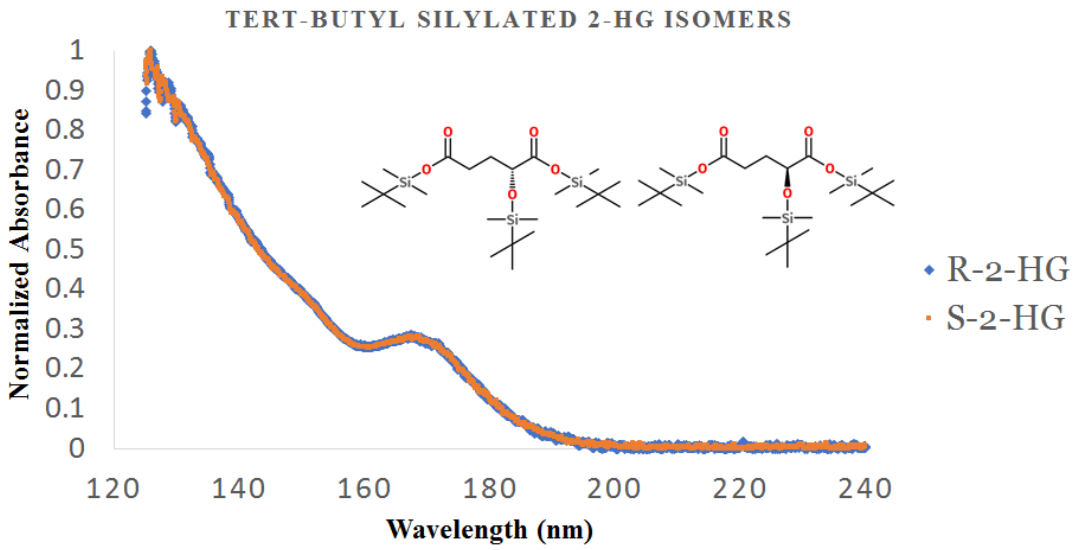

Figure 3.7 VUV spectra of 2-hg enantiomers

To test whether the bulky tert-butyl groups were responsible for the lack of spectral difference, an alternative derivatization was performed. The second derivative produces methyl esters on the carboxyl groups and acetylates the chiral hydroxyl group. The resulting spectra also differs significantly in shape as compared to the tert-butyl 2-hg derivatives but does not produce result in any difference in spectra between the enantiomers (Figure 3.8).

The observed difference between isomers (cholesterols, nucleobases and 2-hg) likely result from the arise from the class of isomers to which the compounds belong. The hydroxycholesterols and the carboxyuracils that were distinguishable by VUV are constitutional isomers. Constitutional isomers, also known as structural isomers, have the

same chemical formula but differ in their connectivity. However, 2-hg enantiomers, by definition, are stereoisomers. Stereoisomers, also called spatial isomers, have the same connectivity and chemical formula but are not arranged in space the same.

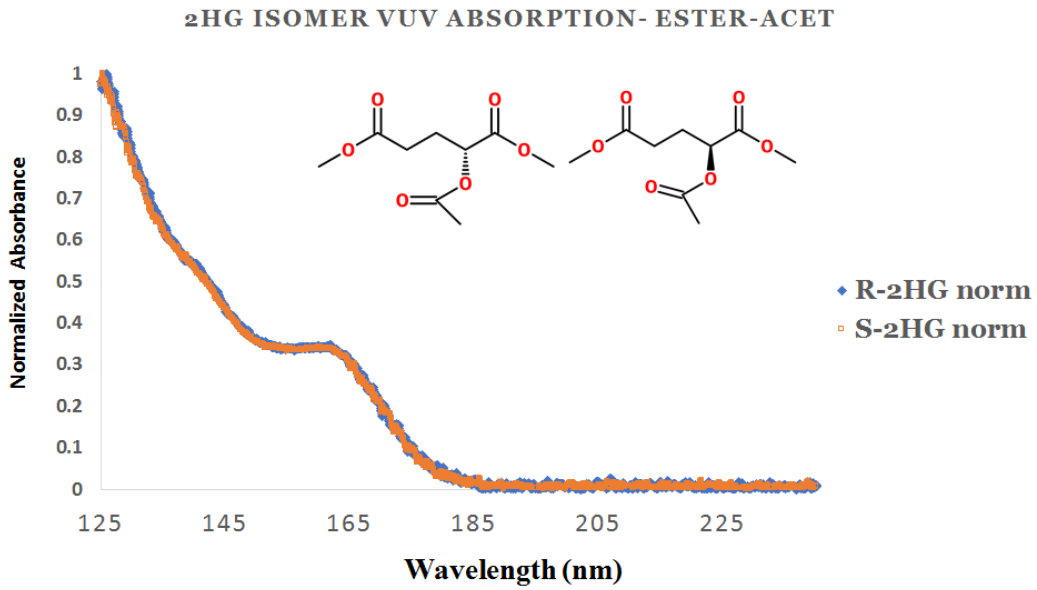

Figure 3.8 VUV spectra of methylated & acetylated 2-hg enantiomers

CONCLUSIONS

VUV is a powerful tool that can be used to distinguish between isomers where MS cannot. However, the capability is limited only to constitutional isomers and it cannot differentiate between enantiomers. In order to detect 2-hg using GC-VUV, a chiral GC column must be used to separate enantiomers as shown in chapter 2. Consequently, MS-based methods were chosen as the methodology of choice to separate and detect 2-hg enantiomers as tandem MS methods are currently more sensitive. The trade-off with the ease, cost, and throughput of GC-VUV would have been worth exploring given that GC-VUV could distinguish between co-eluting 2-hg enantiomers.

Chapter 4: Measurement of 2-hg enantiomers in normal human sera

Parts of this chapter, which include select paragraphs, figures, and tables, are a copy or an adaptation of Strain S. et al. 2020. doi: 10.1016/j.clinms.2019.11.002 [62].

INTRODUCTION

The chiral GC-MS/MS assay developed in chapter 2 was adapted to measure levels of 2-hg enantiomers in serum by stable-isotope dilution mass spectrometry. The assay was used to identify a range of normal serum levels of 2-hg as a clear reference value for normal levels do not currently exist. The human metabolome database reports values for each enantiomer, but the values listed for normal adults cite pediatric aciduria studies [77]–[79]. There are studies comparing 2-hg levels from IDHmut AML to IDHwt patients, but the studies either only measured total 2-hg levels, or only report the 2-hg ratio i.e. the individual levels of each enantiomer levels were either not determined or were left out [15], [80], [81]. A study investigating levels in IDHmut cholangiocarcinoma patients does report each enantiomer separately but only compares the values to IDHwt. Normal values from healthy patients were not reported. Furthermore, a third subset of studies reported normal values but did cite a reference as to where the values were taken from [82]–[84].

A recent study looked at the 97.5 percentile of 2-hg enantiomer levels in a healthy population but only reported that specific percentile and did not give a full range of values [17]. Interestingly, that paper demonstrated some differences in the 97.5 percentile between healthy controls, patients with IDHwt malignancies, and other hematologic malignancies that were not classified as AML. Further work is needed to understand normal levels of 2-hg enantiomers and based upon the current literature, it is not certain as to what the true serum levels of 2-hg enantiomers are and whether they differ between the pediatric and adult populations.

MATERIALS AND METHODS

Chemicals and Reagents

D-α-Hydroxyglutaric acid disodium salt (≥98%), and L-α-Hydroxyglutaric acid disodium salt (≥98%) standards were purchased from Millipore Sigma (St. Louis, MO). The deuterated internal standard (IS), Disodium (RS)-2-Hydroxy-1,5-pentanedioate-2,3,3-d3,OD (≥95%), was purchased from CDN Isotopes (Pointe-Claire, Québec). GC-MS grade ethyl acetate, hydrochloric acid solution (6.0N), sodium chloride (NaCl, ≥99%), glacial acetic acid (≥99%), and (Trimethylsilyl)diazomethane ((TMS)DAM) solution (2.0M) in Hexanes, were purchased from Millipore Sigma (St. Louis, MO). LC-MS grade methanol and LC-MS grade H_2O were obtained from J.T. Baker (Phillipsburg, NJ).

Human Serum Samples

Serum samples from healthy human donors were obtained from Innovative Research (Novi, MI, USA). A total of 60 samples were analyzed and were distributed equally among three races: Black, Hispanic, and Caucasian (Table 4.1). Samples were also equally divided among sex. Each serum sample was aliquoted after thawing and subsequently stored at -80°C.

Demographic		N	Age Mean +/- SD (yrs.)	Age Range (yrs.)
All		60	35.97 +/- 12.62	20-74
Race	Black (B)	20	36.75 +/- 12.19	21-62
	Caucasian (C)	20	38.10 +/- 14.08	20-74
	Hispanic (H)	20	33.05 +/- 11.55	20-58
Sex	Female (F)	30	37.63 +/- 13.82	20-74
	Male (M)	30	34.30 +/- 11.28	20-58

Table 4.1. Demographics of healthy human donors used for measurement of serum 2-hg enantiomers. *See text for full description.

Serum Extraction

Serum (250 µL) was added to a 1.5 mL microcentrifuge tube which was then followed by 3 µL of 100 µM deuterated 2-hg, 10 µL of 6 N HCl, and sodium chloride to saturation (~ 100-300 mg), in that specific order. The tube was capped and vortexed for 30 seconds or until the solution turned a milk-white color. If the solution does not turn to the right color, more sodium chloride can be added, and the tube recapped and vortexed to induce a color change. After successful color change, one milliliter of ethyl acetate was added and subsequently vortexed for another 30 seconds. The tube was then centrifuged at 4000xg for 5 minutes, creating a bilayer separated by a white protein & lipid layer. Of the top organic layer, 900 µL was pipetted out into a 2 mL glass wine vial with a 15 µL reservoir. The glass vial was then placed in a vacuum concentrator to dry. Once dry, the sample was ready for derivatization.

Derivatization

Derivatization was performed for purposes of volatilization and not to separate enantiomers, which was the purpose of DATAN and TSPC-based LC-MS/MS methodologies. To a dried sample in a 2mL glass wine vial was added 100 µL MeOH and 20 µL of 2.0 M (TMS)DAM in hexanes. The sample was then capped with a crimp cap and placed on a shaker at room temperature (25°C) for 30 minutes. After 30 minutes, the reaction was quenched with 20 µL glacial acetic acid and injected immediately for analysis by GC-MS/MS.

GC-MS/MS Analysis

2-hg enantiomers were separated and detected using a Gas-Chromatography Triple Quadrupole (GC-QQQ) Mass Spectrometer (Shimadzu, Kyoto, Japan) with a CP-Chirasil-Dex CB column, 0.25 mm x 25 m x 25 µm (Agilent, Santa Clara, CA) installed. The GC splitless inlet was set at 220°C with an initial oven temperature of 80°C. After injection of

1 µL of derivatized sample, the GC sampled for one minute at 80°C and the oven was ramped at 4°C/min to 180°C and held for 4 minutes, giving a total run time of 30 min. Helium was used as the carrier gas which allowed a column flow of 1.5 mL/min while maintaining constant linear velocity.

For the tandem MS instrument: the interface temperature was set at 200°C, the ion source temperature at 200°C, and an ionization energy of 70 eV which produced positive ions. Two 2-hg specific transitions were monitored, 85.00 m/z > 29.00 m/z at 13.00 V collision energy, and 117.00 m/z > 85.00 m/z at a collision energy of 6.00 V. Similarly, the spiked internal standard transitions were 88.00 m/z > 32.00 m/z at 13.00 V collision energy, and 120.00 m/z > 88.00 m/z at a collision energy of 6.00 V. A solvent cut time of 4 min was used with an event time of 0.04 sec. A summary of the GC-MS/MS parameters is given in Table 4.2.

Parameter	**Setting**
Inlet Temp.	220°C
Injection Pressure	250 kPa
Sampling Time	1 min
Flow Control	Linear Velocity
Column Flow	1.50 mL/min
Total Flow	25 mL/min
Purge Flow	3.0 mL/min
Linear Velocity	49.4 cm/sec
Interface Temp.	200°C
Ion Source Temp.	200°C
Ionization Energy	70 eV
MRM Event Time	0.040 sec
117 > 85 m/z Collision Energy	13.00 V
85 > 29 m/z Collision Energy	6.00 V
Q1/Q3 Resolution	Unit/Unit

Table 4.2. GC-MS/MS parameters used to measure serum levels of 2-hg enantiomers

The Shimadzu Postrun Analysis Software was used to integrate the 2-hg enantiomer peaks and quantitation of endogenous 2-hg enantiomer levels was performed using the following equation:

$$Absolute2hgLevel = \frac{AUC_{endo2hg}}{AUC_{IS}} * Conc_{IS}$$

Where endo2hg = endogenous 2-hg (either enantiomer), IS = internal standard/deuterated 2-hg, AUC = area under the curve, and Conc = concentration. The ratio is defined as R-2-hg:S-2-hg and the total 2-hg as the sum of each absolute 2-hg enantiomer level. Serum levels were reported as the averages of three technical replicates.

Statistics

Normality of the distributions of measured R-2-hg, S-2-hg, Total 2-hg, and the 2-hg split by race and sex was checked by Shapiro-Wilk test of normality using IBM SPSS statistics 25 software. Variances of the distributions were analyzed by Levene's Test of equality of Error Variances using SPSS. Not all the distributions of R-2-hg, S-2-hg, total 2-hg, and the 2-hg ratio were normally distributed when split by sex (Figure A1) or race (Figure A2), nor were the variances equal between male and female (Figure A3) and between Black, Caucasian, or Hispanic race (Figure A4). Consequently, an aligned rank transform was used to run a non-parametric, two-way ANOVA to analyze for differences across race and sex for R-2-hg, S-2-hg, Total 2-hg, and R-2-hg:S-2-hg. The aligned rank transform was first performed using the ARTool (v.1.6.2). [85] The results were then used to run a two-way ANOVA using SPSS.

RESULTS AND DISCUSSION

Stable-isotope dilution GC-MS/MS assay

To volatilize 2-hg, the carboxylic acid functional groups were converted into methyl esters using (TMS)DAM (Figure 4.1A). Targeted detection and quantitation of 2-hg enantiomers was performed using multiple reaction monitoring (MRM) where two primary transitions were monitored. Figure 4.1B shows the molecular structures of the ion species for each MRM transition. MRM transition 1 captures the loss of the second methyl ester functional group while MRM transition 2 detects the loss of two carbon monoxide groups. The tri-deuterated internal standard undergoes an identical fragmentation as the endogenous compound. Positions of the three deuterium atoms are denoted by asterisks in Figure 4.1B.

Typical MRM chromatograms of 2-hg enantiomers as measured in serum is represented in Figure 4.1C. 2-hg enantiomers were separated using a commercially available β-cyclodextrin chiral column with a retention time of approximately 15.20 min and 15.55 min for R-2-hg and S-2-hg, respectively. Retention times were comparable to previously reported retention times using a commercially-available β-cyclodextrin column, but with improved resolution of the enantiomers [35]. Despite shorter retention times reported for DATAN LC methods (4-8 min.), the overall run time for the LC method is 30 minutes due to the equilibration time. The GC-MS/MS method reported here also has an overall runtime of 30 minutes. The 30 minute runtime for the GC-MS/MS allows for the elution of any retained analytes and for the robust separation of 2-hg enantiomers from sample-to-sample without the loss of resolution, intensity, or sample carryover. It is unknown at the time of this report whether the GC-MS/MS method could be shortened to increase data acquisition efficiency for the number of biological samples presented herein.

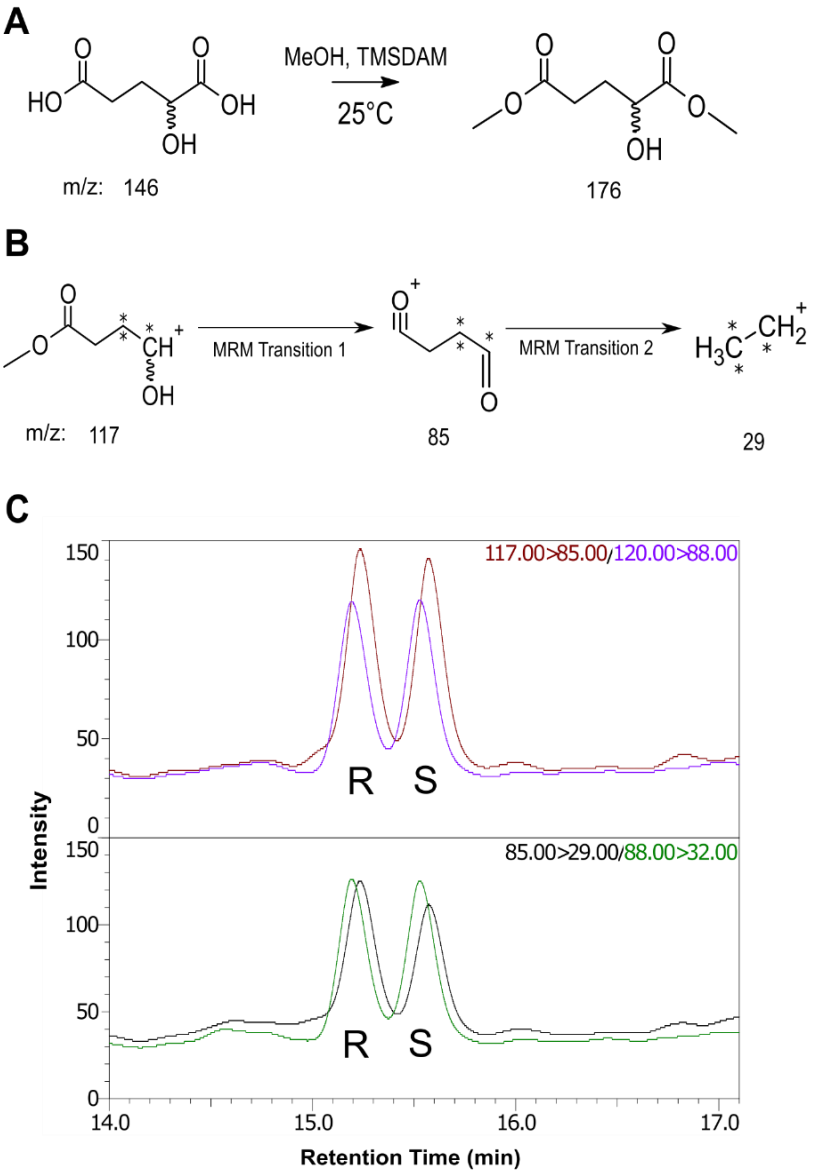

Figure 4.1 Separation and detection of 2-hg enantiomers using GC-MS/MS. Extracted serum sample is derivatized using TMS-DAM (A). Derivatized 2-hg is separated over a β-cyclodextrin column and two MRM transitions are monitored, 117 > 85 and 85 > 29 (B). Corresponding deuterium-labeled internal standards of 2-hg are also detected through the transitions, 120 > 88 and 88 > 32. Asterisks denote the position of deuterium atoms. A representative MRM of 2-hg chromatograms is shown demonstrating sufficient and sensitive separation of both enantiomers from healthy human serum (C).

Basal Levels of 2-hg Enantiomers in Healthy Adult Donors

Serum 2-hg enantiomers levels were measured from 60 healthy human adult donors (Table 4.3). Levels of serum R-2-hg and S-2-hg, reported as the mean ± 95% CI, were similar at 1.09 (0.97 – 1.21) μM and 1.11 (1.00 – 1.22) μM, respectively. Consequently, the ratio of enantiomer levels, R-2-hg:S-2-hg, was observed to be nearly 1:1 at 1.07 (0.95 – 1.20). The average Total 2-hg level, defined as the sum of R-2-hg and S-2-hg, was 2.20 (2.01 – 2.39) μM. Levels of each individual 2-hg enantiomer, along with the quartiles, are mostly in accord with previous studies that reported values of 0.12–1.78 μM for R-2-hg and 0.04–1.5 μM for S-2-hg.[26–28,40] Total 2-hg levels were also similar to previously reported values of 0.7–3.6 μM.[9,21,24,32,41–44] However, of note are the maximum individual values of R-2-hg and S-2-hg, 2.30 and 2.00 μM. These specific measurements are higher than previously reported normal values. Several reasons could exist for the discrepancy. The acquired serum samples are tested for commonly found infectious diseases, but there is no guarantee of the absence of any IDHmut malignancy, or other metabolic disorders. Nevertheless, it is more likely that the values measured herein represent an extended range of values not previously reported.

Measured levels were also equally stratified by race (N=20 per group) and sex (N=30 per group) (Table 4.1). Basal levels of R-2-hg measured in Black (B) donors was 1.34 (1.10 – 1.58) μM, which was a significant increase over the levels measured in Hispanic (H) donors at 0.87 (0.74 – 1.00) μM (p=0.004) (Figure 4.2A). Serum levels of R-2-hg for Caucasians (C) was measured at 1.06 (0.83 – 1.29) μM and was not significantly different between Black (p=0.362) and Hispanic (p=0.114) sera. Additionally, there was a significant difference between Black females and Hispanic females (p=0.024). Production of R-2-hg is known to be regulated by the mitochondrial enzymes, hydroxyacid-oxoacid transhydrogenase (HOT) and R-2-hg dehydrogenase (R-2HGDH). No reported differences in activities of HOT or R-2HGDH have been shown according to

	Race	Mean (95% CI)	Min - Max	Q1	Q2	Q3	95th percentile	Proposed Cutoffs (Mean + 3*SD)
R-2-hg	All	1.09 (0.97 – 1.21)	0.32 – 2.30	0.71	0.98	1.41	2.19	2.52
	B	1.34 (1.10 – 1.58)	0.69 – 2.30	0.79	1.32	1.63	2.30	2.89
	C	1.06 (0.83 – 1.29)	0.44 – 2.08	0.63	1.00	1.24	2.08	2.55
	H	0.87 (0.74 – 1.00)	0.32 – 1.53	0.69	0.77	1.06	1.52	1.71
S-2-hg	All	1.11 (1.00 – 1.22)	0.48 – 2.00	0.79	1.05	1.47	1.82	2.35
	B	1.09 (0.90 – 1.28)	0.48 – 1.82	0.77	1.15	1.40	1.82	2.31
	C	1.27 (1.10 – 1.44)	0.73 – 2.00	0.96	1.16	1.54	1.99	2.37
	H	0.97 (0.77 – 1.17)	0.48 – 1.98	0.70	0.80	1.39	1.96	2.24
Total 2-hg	All	2.20 (2.01 – 2.39)	1.08 – 3.86	1.63	2.09	2.75	3.65	4.36
	B	2.43 (1.20 – 2.81)	1.20 – 3.86	1.73	2.49	2.97	3.85	4.86
	C	2.33 (2.03 – 2.64)	1.30 – 3.76	1.92	2.16	2.74	3.76	4.29
	H	1.84 (1.57 – 2.10)	1.08 – 3.03	1.40	1.67	2.17	3.02	3.53
2-hg Ratio	All	1.07 (0.95 – 1.20)	0.26 – 2.70	0.66	1.06	1.39	1.80	2.50
	B	1.31 (1.08 – 1.54)	0.61 – 2.70	0.92	1.32	1.49	2.67	2.80
	C	0.89 (0.68 – 1.09)	0.26 – 1.81	0.53	0.78	1.24	1.80	2.18
	H	1.02 (0.83 – 1.21)	0.37 – 1.56	0.66	0.99	1.41	1.55	2.24

Table 4.3 Levels of R-2-hg, S-2-hg, Total 2-hg, and 2-hg Ratio in serum of healthy donors. All values shown are reported in µM.

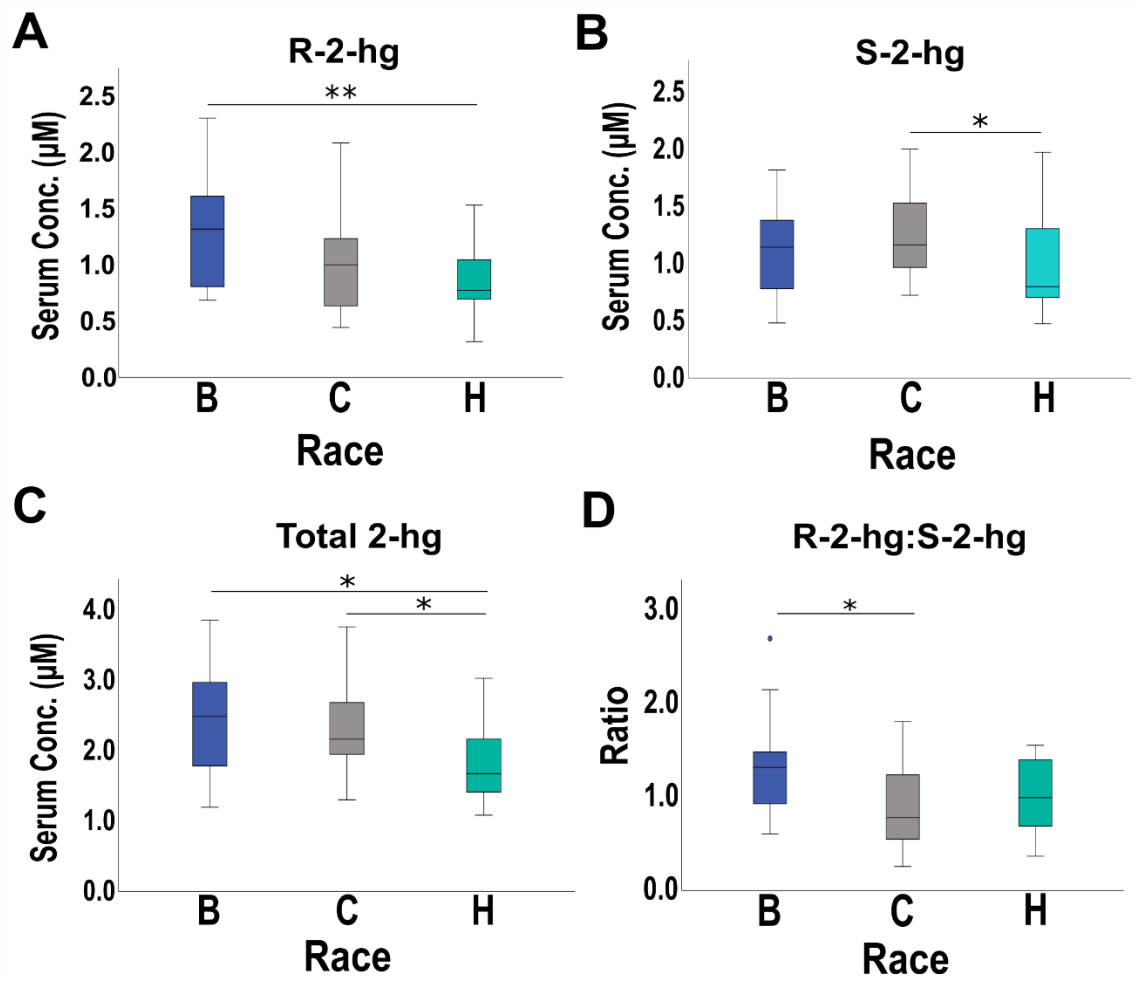

Figure 4.2 Serum levels of healthy donors by race. Differences in race of R-2-hg (A), S-2-hg (B), Total 2-hg (C), and 2-hg Ratio (D), vary according to the parameter. **p-value < 0.01, *p-value <0.05.

race or ethnicity as observed with alcohol dehydrogenase and aldehyde dehydrogenase in Asians, which can have variable activity due to the expression of different isoenzymes [45]. Thus, it is possible that the reported differences in race could be a result of racial differences in basal enzyme activity levels for HOT and R-2HGDH but a more thorough investigation into the biology of serum R-2-hg levels is needed.

Differences in levels between race as measured for S-2-hg serum levels were different from those for R-2-hg (Figure 4.2B). S-2-hg levels for Caucasian sera were 1.27

(1.10 – 1.44) μM, which was higher than levels measured in Hispanic sera at 0.97 (0.77 – 1.17) μM (p=0.019). Black S-2-hg levels were 1.09 (0.90 – 1.28) μM which were not significantly different compared to Hispanic levels (p=0.402) or Caucasian levels (p=0.301). Similar to R-2-hg, there are no reported differences in S-2-hg regulatory enzymes according to race or ethnicity. Further work into the biology of the regulation of serum levels of S-2-hg is needed to better interpret the observed differences in race, especially as the observed differences in race varied between each enantiomer.

Total 2-hg levels were significantly different between Black serum levels at 2.43 (1.20 – 1.81) μM and Hispanic levels at 1.84 (1.57 – 2.10) μM (p=0.17), as well as Hispanic vs. Caucasian levels where Caucasians were 2.33 (2.03 – 2.64) μM (p=0.030) (Figure 4.2C). There were no observed differences in Total 2-hg levels for Black vs. Caucasian Total 2-hg levels (p=0.974). Significant differences for individual R-2-hg levels and S-2-hg levels were still significant when combined. The ratio of the two enantiomers, R-2-hg:S-2-hg, were different between the average Black ratios at 1.31 (1.08 – 1.54) and Caucasian ratios at 0.89 (0.68 – 1.09) (p=.024), but no differences were found in the ratios between Black vs. Hispanic (p=0.189) and Caucasian vs. Hispanic (p=0.620), where Hispanic ratio levels were 1.02 (0.83 – 1.21) (Figure 4.2D). Black donors had one outlier with a ratio of 2.70, above the max boxplot whisker. Though the value does not represent the majority of the Black donor ratios, it is important to note that the individual R-2-hg value, 1.53 μM, and S-2-hg value, 0.57 μM, were normal, demonstrating that the 2-hg ratio alone is likely not a sufficient marker of disease. Finally, no significant differences were observed between sexes (Male vs. Female) for all parameters, which is in agreement with previous studies (Figure 4.3)

Proposed upper limit cutoffs for this assay, which were calculated as three standard deviations above the mean, would be 2.52 μM for R-2-hg, 2.35 μM for S-2-hg, 4.86 μM for total 2-hg, and 2.50 for the ratio. The results of this study also suggest that different cutoffs may need to be considered when determining an absolute increase in 2-hg

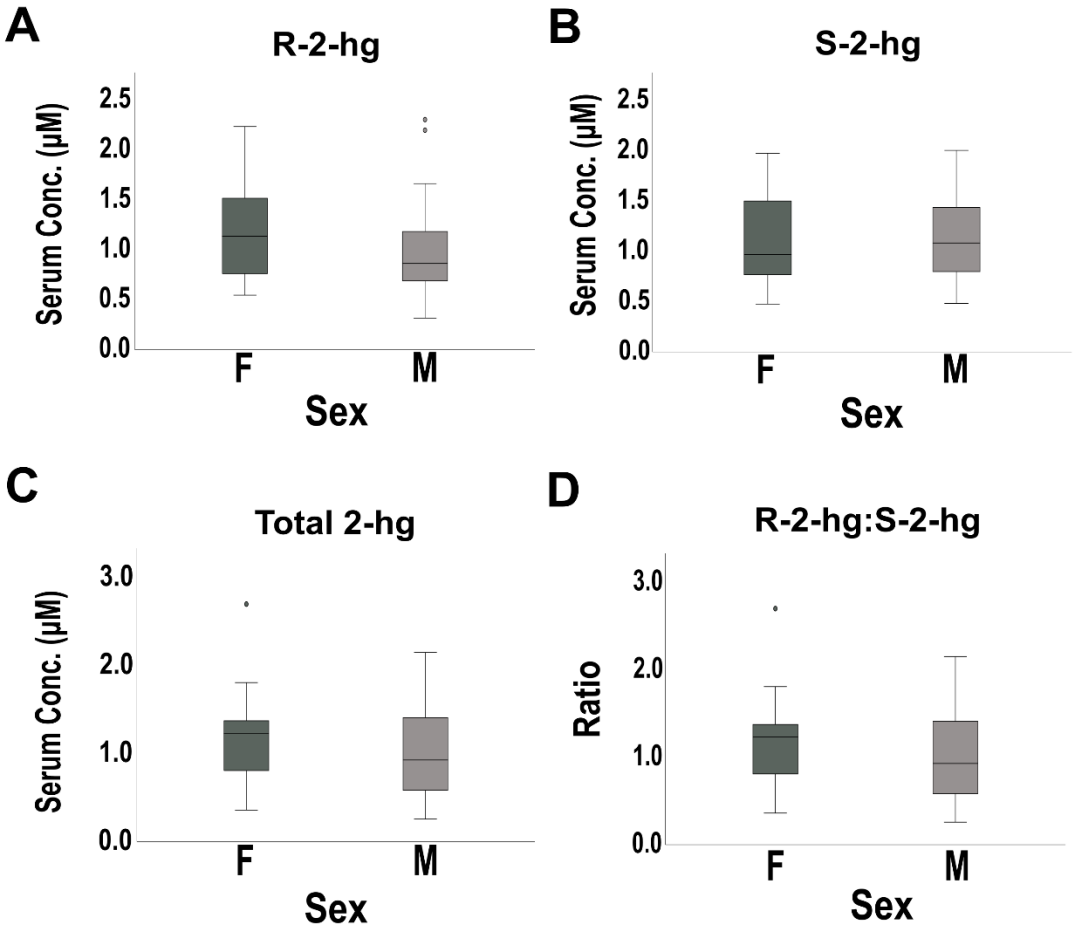

Figure 4.3 Serum levels of healthy donors by sex. No differences were observed between sex for R-2-hg (A), S-2-hg (B), Total 2-hg (C), and 2-hg Ratio (D)

enantiomer levels, for different races. For example, high R-2-hg levels for a Hispanic patient could be deemed normal in a person of the Black race. The use of percent differences in temporal studies could also be used to aid in interpretation and bypass some of the differences observed in basal levels according to race. A larger sample size with a wider variety of races is needed, however, to validate the reported findings, especially as the determination of proper cut-off values for IDHmut status is continually evaluated using a receiver operator characteristic curve [15], [17], [35].

Correlation of 2-hg Enantiomer Levels with Age

The study population was young on average, 35.97 +/- 12.62 (SD) yrs. of age, with a range between 25 and 74. A Pearson correlation was used to determine if any correlation exists between age and R-2-hg, S-2-hg, Total 2-hg, or the 2-hg Ratio. Figure 4.4A-B demonstrates that R-2-hg does not significantly correlate with age (p=0.191, r=0.17), while S-2-hg showed a significant, moderate correlation with age (p=0.000, r=0.50). Total 2-hg levels also demonstrated significant, moderate correlation with age (p=0.001, r=0.40), but the ratio of 2-hg enantiomers did not (p=0.061, r=-0.24) (Figure 4.4C-D).

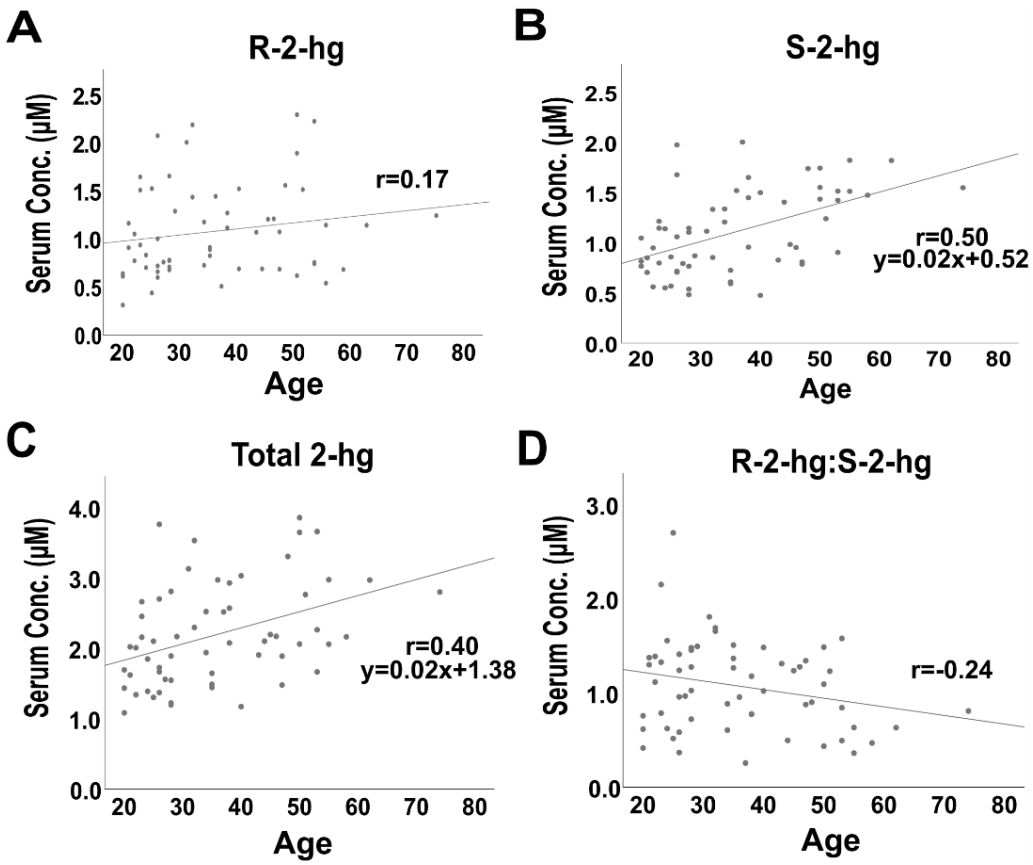

Figure 4.4 Correlation of R-2-hg (A), S-2-hg (B), Total 2-hg (C), and the 2-hg Ratio (D) vs. age. Pearson correlation statistic is shown for each graph and a linear fit equation is given if the Pearson correlation analysis was statistically significant

There is evidence that age is associated with an increase in minimal but chronic, systemic inflammation in the absence of active infection [86]. This age-related inflammation is largely attributed to mitochondrial dysfunction and DNA damage response pathway alterations, among others. Regulation of 2-hg includes mitochondrial enzymes and the effects of mitochondrial dysfunction on 2-hydroxyglutarate have been discussed elsewhere [59], [87]. Any link between S-2-hg, age, and inflammation needs further investigation but is warranted from the correlations presented herein. Though incorporation of older patients into this study would help elucidate any correlation between age and S-2-hg, our focus was on a younger population as IDH mutant gliomas are associated with a younger age at presentation, and secondary glioblastomas, which arise from lower-grade IDHmut gliomas, are predominately found in younger patients (median age of 45 yrs.) [88].

CONCLUSIONS

Normal values in adult patients have been established. The data presented herein also highlights the importance of race and age in order to interpret 2-hg enantiomer levels appropriately. Further work is needed to validate the race and age findings, especially in other races, such as Asian. However, the data shows that a range of 2-hg enantiomer values can be measured and more importantly, that the R-2-hg:S-2-hg ratio can be skewed high in normal patients if the S-2-hg enantiomer level is low. It is important to consider each enantiomer level separately. The application of the suggested cutoff values is used to evaluate 2-hg enantiomers levels from samples obtained from brain tumor patients in chapter 5.

Chapter 5: Levels of 2-hg enantiomers in patients with IDH mutant gliomas

Parts of this chapter, which include select paragraphs, figures, and tables, are a copy or an adaptation of Strain S. et al. 2020. doi: 10.1016/j.clinms.2019.11.002 [62].

INTRODUCTION

Brain Tumors and IDH Mutations

Approximately 20,000 new diagnoses of gliomas are expected to occur every year [89]. Gliomas are primary tumors of the brain that arise from glial cells of the central nervous system. Gliomas represent ~80% of all malignant brain tumors, with the majority being classified as astrocytomas, oligodendrogliomas, and ependymomas [90]. Tumors are further classified using a histopathological grading system (I to IV) where a higher grade is correlated with less differentiation, faster growth, and worse prognosis [91]. Grade II tumors, although initially well differentiated, eventually progress over time and can carry a median survival of only 9.25 yrs. [92]. Grade III and grade IV (glioblastoma) tumors carry a worse prognosis with a median survival of only 2-3 years and 3-12 months, respectively [93], [94]. Overall, gliomas represent a deadly set of cancers, and new therapeutic modalities need to be developed. Next-generation sequencing of glioblastomas in 2008 revealed a novel mutation in a gene involved in cellular respiration, isocitrate dehydrogenase (IDH) [95]. It was later found that IDH mutations occur in a significant number of grade II/III tumors as well (Figure 5.1) [3]. Interestingly, secondary GBMs, which progress from lower grade gliomas, frequently harbor IDH mutations. Primary GBMs do not progress from lower grade gliomas and <10% are IDH mutated [3], [95].

Currently, diagnosis of brain tumors is made by neurological examination and, when the tumor is large enough, by imaging (via CT and/or MRI) [96]. Many patients present with advanced disease and treatment options vary based upon the location

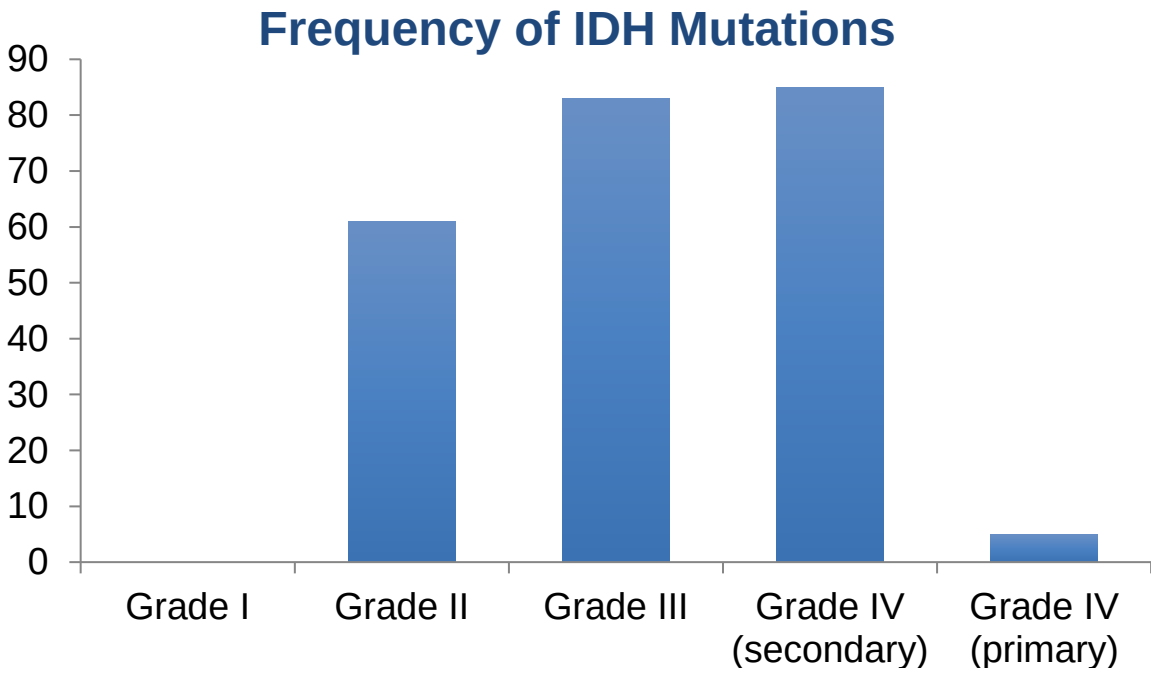

Figure 5.1 Frequency of IDH mutations by tumor grade. Figure created from data obtained by Yan et al. 2009 [3].

and stage of disease. However, surgical resection is typically the first step in treatment, followed by radiation and/or chemotherapy as indicated [89], [96]. After resection, most tumors are histopathologically graded, classified for tumor type, and analyzed for mutations in a standard panel of genes. Protocols differ across institutions, but at Texas Oncology where samples were obtained for this dissertation, mutation status is analyzed by immunohistochemistry (IHC) staining for IDH, p-53, and Ki-67. A 315 gene array using a Next Generation Sequencing assay can also be conducted at the discretion of the facility. Currently, there are no methods other than monitoring clinical symptoms and imaging to assess treatment response and relapse/progression of disease. However, the recent discovery that R-2-hg is made by the mutant IDH enzyme in IDHmut gliomas has provided a new potential tool for clinical management of patients with IDH mutant gliomas [7]. A blood test for levels of R-2-hg could be used to aid in diagnosis gliomas with an IDH mutation, assess treatment response, and screen for early signs of relapse or progression.

Such a test would also be a useful assay for assessing the efficacy of new therapeutics currently in clinical trials that specifically target the IDHmut enzyme [97]–[99].

2-hg levels as a biomarker for IDHmut gliomas

Initial pilot studies have shown no difference in total 2-hg levels in the blood of patients with IDHmut tumors as compared to patients with IDHwt gliomas [100]. Total 2-hg levels were measured by conventional mass spectrometry which do not differentiate between, R-2-hg, the molecule produced by the tumor, and its enantiomer, S-2-hg. Thus, no correlation of 2-hg levels with mutant status or tumor burden were established in the above studies. In regards to urinary 2-hg, one study reported an increase in urine 2-hg levels, which correlated with mutation status [101], while a separate study reported that 2-hg levels were actually higher in IDHwt patients [102]. In patients with other IDHmut tumors, such as AML and cholangiocarcinoma, some studies report that circulating levels of 2-hg correlates with clinical outcome and IDH mutation status [80], [103]. Yet, in a similar manner to glioma studies, not all investigations have agreed. One AML study reported that total 2-hg levels were a poor predictor of outcome for patients with IDHmut AML, and an increase in 2-hg levels did not always correspond to the presence of an IDH mutation [81]. The discrepancy in results from the different studies, likely arises from the fact that total 2-hg levels were measured, rather than each of the (R) and (S) enantiomers. Recent studies have demonstrated the importance of measuring individual 2-hg enantiomers in patients with IDH mutant tumors [15], [41], [104], [105]. Measuring the ratio of R-2-hg:S-2-hg is reportedly more specific for minimal residual disease in AML patients using mass spectrometry-based methods [15]. Additionally, the CSF of patients with IDH mutant gliomas was reported to have seven-fold higher levels of R-2-hg as compared to CSF from patients with IDHwt gliomas [41].

In summary, the utility of the oncometabolite, R-2-hg, for clinical management of patients with IDH mutant gliomas has yet to be studied. Thus, the absolute levels of R-2-

hg, or the ratio of R-2-hg:S-2-hg, could have a significant impact as a biomarker in the management of patients with IDH mutant gliomas. The goal of the experiments presented in this chapter is to measure R-2-hg and S-2-hg in patient samples to determine if the absolute levels of R-2-hg, or the ratio of R-2-hg:S-2-hg in serum & urine, could have a significant impact as a biomarker in the management of patients with IDHmut gliomas.

METHODS

Biological samples

Serum and urine samples from patients with IDH mutated or IDH wild-type (IDHwt) gliomas were collected from an ongoing, IRB-approved study at The Austin Brain Tumor Center (Texas Oncology, Austin, TX). The serum obtained from 11 patients was initially used as a pilot study to demonstrate feasibility and justify the continued collection of patient samples. A similar study was also set in place at the University of Texas Medical Branch (Galveston, TX) which only collected serum before treatment. Additional samples from 76 more patients were used in an expanded cohort to bring the total number of patients to 87. Patients were enrolled as outlined in the IRB-approved protocols (Appendix B).

Sample Analysis

Biological samples were extracted, derivatized, and analyzed by GC-MS/MS according to the protocols listed in chapter 2.

Statistical Analysis

Individual t-tests were used to determine differences between R-2-hg, S-2-hg, Total 2-hg, or 2-hg Ratios between groups in the expanded cohort. Levene's test was used to compare variances between groups.

RESULTS AND DISCUSSION

Pilot Study (n=11 patients)

To demonstrate clinical feasibility for this assay to be used in patients with gliomas,

Patient	R-2-hg	S-2-hg	Total 2-hg	2-hg Ratio
001	**2.94**	1.24	4.18	**2.37**
002	**4.39**	1.92	**6.31**	**2.28**
003	2.09	**4.01**	**6.09**	0.52
004	1.40	2.08	3.48	0.67
005	1.16	1.23	2.39	0.94
006	1.23	**5.76**	**6.99**	0.21
007	0.68	1.46	2.14	0.47
008	1.19	**2.69**	3.88	0.44
009	1.58	**2.26**	**3.84**	0.70
010	0.87	**4.14**	**5.01**	0.21
011	2.34	**4.36**	**6.69**	0.54

Table 5.1 Pilot study patient demographics, tumor properties, and sample collection context.

Patient	Age (yrs.)	Race	Tumor Type	Tumor Grade	IDH Status	Tumor Stability	Sample Context
001	32	C	A	II	Mut	TP	No resection
002	57	C	A/O	III	Mut	TP	Surveillance
003	30	C	A	II	Mut	Shrinking	Post-GTR/XRT During TMZ
004	54	Asian	A	IV	WT	No Tumor	Post-GTR/XRT+TMZ During CCNU + Optune
005	40	Asian	A	IV	Mut	TP	Surveillance
006	56	C	A	IV	WT	TP	Post-STR/XRT/TMZ
007	40	C	A	III	Mut	Stable	During CCNU + Eflornithine
008	64	C	A	IV	WT	Stable	Post-GTR/XRT/TMZ During Optune
009	54	H	A	III	WT	No Tumor	Post-GTR/XRT/TMZ During Optune
010	64	C	A	III	Mut	No Tumor	Post-STR/XRT/TMZ
011	60	C	A	IV	WT	TP	Post-STR/XRT+TMZ/TMZ

C= Caucasian, H= Hispanic; A = astrocytoma, A/O = anaplastic oligodendroglioma; GTR = gross total resection, STR = sub-total resection, XRT = radiation therapy, TMZ = temozolomide, CCNU = lomustine; TP = tumor progression

Table 5.2. Pilot study patient demographics, tumor properties, and sample collection context.

2-hg enantiomers were measured in serum samples obtained from a pilot study of 11 patients with IDHmut and IDHwt gliomas (Table 5.1). Patient demographics, tumor properties, and sample context are given in Table 5.2. In reference to the reported normal value cutoffs proposed above, serum levels of R-2-hg were increased in 2 out of 3 patients with actively growing IDHmut tumors (001, 002, and 005). Three other patients, 003, 007, and 010 also had IDHmut tumors but either had shrinking or stable tumors. Surprisingly, the S-2-hg level was increased in a number of samples (003, 006, 008, 010, and 011) and no correlation between IDHmut status or any other variable in Table 5.2 could explain the observed increase. It is unclear for this pilot study as to why S-2-hg was increased. Tumor hypoxia, treatment with chemotherapy, or another other, yet unidentified mechanism could be the causative agents for this observation.

Distinguishing between each enantiomer is exemplified in the levels of total 2-hg measured across all 11 patients. Those with increased total 2-hg levels included some of those with increased levels of either R-2-hg or S-2-hg, but not all patients with an increase in one enantiomer level, such as patient 001 and patient 008, demonstrated an increase in total 2-hg levels. This shows that measuring total 2-hg alone is insufficient and that the source of any observed increase in 2-hg could come from either enantiomer. Furthermore, reporting only the 2-hg ratio, can mask any increase in R-2-hg as a potentially large increase in S-2-hg, such as the levels shown from patient 006, could hypothetically cause the ratio to be normal which could mask any subtle, yet significant increase in R-2-hg.

Furthermore, using the above proposed cutoff for the 2-hg ratio yielded no sample with an increase in the R-2-hg:S-2-hg ratio. The proposed cutoff could be too high as it included outlier values but further work beyond the pilot study is needed to definitively determine cutoff values. Lastly, when utilizing race specific cutoffs for 9 of the 11 patients (two were of Asian race), a number of measured levels are labeled as an increase (Table 5.3). For example, the patients 001 and 002 with actively growing IDH mutant tumors were shown to have an increase in their 2-hg ratio, and the Hispanic patient, patient 009, had an

increase in S-2-hg and total 2-hg levels. Interestingly, with the race cutoff correction, of the 6 of the seven who received prior radiation therapy, an increase in S-2-hg was observed (003, 006, 008, 009, 010, 011). In conclusion, we demonstrate the potential importance of taking into account race when determining an individual's normal levels of 2-hg enantiomers.

Patient	R-2-hg	S-2-hg	Total 2-hg	2-hg Ratio
001	**2.94**	1.24	4.18	**2.37**
002	**4.39**	1.92	**6.31**	**2.28**
003	2.09	**4.01**	**6.09**	0.52
004	1.40	2.08	3.48	0.67
005	1.16	1.23	2.39	0.94
006	1.23	**5.76**	**6.99**	0.21
007	0.68	1.46	2.14	0.47
008	1.19	**2.69**	3.88	0.44
009	1.58	**2.26**	**3.84**	0.70
010	0.87	**4.14**	**5.01**	0.21
011	2.34	**4.36**	**6.69**	0.54

Table 5.3. Serum levels of 2-hg enantiomers for a pilot study of 11 patients using race-specific cutoffs. All values shown are reported in µM. Bold denotes increase above proposed cutoff. Red bold indicates an increase using race-specific cutoffs.

Correlation between urine and serum

Urine levels were also taken at the same time the serum samples were collected. A comparison of serum and urine levels for R-2-hg (Figure 5.2A) and S-2-hg (Figure 5.2B) was performed to examine whether the two correlated. The general trend between serum and urine holds, however, not every sample is identical. For instance, R-2-hg levels for patient 008 and 009 were comparable to 001 and 002 in urine, but not in serum. The likely discrepancy likely arises from urine not being normalized to creatinine output, which is marker of normal kidney function. Proper measurement of creatinine output is also usually

performed over a 24-hr period to account for any variation in volume output. Other variables such as diet and secretion of other urinary metabolites, like lactate and ketoacids, can also affect urinary organic acid output [106]. Thus, serum levels are likely to have more utility as a biomarker as it will not experience such issues.

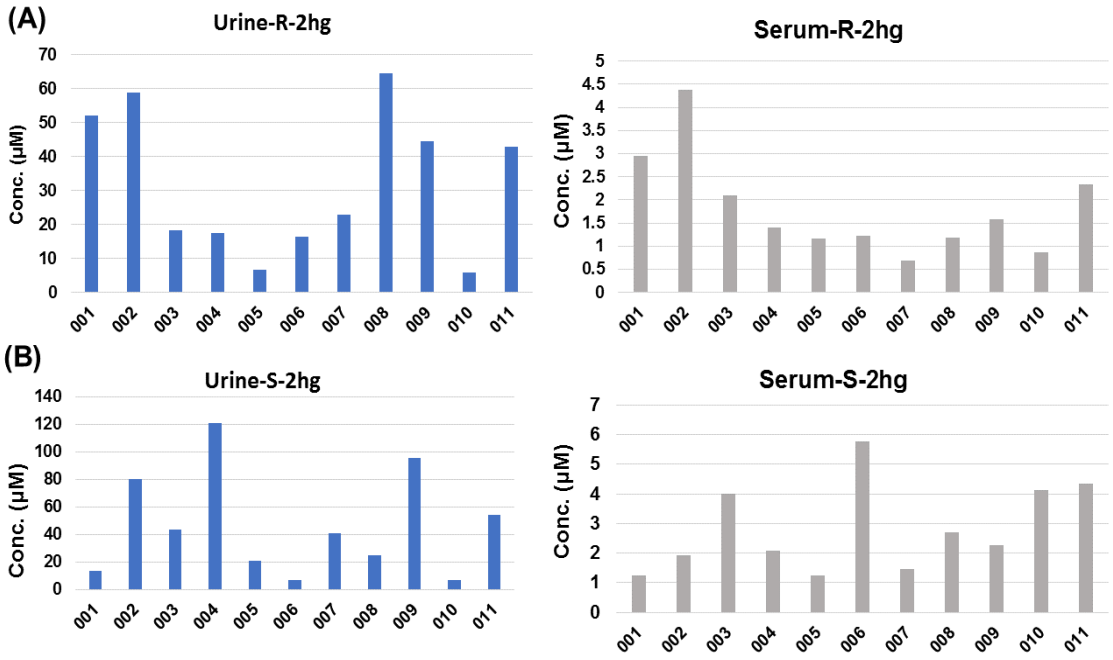

Figure 5.2 Comparison urine and serum R-2-hg levels (A) and S-2-hg levels (B).

Expanded Cohort

Sample collection was continued, and serum and urine samples were analyzed from a total of 87 patients. The following patients variables were also collected for each sample: subject ID, date of birth, sex, ethnicity, tumor type, tumor grade, IDH status, IDH mutation allele, 1p19q status, Ki-67 status, date of tumor dx, age at diagnosis, location of tumor, sample collection type and date, date of baseline scan, dimensions of tumor, volume of tumor, MRI enhancement and degree of enhancement, other significant radiological features, sample obtained prior to or post resection, extent of resection (subtotal or gross), prior treatment

history, adjuvant therapy before or during sample collection, tumor growth before sample collection, and any other relevant clinical context during sample collection. R-2-hg and S-2-hg levels from a total of 128 have samples are shown in Table 5.4. Samples were not adjusted for race due to the preliminary nature of the results obtained from chapter 4. The application of the results from race adjustment was demonstrated in the pilot study as there is still a lack of data from other races, such as Asian.

Of the 128 samples analyzed, 75 samples (58.6%) were taken from patients with a tumor and 53 (41.4 %) from patients without a tumor as evident by MRI. Of those with a tumor, 45 (60%) had an actively growing tumor and 30 (40%) had a stable tumor. IDH mutations were prevalent in 34/45 actively growing tumors and 23/30 stable tumors (Figure 5.3). 8 samples were taken prior to treatment (tx), 51 were taken during treatment, 69 were taken post-treatment, where post-treatment can include those with and without evidence of disease by MRI (post-tx surveillance) (Figure 5.4).

The majority of patients were enrolled in cohort 2 meaning they were receiving, or about to receive, adjuvant therapy with chemotherapy or radiotherapy (XRT) following surgical resection (Figure 5.4). Only 6 samples were taken for cohort 1 where patients received surgery only, and only 2 were enrolled in cohort 3 where no current tx was taking place. Lastly, the vast majority of patients were not treatment naïve at the time of enrollment. 119 (93%) samples were collected from patients with a prior history of treatment with chemotherapy and/or XRT (Figure 5.4). Only 9 samples total were collected from treatment naïve patients.

ID Number	Date of Collection	R-2-hg (μM)	S-2-hg (μM)	Total 2-hg (μM)	2-hg Ratio
001	2/5/2018	**2.94**	1.24	4.18	2.37
001	7/23/2018	**2.80**	1.52	4.33	1.84
001	10/15/2018	**7.27**	**2.61**	**9.88**	**2.79**
002	2/5/2018	**4.39**	1.92	**6.31**	2.28
002	9/6/2018	**3.04**	0.99	4.03	**3.06**
003	2/6/2018	2.09	**4.01**	**6.09**	0.52
003	6/13/2018	1.10	1.22	2.32	0.90
003	8/9/2018	1.33	1.91	3.24	0.70
004	2/22/2018	1.78	2.00	3.78	0.89
004	6/13/2018	2.35	**5.21**	**7.56**	0.45
004	8/9/2018	2.42	**3.04**	**5.47**	0.80
005	3/22/2018	1.61	1.32	2.92	1.22
006	2/26/2018	1.16	1.23	2.39	0.94
007	3/1/2018	1.23	**5.76**	**6.99**	0.21
008	3/1/2018	0.68	1.46	2.14	0.47
008	7/16/2018	0.72	1.53	2.25	0.47
009	3/1/2018	1.19	**2.69**	3.88	0.44
009	5/24/2018	1.39	**3.06**	**4.45**	0.45
009	8/20/2018	1.03	1.43	2.47	0.72
010	3/1/2018	1.58	2.26	3.84	0.70
010	4/24/2018	2.23	2.04	4.27	1.10
010	7/30/2018	2.23	2.33	**4.56**	0.96
011	3/5/2018	0.87	**4.14**	**5.01**	0.21
011	6/13/2018	1.17	**2.94**	4.11	0.40
011	10/15/2018	1.02	**4.79**	**5.81**	0.21
012	3/5/2018	2.34	**4.36**	**6.69**	0.54
012	5/14/2018	2.31	**4.75**	**7.07**	0.49
012	7/12/2018	2.07	**4.05**	**6.11**	0.51
012	8/9/2018	2.24	**3.79**	**6.02**	0.59
012	9/6/2018	2.38	**3.86**	**6.24**	0.62
013	3/8/2018	1.10	0.77	1.87	1.43
014	3/8/2018	**15.37**	2.06	**17.43**	**7.46**
014	7/2/2018	**7.14**	1.52	**8.66**	**4.71**
014	9/6/2018	**3.83**	1.73	**5.57**	2.21
015	3/8/2018	0.80	0.74	1.54	1.09
015	6/4/2018	0.79	0.73	1.52	1.07
015	7/2/2018	0.73	0.60	1.34	1.22
015	9/6/2018	1.62	1.26	2.88	1.28
016	6/13/2018	0.95	1.45	2.40	0.66
016	8/24/2018	1.08	1.63	2.71	0.66

016	10/11/2018	0.77	1.34	2.11	0.57
017	5/17/2018	1.71	0.94	2.65	1.82
018	5/17/2018	**5.06**	**3.95**	**9.01**	1.28
019	7/12/2018	1.04	2.26	3.30	0.46
019	10/11/2018	1.07	1.83	2.90	0.59
020	5/17/2018	1.31	**2.86**	4.17	0.46
021	6/18/2018	2.39	**3.24**	**5.63**	0.74
021	10/15/2018	1.80	1.83	3.63	0.99
022	6/18/2018	0.92	**3.52**	**4.44**	0.26
022	9/6/2018	1.55	**3.55**	**5.10**	0.44
022	10/1/2018	1.16	1.37	2.52	0.85
023	5/21/2018	1.03	1.10	2.13	0.93
023	9/24/2018	0.92	0.76	1.69	1.21
025	8/2/2018	1.26	1.20	2.46	1.05
026	6/4/2018	1.02	**2.36**	3.38	0.43
026	9/6/2018	1.55	**2.64**	4.19	0.59
027	8/2/2018	1.56	**3.64**	**5.20**	0.43
028	7/30/2018	1.82	**2.91**	**4.73**	0.62
029	6/4/2018	**3.46**	1.28	**4.74**	**2.71**
030	6/4/2018	1.28	1.81	3.09	0.71
030	8/6/2018	1.53	**2.49**	4.01	0.61
032	6/21/2018	0.88	1.52	2.40	0.58
032	10/15/2018	1.37	**3.31**	**4.68**	0.41
033	6/13/2018	0.71	**2.96**	3.67	0.24
034	6/13/2018	1.79	1.84	3.62	0.97
034	10/8/2018	1.28	1.25	2.53	1.03
035	6/18/2018	1.61	1.81	3.41	0.89
036	6/21/2018	1.26	1.08	2.34	1.18
036	8/2/2018	1.64	1.34	2.98	1.22
036	9/27/2018	1.42	1.06	2.48	1.33
037	6/25/2018	1.31	**3.62**	**4.92**	0.36
038	6/25/2018	1.74	1.42	3.16	1.22
040	6/25/2018	0.67	1.03	1.70	0.65
040	8/21/2018	1.07	1.15	2.22	0.93
040	10/11/2018	0.78	1.21	1.99	0.64
041	6/25/2018	2.06	1.05	3.11	1.97
041	9/17/2018	1.53	0.97	2.51	1.58
042	6/25/2018	1.02	**4.97**	**6.00**	0.21
043	6/25/2018	0.82	1.38	2.20	0.59
044	6/28/2018	1.69	1.13	2.81	1.49
045	8/23/2018	0.97	1.88	2.85	0.52

046	6/28/2018	1.92	0.79	2.71	2.43
047	6/28/2018	0.80	1.21	2.01	0.66
048	7/2/2018	0.83	1.06	1.89	0.78
049	8/23/2018	1.46	**5.02**	**6.49**	0.29
050	7/2/2018	0.88	**2.80**	3.68	0.31
050	9/13/2018	0.95	**2.38**	3.33	0.40
051	7/9/2018	0.82	1.17	1.98	0.70
052	7/9/2018	0.94	1.34	2.29	0.70
053	7/9/2018	1.19	**2.58**	3.78	0.46
053	9/10/2018	1.09	2.28	3.37	0.48
054	7/9/2018	1.05	2.32	3.37	0.45
055	7/12/2018	1.46	**3.19**	**4.65**	0.46
055	9/11/2018	1.62	**3.24**	**4.86**	0.50
056	7/12/2018	1.91	1.34	3.25	1.42
057	7/12/2018	0.91	0.87	1.78	1.04
058	7/16/2018	1.50	**2.88**	**4.39**	0.52
059	7/16/2018	**2.67**	1.25	3.91	2.14
059	10/15/2018	2.49	1.62	4.11	1.54
060	7/16/2018	**3.30**	**2.93**	**6.22**	1.13
060	9/12/2018	1.22	1.88	3.10	0.65
061	7/19/2018	1.76	0.99	2.75	1.79
061	9/12/2018	1.61	1.06	2.67	1.52
062	7/19/2018	1.18	1.57	2.75	0.75
063	7/19/2018	1.41	0.98	2.39	1.44
063	10/12/2018	1.45	0.90	2.35	1.62
064	7/19/2018	**2.54**	1.44	3.97	1.77
065	7/19/2018	1.80	2.24	4.04	0.80
066	7/19/2018	1.14	1.90	3.05	0.60
067	7/26/2018	0.76	1.70	2.45	0.45
068	7/26/2018	1.05	1.44	2.49	0.73
070	8/9/2018	1.68	1.27	2.96	1.32
071	8/20/2018	1.33	1.05	2.38	1.27
072	8/20/2018	0.63	**3.81**	**4.44**	0.16
073	8/21/2018	0.73	1.32	2.05	0.55
074	8/23/2018	1.27	1.66	2.93	0.77
075	9/6/2018	1.13	1.57	2.70	0.72
076	9/10/2018	1.56	**3.46**	**5.02**	0.45
077	9/10/2018	0.90	**2.50**	3.40	0.36
078	9/10/2018	0.99	**2.46**	3.45	0.40
079	9/10/2018	1.71	1.67	3.38	1.03
080	9/10/2018	0.88	1.97	2.85	0.45

081	9/10/2018	0.92	1.76	2.69	0.52
082	9/20/2018	**42.90**	**11.03**	**53.93**	**3.89**
083	9/24/2018	1.33	1.64	2.97	0.82
085	10/1/2018	0.85	1.58	2.43	0.54
086	10/4/2018	0.88	1.63	2.51	0.54
087	10/8/2018	1.32	2.26	3.58	0.59
UTMB-002	01/26/2018	**2.64**	0.88	3.52	**3.01**

Table 5.4 2-hg enantiomer levels measured from sera of 87 patients. Values are reported in μM and bold denotes an increase over the cutoff values as determined in chapter 4.

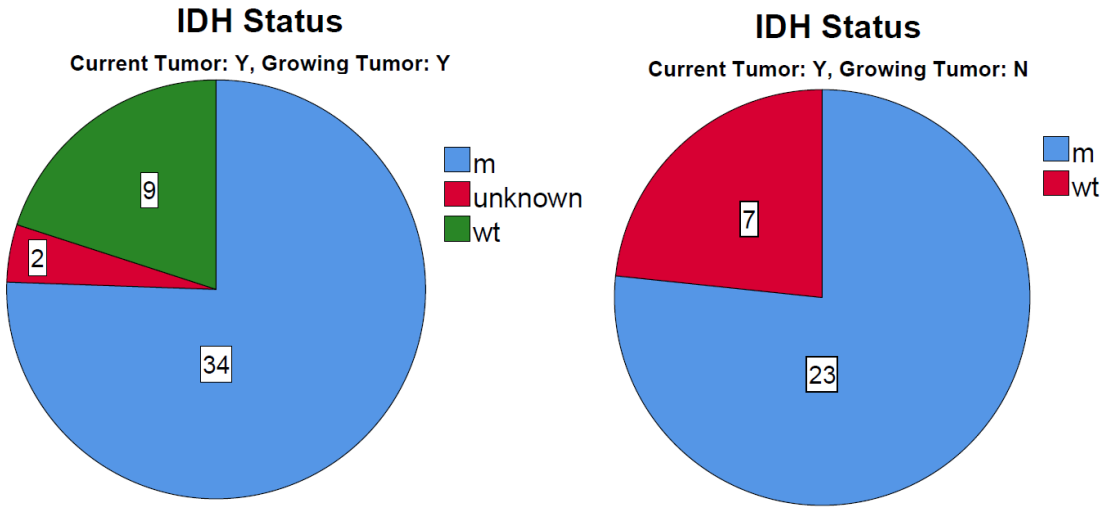

Figure 5.3 IDH Status in patients with stable and growing tumors

Comparison of R-2-hg levels from patients with actively growing IDHmut tumors vs. those with actively growing IDHwt tumors showed no difference (p=0.388) (Figure 5.5A). However, the standard deviation (1.288) and range (6.604) of the IDHmut group was greater than that observed for the IDHwt group (std. dev.= 0.570; range=1.616). Given that the sample size for growing IDHwt tumors was small (n=9), it is likely that a larger sample size is needed to verify that there truly is no difference between groups. Interestingly, there was an increase in R-2-hg levels from samples with stable IDHwt tumors as compared to samples from stable IDHmut tumors (p=0.039) (Figure 5.6A). This was a result of a few

samples in the IDHwt group having an increase in R-2-hg levels (discussed in further detail below).

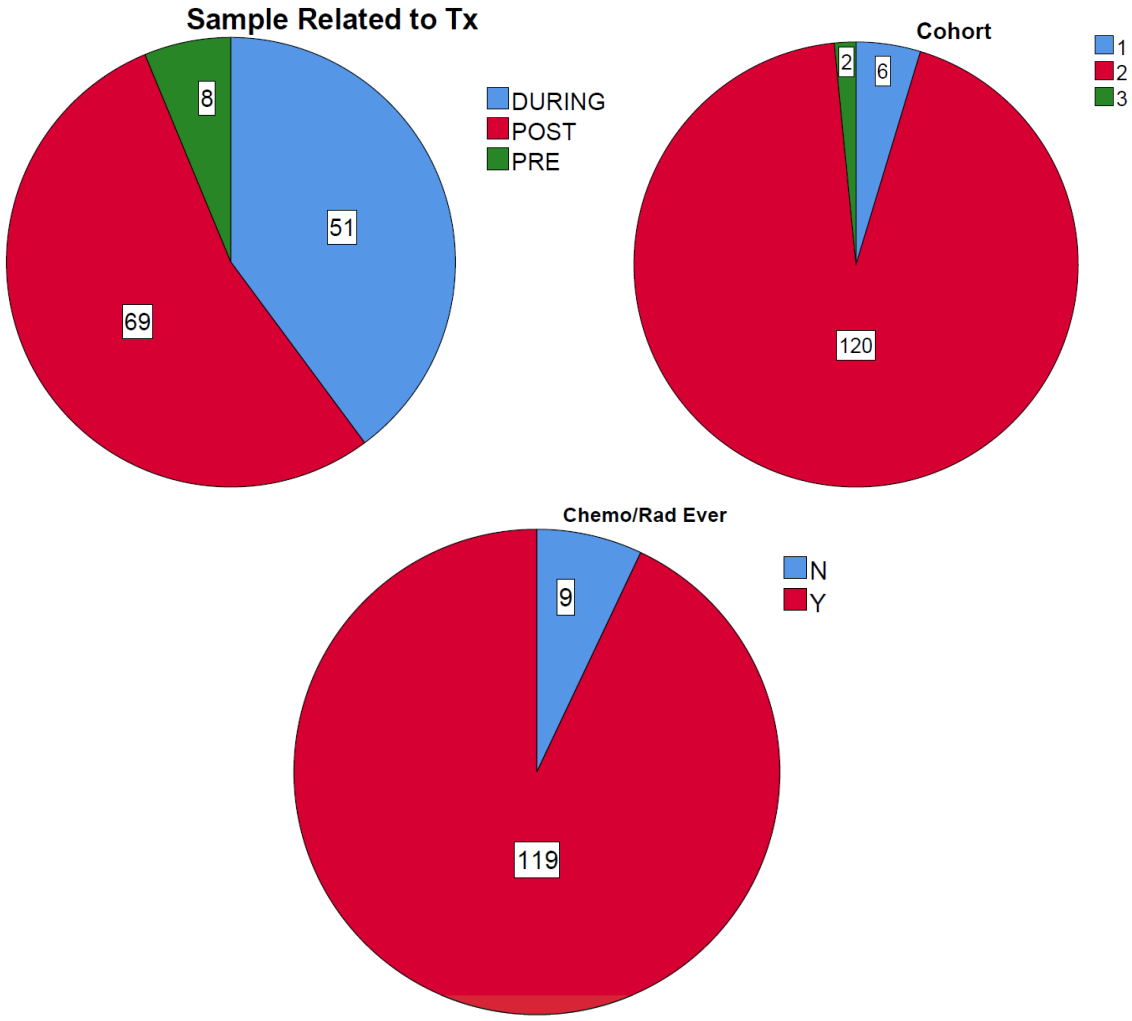

Figure 5.4 Context of samples taken from expanded cohort. Samples were stratified as it related to tx context, cohort, and whether it was taken from a patient that ever received chemo/rad tx.

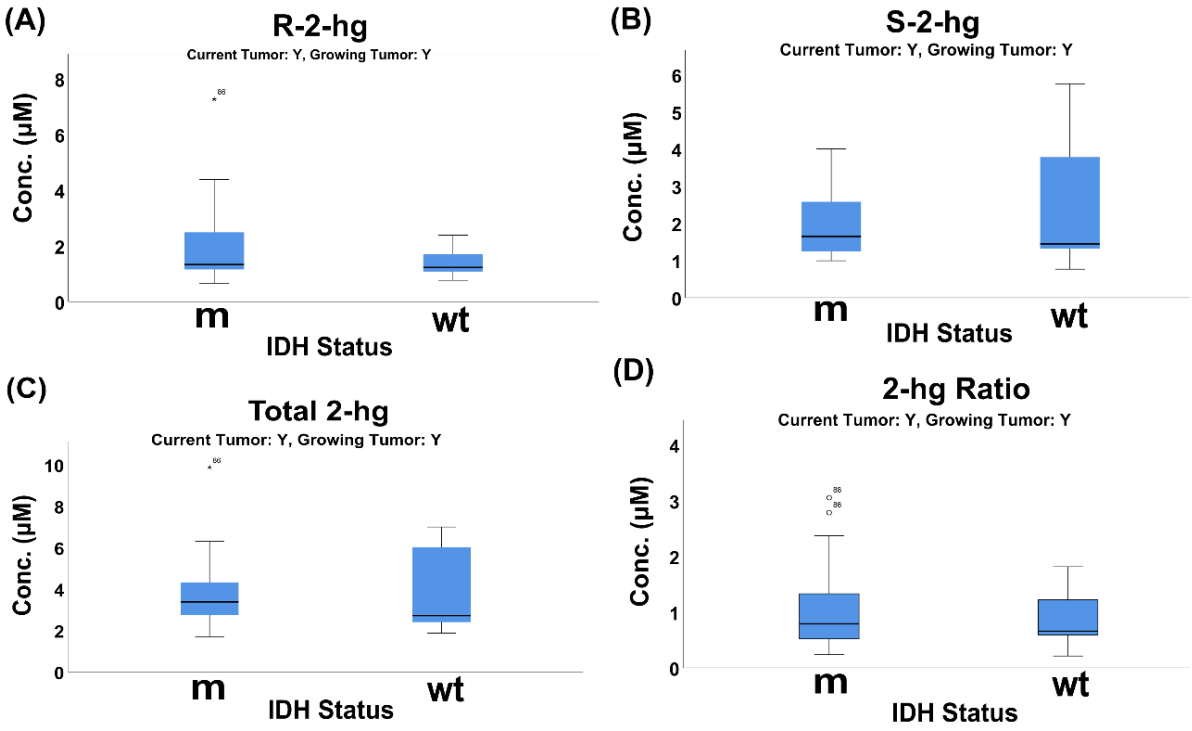

Figure 5.5 2-hg enantiomer levels from samples taken from patients with growing tumors and stratified by IDH status

Measurements of S-2-hg and Total 2-hg also followed the same trend. No difference was observed for between growing IDHmut and IDHwt tumors (S-2-hg, p=0.545; Total 2-hg, p=0.984) (Figure 5.5B-5.5C) but a difference was observed between stable tumors (S-2-hg, p=0.000; Total 2-hg, p=0.003) (Figure 5.6B-5.6C). There were no differences observed for the 2-hg ratio for either stable tumors (p=0.313) (Figure 5.5D) or growing tumors (p=0.434) (Figure 5.6D). Similar to R-2-hg, the standard deviation and range of samples for the 2-hg ratio from IDHmut patients were increased as compared to IDHwt patients, further suggesting that a large sample will be needed to confirm no difference between groups.

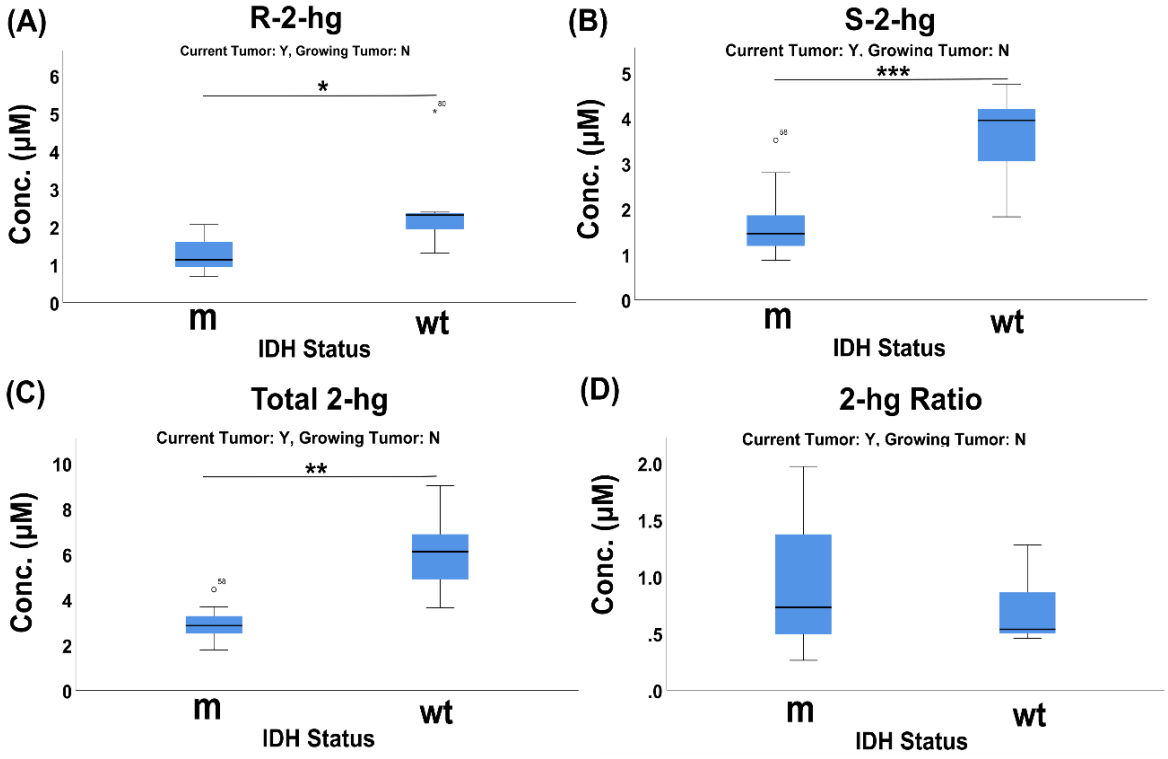

Figure 5.6 2-hg enantiomer levels from samples taken from patients with stable tumors and stratified by IDH status

When all patients with a tumor, regardless of tumor growth, are compared, S-2-hg levels and Total 2-hg levels were found to be increased in patients with IDHwt tumors as compared to samples from IDHmut tumors (p=0.004). Other correlations were also explored to find the possible reason for the observed increase in S-2-hg levels. While no differences were observed between prior treatment with chemo/XRT groups (Yes vs. No), 42/42 (100%) samples with increased S-2-hg were taken from patients either during or after treatment with chemotherapy/XRT. 40/42 (95%) samples came from patients that had ever had treatment with chemo/XRT in their lifetime. This was consistent with the results observed in the pilot study. However, it is important to state that not all of the samples taken from those who did receive prior chemotherapy and/or during/after treatment, had an increase in S-2-hg levels. Further variables will need to be explored to completely

understand the cause of the observed increase in S-2-hg levels, such as the amount of hypoxia and/or the pH content of the tumor microenvironment.

Of the fifteen samples found to have an increase in R-2-hg levels, ten samples were obtained from patients that had evidence of a tumor. Of those ten, nine had actively growing IDHmut tumors. The tenth sample was taken from a patient with a stable IDHwt tumor. The results are consistent with the data from the pilot study in that, of the samples with higher R-2-hg levels, the majority come from patients with IDHmut gliomas. However, not all samples with growing IDHmut tumors (n=34) had an increase in R-2-hg levels. Additionally, the other five samples with an increase in R-2-hg levels were obtained from patients without a tumor as evident by MRI at the time of sample collection. These patients were either undergoing treatment or were post-tx and the increase of observed R-2-hg levels included those who had either a prior IDHwt or IDHmut tumor. One explanation of the data could potentially be from the fact that some residual tumor was present that was not detected by conventional imaging modalities. For those that previously had an IDHwt tumor, there could be some heterogeneity in the tumor (mix of IDHmut and IDHwt). Of particular note is one patient in remission for 4 years with a history of an IDHmut tumor that eventually mutated into a glioblastoma tumor. This patient, patient 082, had R-2-hg and S-2-hg levels significantly higher than any patient at 42 μM and 11 μM, respectively. The patient's case is unique in that the evolved tumor had over 20 driver mutations with >140 variants of unknown significance. Within the unknown biology of this tumor likely lies a mechanism that could be driving the observed continual increase in serum levels of both R-2-hg and S-2-hg.

As mentioned previously, the majority of the samples were taken from patients with a history of disease. Only two samples were obtained from treatment naïve patients (064, UTMB-002), prior to any planned treatment. Both patients had an actively growing IDHmut glioma and had R-2-hg levels above the cutoff. Samples from patient 003, were taken post-surgery (IDHmut tumor) but were chemoXRT naïve. Interestingly, samples

from patient 003 showed a decrease in R-2-hg levels at the same time the tumor was shrinking (as shown by MRI). Consequently, this could mean that relative individual levels could be more useful as a biomarker instead of following absolute cutoffs. Furthermore, only the UTMB-002 sample demonstrated an increase in the 2-hg ratio, demonstrating that the ratio in and of itself is not a sufficient biomarker.

Although increased R-2-hg levels observed from patients that currently had no evidence of tumor could be concerning, recent investigations have shown that an increase in 2-hg levels can occur in the absence of IDH mutation. Elevated 2-hg has now been observed in papillary thyroid carcinoma, breast cancer, AML, renal cell carcinoma, colorectal cancer cells and even non-cancerous tissues such as heart cells during ischemic preconditioning and hematopoietic stem cells during respiratory chain disruption [81], [107]–[112]. These studies challenge the current view that the mutated IDH enzyme is primarily responsible for the increase in intracellular levels of R-2-hg and that other unknown enzymes may be causing an increase in circulating R/S 2-hg levels. The reason, explored in detail elsewhere [113], is likely due to enzyme promiscuity.

Lastly, no specific correlation was observed between 2-hg enantiomer levels and specific allele IDH mutation, tumor type, or tumor grade.

2-hg Lactone

Lactone enantiomers were also measured in the 128 samples using the methodology as outlined in chapter 2 (Table 5.5). Results demonstrate comparable lactone measurements as shown in Table 2.2.

Biological Sample	R-2-hg Surrogate Marker: % Difference of 2-hg enantiomer ratios between MRM transitions	% Peak Area Ratio Lactone S-2-hg:Linear S-2-hg
Serum	0-55	0-83

Table 5.5 Measurement of serum 2-hg lactone enantiomers from the expanded cohort

CONCLUSIONS

In summary, an increase in R-2-hg levels was observed in some patients with an actively growing IDHmut tumor but an R-2-hg increase was never observed in patients with a stable or actively growing IDHwt tumor. However, increased R-2-hg levels were observed in samples from patients without evidence of a tumor. An increase in S-2-hg was observed in a number of patients who have previously received prior chemotherapy/XRT or who were currently receiving chemotherapy/XRT, irrespective of IDHmut status (though higher levels were observed in IDHwt patients overall). In conclusion, the specificity of R-2-hg and S-2-hg from this data is poor and more variables, such as hypoxia, blood-barrier integrity, and concurrent mutations, are needed to correlate the above findings for clinical use.

Chapter 6: Conclusion and Future Work

Parts of this chapter, which include select paragraphs, figures, and tables, are a copy or an adaptation of Strain S. et al. RCM. 2019. doi: 10.1002/rcm.8485. [61] *and Strain S. et al. 2020. doi: 10.1016/j.clinms.2019.11.002* [62].

The primary goals of the work presented herein were to 1) build a clinically amenable MS-based assay for the separation and detection of 2-hg enantiomers, and 2) determine the utility of R-2-hg as a biomarker for IDH-mutant gliomas. Current methods used to detect 2-hg enantiomers suffered from either low sensitivity and/or from the use of protocols that can lead to confounding results. Additionally, to date, no one has measured serum levels of 2-hg enantiomers from patients with IDHmut gliomas.

The novel assay described herein to separate 2-hg enantiomers was a gas chromatography-tandem Mass Spectrometry (GC-MS/MS) assay that utilized a simple non-chiral derivatization and a chiral column to separate 2-hg enantiomers. A simplified extraction protocol was then used to extract 2-hg metabolites and the quantitation of enantiomer levels was achieved by using stable-isotope dilution MS.

The GC-MS/MS assay also distinguished between the 2-hg enantiomers and their corresponding lactones in serum and urine. Separation between the lactone and the linear forms of 2-hg was achieved by monitoring transitions unique to each molecule. This is the first report demonstrating the simultaneous detection of both the (R) and (S) 2-hg lactone enantiomers. Current assays used to detect 2-hg enantiomers either have not addressed the detection of both the lactone and acyclic 2-hg molecules or do not have the capability to do so. The amount of 2-hg lactone detected as shown in chapter 2 varied from sample to sample and is non-negligible. However, further work is needed to understand the biological importance of each 2-hg lactone.

Additionally, ion structures were proposed for the top 4 major ions of 2-hg by comparison of isotopologues from the deuterated and ^{13}C-labeled 2-hg. Of the ions

identified, only one fragment, 117 *m/z*, was unique to the linear 2-hg compound which could have likely led to the confusion by prior studies that the 85 *m/z* must be a cyclic fragment. A new ion structure was proposed with the same molecular formula as the cyclic 85 *m/z*, but one that arose from methanol elimination of the linear 117 *m/z* fragment. The 85 *m/z* fragment then, along with the 57 and 29 *m/z* fragments, were the result of secondary fragmentation. Herein is also the first detailed EI fragmentation method for the acyclic 2-hg compound which showed that methyl ester loss and methanol elimination took precedence over other common mechanisms like the McLafferty rearrangement.

Though the GC-MS/MS assay presented has major advantages over current methods utilized today, the assay could be further improved by 1) finding a robust solid phase extraction protocol which will eliminate the need for liquid-liquid extractions and 2) employing the use of chemical ionization (CI), which allows for the detection of the parent 2-hg molecule (molecular ion) itself rather than its fragments. The interpretation of CI spectra is less complex and would still allow for the simultaneous detection of the lactone enantiomers as well as the linear compounds.

In chapter 3 was demonstrated the power of a GC-VUV assay for the distinguishing of biological isomers. However, this technique is currently only limited to constitutional isomers and cannot readily separate stereoisomers, like 2-hg, by absorption spectra alone. Modification of the GC-VUV by the placement of a filter to allow the sample to be exposed to circularly polarized light and would potentially allow for a difference in absorption spectra between the enantiomers. Currently, the light source in the VUV system is a simple deuterium lamp (Figure 3.1) that emits unpolarized light with a broad spectrum of wavelengths.

The second half of this dissertation then focused on the clinical application of the results from chapters 2 and 3. Chapter 4 addressed a current gap that existed for a reliable reference of 2-hg enantiomer levels. Serum 2-hg enantiomers levels from 60 normal human donors were used to build a reference table for the range of normal values for R-2-hg, S-2-

hg, Total 2-hg, and the 2-hg ratio. As the role of R-2-hg levels as a biomarker becomes further defined, there will be a need for reliable and cutoffs to determine what constitutes an increase in 2-hg enantiomer levels. The data also highlighted the importance of race and age in the development of normal values in order to interpret 2-hg levels appropriately. Interestingly, there was also a moderate association of S-2-hg levels with age. All the findings are still preliminary and further validation using samples from other races and older individuals is needed.

Lastly, in chapter 5, 2-hg enantiomers were measured in samples from patients with IDHmut and IDHwt gliomas. First, a proof of concept was implemented by looking at 11 patients with clinical disease. In that study, R-2-hg levels were increased in 2/3 patients with actively growing disease and S-2-hg levels were increased in a number of samples, regardless of IDH status. Given the promising results, an expanded cohort of 128 samples from a total of 87 patients was implemented. R-2-hg levels were observed to be increased in a number of patients with growing IDHmut gliomas, however, not all patients with growing IDHmut gliomas demonstrated an increase in R-2-hg levels. S-2-hg levels were also increased in a number of patients that received or were currently receiving treatment with chemoXRT, but the compliment did not hold true. It is likely that other variables are needed to explain the observed findings. The increased values as measured from the brain tumors have never been recorded previously and were significantly different than the values measured from normal human sera. Additionally, it was shown that total 2-hg levels and the 2-hg ratio alone is insufficient and that the separation and detection of each enantiomer is more important to study the use of 2-hg as a biomarker. In order to elucidate the observed lack of specificity, future work will need to focus on the following: more samples from treatment naïve patients, full genetic sequencing of every tumor, and a robust, methodology to measure tumor microenvironment variables, such as pH, oxygen levels, and the integrity of the blood-brain barrier. Overall, the work presented herein takes

a significant first step in providing the tools and framework for understanding the clinical implications of tumor biology on circulating R-2-hg and S-2-hg levels.

Appendix A: Statistical Assumptions

NORMALITY AND VARIANCE TESTS

Tests of Normality[a]

	Kolmogorov-Smirnov[b]			Shapiro-Wilk		
	Statistic	df	Sig.	Statistic	df	Sig.
R2hg-SerumConc-117 (pmol/uL)	.133	30	.184	.919	30	.025
S2hg-SerumConc-117 (pmol/uL)	.151	30	.080	.936	30	.069
Total2hg-117	.122	30	.200*	.941	30	.100
RSratio2hg-117	.111	30	.200*	.933	30	.060

*. This is a lower bound of the true significance.

a. Sex = F

b. Lilliefors Significance Correction

Tests of Normality[a]

	Kolmogorov-Smirnov[b]			Shapiro-Wilk		
	Statistic	df	Sig.	Statistic	df	Sig.
R2hg-SerumConc-117 (pmol/uL)	.146	30	.102	.897	30	.007
S2hg-SerumConc-117 (pmol/uL)	.100	30	.200*	.969	30	.522
Total2hg-117	.146	30	.100	.951	30	.185
RSratio2hg-117	.141	30	.130	.940	30	.091

*. This is a lower bound of the true significance.

a. Sex = M

b. Lilliefors Significance Correction

Figure A1. Normality tests for distribution of R-2-hg, S-2-hg, Total 2-hg, and 2-hg Ratio as divided by sex. P-value < 0.05 indicates distribution is not normally distributed

Tests of Normality[a]

	Kolmogorov-Smirnov[b]			Shapiro-Wilk		
	Statistic	df	Sig.	Statistic	df	Sig.
R2hg-SerumConc-117 (pmol/uL)	.135	20	.200*	.913	20	.071
S2hg-SerumConc-117 (pmol/uL)	.127	20	.200*	.955	20	.448
Total2hg-117	.106	20	.200*	.961	20	.571
RSratio2hg-117	.162	20	.177	.911	20	.066

*. This is a lower bound of the true significance.

a. Race = B

b. Lilliefors Significance Correction

Tests of Normality[a]

	Kolmogorov-Smirnov[b]			Shapiro-Wilk		
	Statistic	df	Sig.	Statistic	df	Sig.
R2hg-SerumConc-117 (pmol/uL)	.149	20	.200*	.902	20	.045
S2hg-SerumConc-117 (pmol/uL)	.168	20	.141	.950	20	.366
Total2hg-117	.183	20	.079	.931	20	.163
RSratio2hg-117	.170	20	.131	.938	20	.223

*. This is a lower bound of the true significance.

a. Race = C

b. Lilliefors Significance Correction

Tests of Normality[a]

	Kolmogorov-Smirnov[b]			Shapiro-Wilk		
	Statistic	df	Sig.	Statistic	df	Sig.
R2hg-SerumConc-117 (pmol/uL)	.174	20	.115	.933	20	.180
S2hg-SerumConc-117 (pmol/uL)	.241	20	.004	.859	20	.008
Total2hg-117	.149	20	.200*	.915	20	.081
RSratio2hg-117	.155	20	.200*	.916	20	.082

*. This is a lower bound of the true significance.

a. Race = H

b. Lilliefors Significance Correction

Figure A2. Normality tests for distribution of R-2-hg, S-2-hg, Total 2-hg, and 2-hg Ratio as divided by race. P-value < 0.05 indicates distribution is not normally distributed

Levene's Test of Equality of Error Variances[a,b]

		Levene Statistic	df1	df2	Sig.
R2hg-SerumConc-117 (pmol/uL)	Based on Mean	3.860	2	57	.027
	Based on Median	3.953	2	57	.025
	Based on Median and with adjusted df	3.953	2	52.830	.025
	Based on trimmed mean	3.878	2	57	.026

Tests the null hypothesis that the error variance of the dependent variable is equal across groups.

a. Dependent variable: R2hg-SerumConc-117 (pmol/uL)

b. Design: Intercept + Race

Levene's Test of Equality of Error Variances[a,b]

		Levene Statistic	df1	df2	Sig.
S2hg-SerumConc-117 (pmol/uL)	Based on Mean	.162	2	57	.851
	Based on Median	.128	2	57	.880
	Based on Median and with adjusted df	.128	2	46.757	.880
	Based on trimmed mean	.138	2	57	.872

Tests the null hypothesis that the error variance of the dependent variable is equal across groups.

a. Dependent variable: S2hg-SerumConc-117 (pmol/uL)

b. Design: Intercept + Race

Levene's Test of Equality of Error Variances[a,b]

		Levene Statistic	df1	df2	Sig.
Total2hg-117	Based on Mean	1.960	2	57	.150
	Based on Median	1.811	2	57	.173
	Based on Median and with adjusted df	1.811	2	55.191	.173
	Based on trimmed mean	2.009	2	57	.144

Tests the null hypothesis that the error variance of the dependent variable is equal across groups.

a. Dependent variable: Total2hg-117

b. Design: Intercept + Race

Levene's Test of Equality of Error Variances[a,b]

		Levene Statistic	df1	df2	Sig.
RSratio2hg-117	Based on Mean	.029	2	57	.971
	Based on Median	.001	2	57	.999
	Based on Median and with adjusted df	.001	2	48.088	.999
	Based on trimmed mean	.013	2	57	.987

Tests the null hypothesis that the error variance of the dependent variable is equal across groups.

a. Dependent variable: RSratio2hg-117

b. Design: Intercept + Race

Figure A3. Test of equal variances across race

Levene's Test of Equality of Error Variances[a,b]

		Levene Statistic	df1	df2	Sig.
R2hg-SerumConc-117 (pmol/uL)	Based on Mean	.000	1	58	.985
	Based on Median	.025	1	58	.875
	Based on Median and with adjusted df	.025	1	54.857	.875
	Based on trimmed mean	.005	1	58	.946

Tests the null hypothesis that the error variance of the dependent variable is equal across groups.

a. Dependent variable: R2hg-SerumConc-117 (pmol/uL)

b. Design: Intercept + Sex

Levene's Test of Equality of Error Variances[a,b]

		Levene Statistic	df1	df2	Sig.
S2hg-SerumConc-117 (pmol/uL)	Based on Mean	.588	1	58	.446
	Based on Median	.317	1	58	.575
	Based on Median and with adjusted df	.317	1	56.634	.575
	Based on trimmed mean	.577	1	58	.451

Tests the null hypothesis that the error variance of the dependent variable is equal across groups.

a. Dependent variable: S2hg-SerumConc-117 (pmol/uL)

b. Design: Intercept + Sex

Levene's Test of Equality of Error Variances[a,b]

		Levene Statistic	df1	df2	Sig.
Total2hg-117	Based on Mean	.852	1	58	.360
	Based on Median	.679	1	58	.413
	Based on Median and with adjusted df	.679	1	57.828	.413
	Based on trimmed mean	.846	1	58	.361

Tests the null hypothesis that the error variance of the dependent variable is equal across groups.

a. Dependent variable: Total2hg-117

b. Design: Intercept + Sex

Levene's Test of Equality of Error Variances[a,b]

		Levene Statistic	df1	df2	Sig.
RSratio2hg-117	Based on Mean	.557	1	58	.459
	Based on Median	.527	1	58	.471
	Based on Median and with adjusted df	.527	1	54.326	.471
	Based on trimmed mean	.469	1	58	.496

Tests the null hypothesis that the error variance of the dependent variable is equal across groups.

a. Dependent variable: RSratio2hg-117

b. Design: Intercept + Sex

Figure A4. Test of equal variances across sex

Appendix B: IRB Protocols

The IRB protocol listed below is an adaptation of the protocol that was used to collect samples at Austin Brain Tumor Center in Austin, TX, reformatted for the purposes of this dissertation. The same protocol was submitted to the UTMB IRB with an addendum to only collect blood samples under cohort 1.

Measurement of 2-hydroxyglutarate enantiomer levels for use as a biomarker in management of patients with IDH mutant gliomas

Study Chair
Morris Groves, M.D.
Austin Brain Tumor Center
Texas Oncology
Austin, TX

Study Co-Chairs
Mark Emmett, Ph.D.
Biochemistry and Molecular Biology
University of Texas Medical Branch
Galveston, TX

Kelly Olino, M.D.
Surgical Oncology
University of Texas Medical Branch
Galveston, TX

Table of Contents:

1.0 Background

IDH mutations and glioma

Next-generation sequencing of brain tumors with poor long-term survival, grade IV gliomas (glioblastoma), has revealed recurrent mutations in a cellular metabolism gene, isocitrate dehydrogenase (IDH)[95]. Further investigation showed that *IDH* mutations were mainly prevalent in >80% of grade II/III gliomas and secondary grade IV gliomas (tumors that progressed from a lower grade).[3] *IDH* mutations have also been identified in other human cancers such as acute myeloid leukemia, intrahepatic cholangiocarcinoma, and chondrosarcoma.[5], [6], [14] The IDH enzyme normally catalyzes the conversion of isocitrate to α-ketoglutarate (α-KG) in the Krebs cycle (**fig. 1a**).[114] However, the enzyme activity of mutant *IDH* (mutIDH) produces high levels of the oncometabolite, (R)-2-hydroxyglutarate [(R)-2HG], instead (**fig 1b**).[7] (R)-2HG has been reported to exert proliferative and various other tumorigenic effects on cancer cells and has been proposed as a novel biomarker for mutant *IDH* status.[11], [29]

Initially, levels of circulating total 2-hydroxyglutarate (2HG) were studied for use a biomarker in patients with *IDH* mutant cancers.[5], [41], [80], [81], [101], [102], [105], [115] Total 2HG levels were measured by conventional mass spectrometry which did not differentiate between, (R)-2HG, the molecule produced by the tumor, and its naturally occurring enantiomer, (S)-2HG. (S)-2HG is made normally in the body during metabolism of α-KG by L-malate dehydrogenase and can be present in circulation at levels comparable to (R)-2HG (**fig. 1c & 1d**).[11] Studies

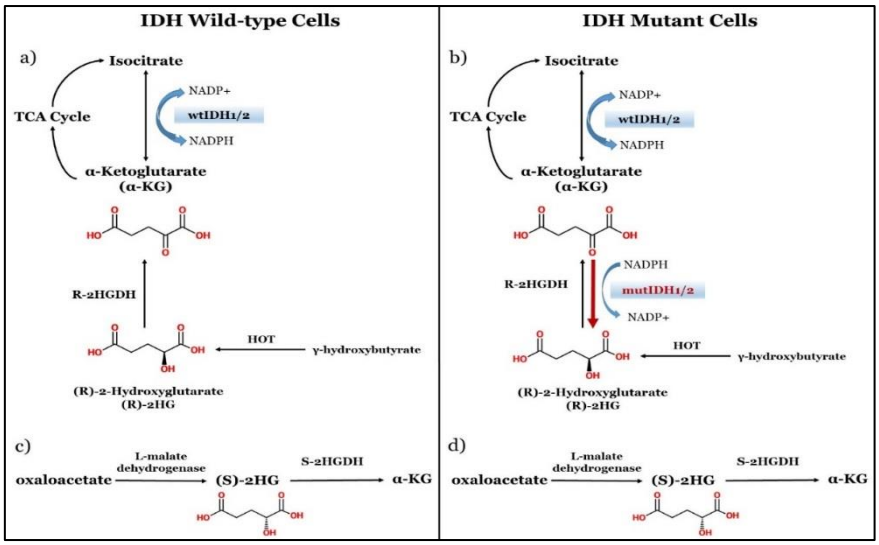

Figure B1. Isocitrate dehydrogenase metabolic pathways in IDH wild-type cells and IDH mutant cells.

measuring total serum 2HG as a biomarker have reported inconsistent results. Total 2HG levels have been shown to be correlated with mutation status in serum of AML patients and cholangiocarcinoma patients.[80], [103] Conversely, another study has shown that total 2HG levels are a poor predictor of outcome in AML

patients.[81] Another separate study with glioma patients reported an increase in mean total 2HG levels in the urine, but not in serum.[101] The discrepancy between results of the aforementioned studies likely arises from measuring total 2HG levels and not distinguishing between (R)-2HG and (S)-2HG. Methods that do not differentiate between (R)-2HG and (S)-2HG can lead to a loss of correlation between an increase in the relevant (R) enantiomer of 2HG and clinically significant information, such as an increase in tumor burden.

The proposed study will address the use of 2HG as a clinical biomarker by distinguishing between the metabolite produced by an *IDH* mutant tumor, (R)-2HG, and the metabolite produced by normal cells, (S)-2HG. The levels (R) & (S) 2HG will be measured in the serum and urine of glioma patients, with and without *IDH* mutations, and reported as a ratio of the two molecules, (R)-2HG:(S)-2HG. A recent study measuring each 2HG enantiomer in the blood of AML patients has reported that (R)-2HG:(S)-2HG is a more specific marker for *IDH* mutation status and clinical status.[15]

Currently, it is not known if, and how, *IDH1* mutations can be used to guide treatment. The study proposed will address this question. The study will be useful in demonstrating the utility of measuring 2HG enantiomers as a diagnostic tool for identifying patients with *IDH* mutant gliomas, assessing tumor burden, and monitoring treatment response. Additionally, the assay can be used for the evaluation of the effectiveness of novel therapeutics targeted to *IDH* mutant tumors that are currently in clinical trials, which would be advantageous due to current limits of tumor monitoring via imaging.[97]

<u>The potential benefit for management of patients with mutIDH low-grade gliomas</u>

The study will also demonstrate the utility of measuring 2HG enantiomers to inform and improve the treatment of patients with low-grade gliomas. Low-grade gliomas (LGGs) are slow growing and progression is hard to measure by imaging. This creates difficulty in making treatment decisions, particularly in asymptomatic patients. The management of patients with LGG include: 1) deferment of treatment with serial MRI to monitor for evidence of progression, 2) surgery if technically possible while preserving neurologic function, 3) chemotherapy, and/or 4) radiotherapy. Each type of therapeutic intervention carries significant side effects that range from cognitive impairment to systemic bone marrow toxicity and even relapse with a more aggressive tumor. Due to the need to balance the benefits and drawbacks of treatments, new method to measure tumor burden, stability and progression in LGG patients is needed. Since >80% of grade II tumors harbor *IDH* mutations, the use of a 2HG biomarker, specifically the measurement of (R)-2HG & (S)-2HG, could significantly aid in treatment planning for a large number of LGG patients.[11]

2.0 Rationale and Objectives

<u>Rationale</u>

2-hydroxyglutarate is currently being studied for use a clinical biomarker in patients with *IDH* mutant cancers.[5], [41], [80], [81], [101], [102], [105], [115]

To date, the utility of the tumor producing metabolite, (R)-2-HG, for clinical management of patients with *IDH* mutant gliomas has yet to be studied. Thus, the absolute levels of (R)-2HG, or the ratio of (R)-2HG:(S)-2HG, could have a significant impact as a biomarker in management of patients with *IDH* mutant gliomas.

Primary Objective:

To determine whether absolute levels of (R)-2HG or (R)-2HG:(S)-2HG in serum/urine can be used as a biomarker for tumor burden in patients with *IDH* mutant gliomas.

Secondary Objectives:

1. To determine whether absolute levels of (R)-2HG or (R)-2HG:(S)-2HG in serum/urine can predict tumor growth prior to evidence of growth on imaging
2. To correlate absolute levels of (R)-2HG or (R)-2HG:(S)-2HG in serum/urine with treatment response for patients undergoing treatment with surgery, chemotherapy and/or radiotherapy.
3. To determine whether absolute levels of (R)-2HG or (R)-2HG:(S)-2HG in serum/urine can predict the IDH mutant status of tumor
4. To determine whether absolute levels of (R)-2HG or (R)-2HG:(S)-2HG in serum/urine correlate with tumor grade
5. To correlate absolute levels of (R)-2HG or (R)-2HG:(S)-2HG in serum/urine with allelic variants of tumor IDH mutation

3.0 Inclusion/Exclusion Criteria

Subjects must meet all of the inclusion criteria in order to be eligible to participate in the study.

Inclusion criteria are:

1. Any patient with, or presumed to have a, grade II, III, or IV glioma with an IDH mutation (mutIDH group) or without an IDH mutation (control).
2. Subject has provided informed consent and is willing and able to comply with the study procedures.
3. Adults at least 18 years of age at the time of consent.

Subjects meeting any of the exclusion criteria at baseline will be excluded from study participation.

Exclusion criteria are:

1. Patient has been diagnosed with an inborn error of metabolism
2. Patients with renal failure (creatinine>1.6, GFR < 90) or liver failure (elevated aminotransferases > 3X ULN, prolonged prothrombin time > 2X ULN, elevated bilirubin > 2X ULN and/or jaundice).

All patients will read and sign an informed consent document prior to participating in this study. The informed consent document will be explained to the patient to ensure that the participant understands the purpose of the collection. If the individual does not understand the protocol, the principal investigator or the attending physician will be notified of the patient's concerns or lack of knowledge. The informed consent process will be documented in the patient's medical record.

4.0 Study Design

Patients will be stratified into three cohorts as detailed below.

Cohort 1 will consist of patients who have or will undergo treatment by surgical resection only. Patients will: 1) be presumed to have or have had a primary brain tumor based on radiographic imaging 2) have had surgical resection or have plans for surgical resection of their tumor and 3) have plans for follow-up with an investigator in this study. When possible, blood and urine samples will be taken preoperatively within 30 days prior to resection. Tumor volume will also be measured preoperatively using T2/FLAIR brain MRI within 30 days prior to resection. Within 30 days after surgical resection, imaging will be performed and another blood/urine sample will be taken at the post-surgical follow-up. All blood/urine samples will be collected within 14 days of MRI imaging. Patients will be subsequently be followed up at regular intervals, during which blood and urine will be collected, in addition to further MRI evaluations. Typical time to follow-up for patients is every 2-3 months for the first year after resection and every 4 months for the year after. However, patients with grade IV gliomas typically have blood taken twice a month (day 1 and day 22 of a 28-day cycle). If progression occurs and adjuvant therapy is indicated, patient will be placed into cohort 2. Patients will be followed until the end of the study, or until discontinuation for other reasons listed in **7.0 study withdrawal/discontinuation**.

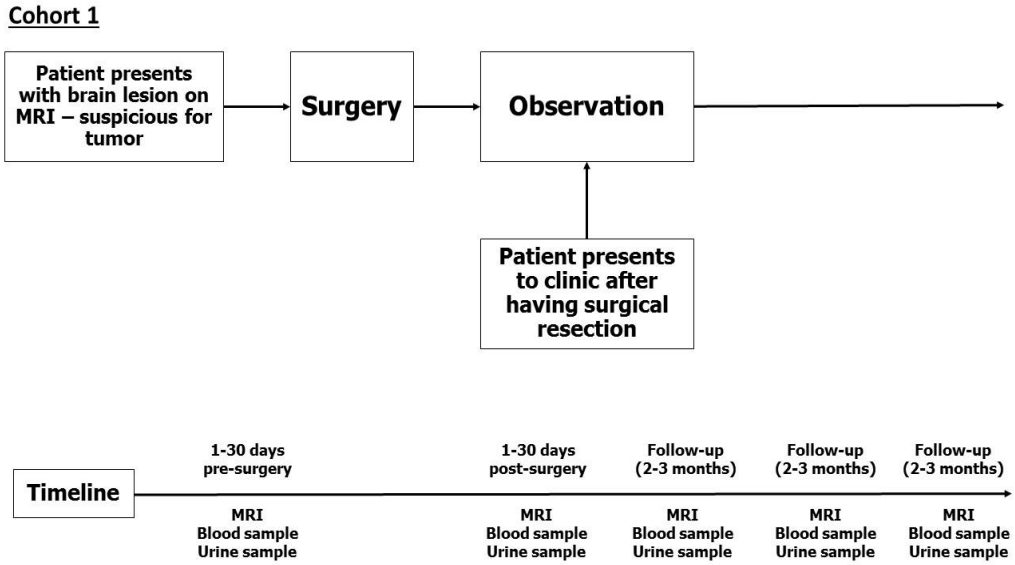

Figure B2**.** Patient sample collection workflow for cohort 1

Cohort 2 will consist of patients who have or will undergo treatment by surgical resection followed by adjuvant therapy (chemotherapy/radiotherapy). Patients will: 1) be presumed to have a primary brain tumor based on radiographic imaging 2) have had surgical resection or have plans for surgical resection of their tumor and 3) have plans for follow-up with an investigator in this study for chemotherapy/radiotherapy. When possible, blood and urine samples will be taken preoperatively within 30 days prior to resection. Tumor volume will also be measured preoperatively using T2/FLAIR brain MRI within 30 days prior to resection. Within 30 days after surgical resection, imaging will be performed and another blood/urine sample will be taken at the post-surgical follow-up. All blood/urine samples will be collected within 14 days of MRI imaging. Further imaging and sample collection will take place at each clinic visit during and after completion of adjuvant therapy. Patients will then enter observation follow-up as described in cohort 1. Patients will be followed until the end of the study, or until discontinuation for other reasons listed in **7.0 study withdrawal/discontinuation**.

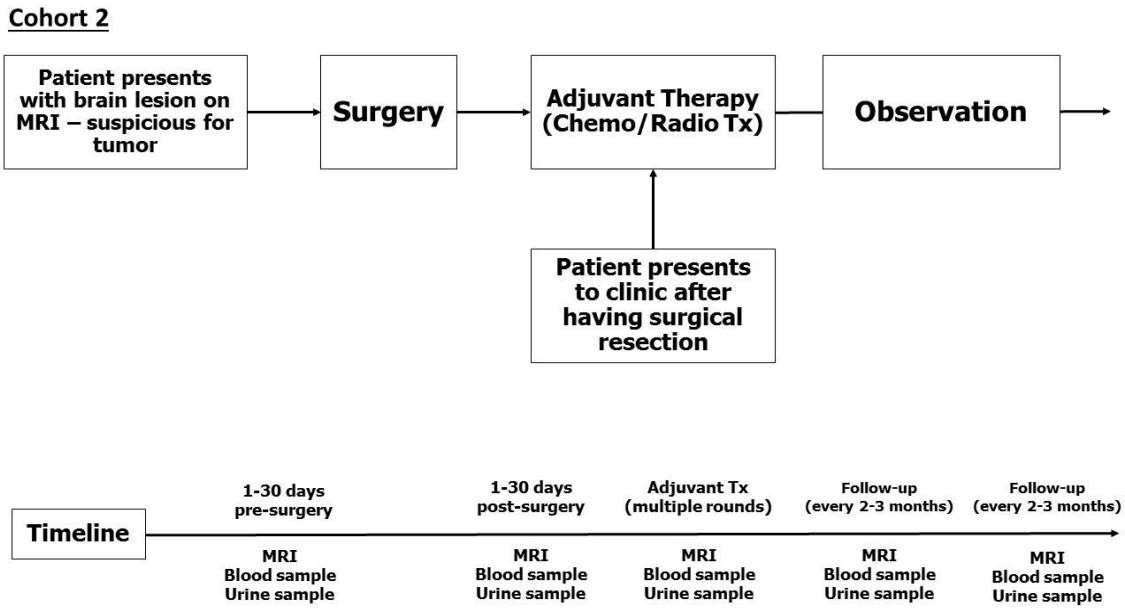

Figure B3. Patient sample collection workflow for cohort 2

Cohort 3 will consist of patients are on a surveillance treatment plan. These patients will typically have a stable or slow-growing, that is presumed to be a low-grade IDH mutant glioma that is based upon radiographic features alone.[116] Tumors in these patients are presumed to be low-grade based upon characteristic radiographic features. MRI imaging, and peripheral blood/urine samples will be collected at each clinic follow-up until the study ends, or if the patient's tumor progresses. All blood/urine samples will be collected within 14 days of MRI imaging. If the patient's tumor progresses, the patient will be placed in cohort 1 or 2, depending upon the chosen treatment plan. The number of patients in this cohort is expected to be small (<10).

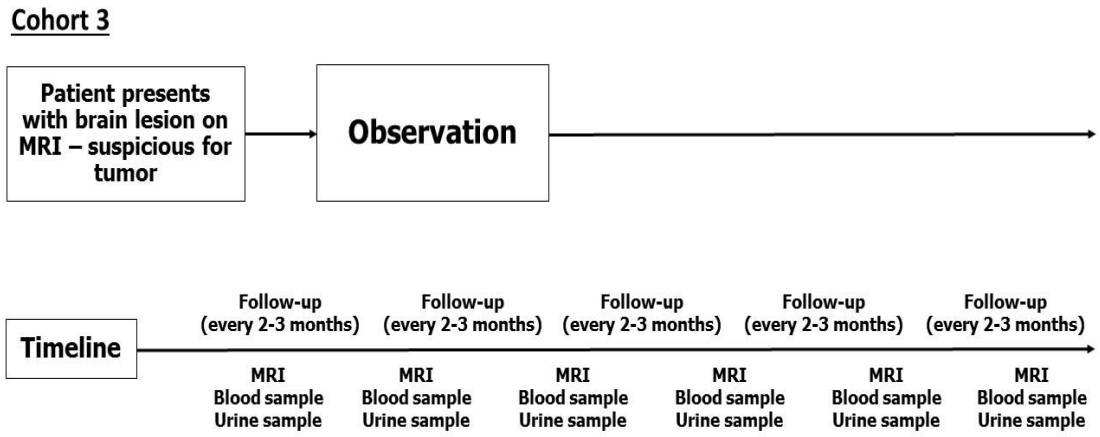

Figure B4. Patient sample collection workflow for cohort 3

Additional optional sample collection

When permissible, optional patient samples will be collected for analysis of 2HG enantiomers to provide additional information of a patient's tumor. If possible, cerebrospinal fluid (CSF) will be collected either preoperatively or perioperatively. Additionally, if a patient is indicated to undergo a spinal tap for any reason, any residual CSF will be collected and frozen. Lastly, any frozen tumor tissue that remains available may be requested, for use in additional studies.

Power Analysis

To date, no study has individually measured (R)-2HG or (S)-2HG in the blood of patients with IDH mutant gliomas. Therefore, proper statistical modeling to estimate the needed number of patient for the study cannot be performed. However, the first initial 10 samples will be used in a pilot study to estimate the total number of samples needed for this study. Specifically, samples from the first initial 10 patients (5 in mutIDH group; 5 in control group) in cohorts 1 and 2 will be used to perform a statistical power analysis to determine how many patients will be needed to stop accruing samples. When this stopping number has been reached, the study will end.

A previous study that has measured (R) and (S) 2HG in cerebrospinal fluid of patients with *IDH* mutant gliomas accrued a total of 84 patients (16 mutIDH, 68 wtIDH). Even with an unbalanced sample size, the study was able to show statistically significant difference in (R)-2HG (and higher ratio) between patients with *IDH* mutants gliomas and *IDH* wild-type gliomas. We anticipate accruing a similar number of total patients. Approximately 100 patients will be recruited for the initial study and another 50 for a validation study. A total of approximately 150 total, with a close balance in the number of patients with wtIDH and mutIDH tumors. A conservative estimate of a difference of enantiomer levels of 33.3%, to achieve a power of 0.95, with a significance level of 0.05, a minimal sample size of 92 would be required.

As stated above we plan accruing approximately 150 patients. On average we anticipate an average 8-12 samples per patient, depending closely upon their treatment plan. For example when a patient is undergoing active treatment, they might have 6-8 samples taken in the first year and then 4-6 samples taken in while under surveillance the next year.

To date, no studies have investigated 2HG enantiomer levels in the serum or urine of patients with mutIDH gliomas. Therefore, we plan on using the pilot data to make predictions about what range of (R)/(S) 2HG levels are meaningful, and how these levels can be correlated to imaging findings and clinical outcome.

5.0 Study Procedures

Sample Collection

Peripheral venous blood will be acquired via venipuncture, where approximately 25mL of blood will be drawn into rapid serum tubes for analysis. Fifteen milliliters will be used for standard laboratory analysis (5mL for complete blood counts, 5mL for complete metabolic panel, and 5mL in case of need for further testing later). The last 10mL will be acquired to collect serum for use in the study. Serum is separated according to manufacturer recommendations. Briefly, blood in rapid serum tubes will be inverted 5-6 times to mix blood with clot activator. The tubes will then be centrifuged at 23-27°C at 2000g for 4 minutes, decanted into cryotubes, and stored immediately at -80°C. Approximately 10mL of urine will be collected, decanted into cryotubes, and frozen immediately at -80°C. All frozen samples for analysis will be de-identified and shipped overnight in dry ice to UTMB and analyzed as described below.

Serum analysis for levels of (R) & (S) 2HG

2HG analysis will be performed using chiral Gas-chromatography-Mass spectrometry (GC-MS). This method utilizes a chiral gas chromatography column which separates the two molecules in time before mass analysis with the mass spectrometer (**fig. 5**). GC-MS is a robust, quick, and versatile technique that identifies a molecule based upon the retention time (as measured by GC) and its mass (as measured by mass spectrometry). Separation in retention time using chiral GC is necessary since the two enantiomers of 2HG have the same mass. As stated before, previous studies did not separate the two molecules and measured both at the same time. Individual changes in (R)-2HG and (S)-2HG concentrations could not be determined. The procedure to measure 2HG enantiomers by chiral GC-MS is as follows. Metabolites, which in include the 2HG enantiomers, will be extracted using 80% methanol, as previously described.[117] One mL of sample is mixed with 4 mL of 80% methanol (-80°C) and centrifuged at 140000xg for 20min at 4°C. The supernatant is then removed, dried by vacuum centrifugation and derivatized using trimethylsilyl-diazomethane. This allows the molecules to enter the gas phase for analysis with GC-MS. A β-cyclodextrin column (a chiral column) will be used as the chiral GC column to separate the two 2HG enantiomers. The enantiomers are then fragmented via electron ionization for mass analysis.

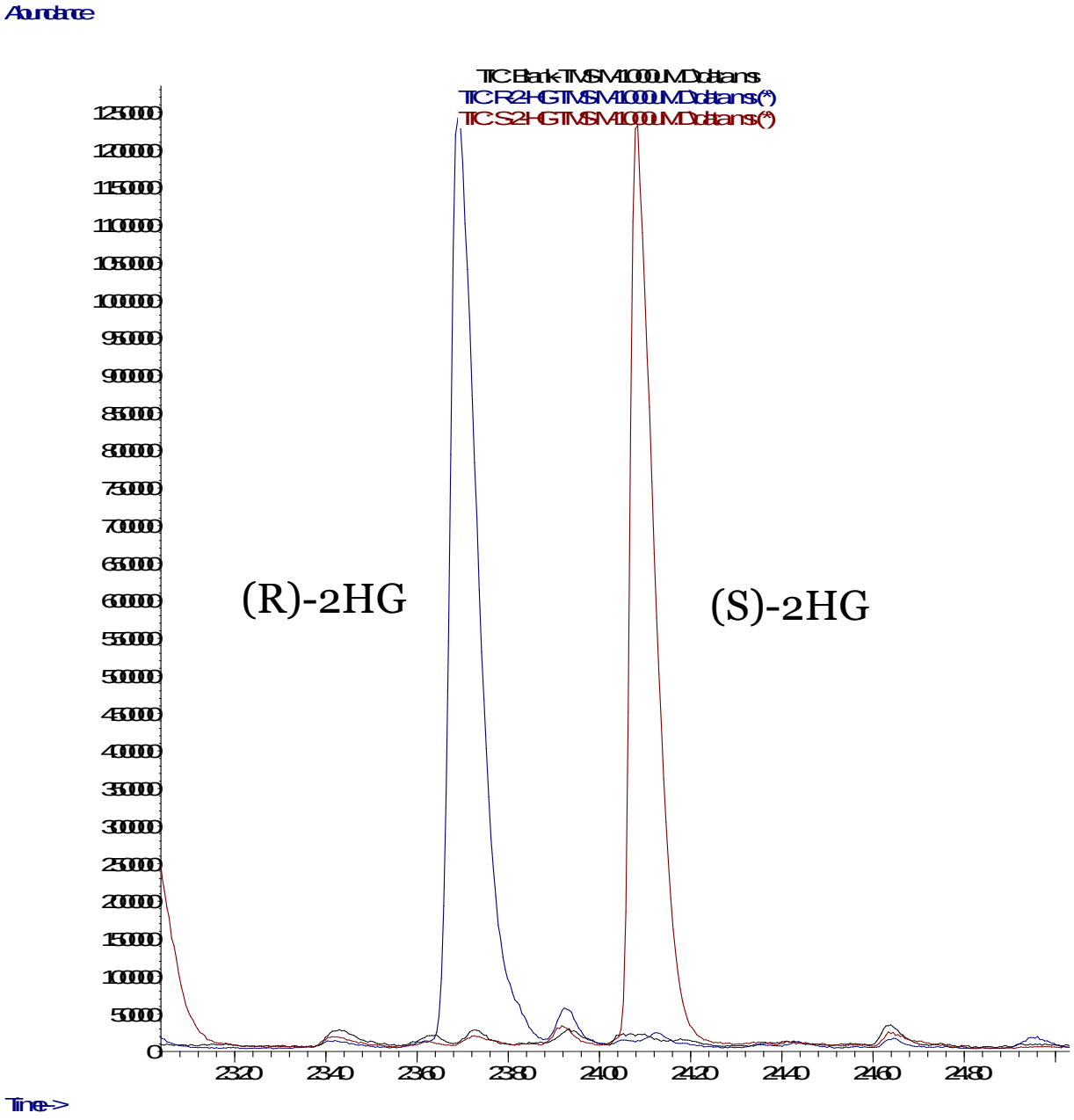

Figure B5. Separation of (R)-2HG (blue peak) and (S)-2HG (red) using chiral gas chromatography

6.0 Study Procedure Risks

Blood collection will already be a part of standard medical care for the patient. Therefore, the study poses no added risk to the patient. Urine collection may not be a part of the standard medical care but poses negligible added risk. Overall, blood and urine collection pose a minimal-to-no risk to the patient. Rare but potential risks for blood collection are listed below.

Venipuncture Blood Draw

Possible risks include hematoma, pain, phlebitis, vasovagal reaction, and anxiety/fear.

7.0 Study Withdrawal/Discontinuation

A study subject will be discontinued from participation in the study if any of the following occur:

- A medical condition or situation occurs such that continued participation in the study would not be in the best interest of the subject in the opinion of the treating investigator
- Development of any exclusion criteria
- Subject withdrawals consent to continue in the research for any reason
- Study ends due to sufficient number of samples collected

8.0 Ethics and Protection of Human Subjects

The investigator will ensure that this study is conducted in full conformity with the principles set forth in The Belmont Report: Ethical Principles and Guidelines for the Protection of Human Subjects of Research of the US National Commission for the Protection of Human Subjects of Biomedical and Behavioral Research (April 18, 1979) and codified in 45 CFR Part 46 and/or the ICH E6; 62 Federal Regulations 25691 (1997).

The investigator must provide for the review and approval of this protocol and the associated informed consent documents and recruitment material by an appropriate independent ethics committee (IEC) or IRB registered with the OHRP. Any amendments to the protocol or consent materials must also be approved before they are placed into use. In the United States and in other countries, only institutions holding a current US Federalwide Assurance issued by OHRP may participate.

Informed consent is a process that is initiated prior to the individual's agreeing to participate in the study and continuing throughout the individual's study participation. Extensive discussion of risks and possible benefits of this therapy will be provided to the subjects and their families. Consent forms describing in detail the study interventions/products, study procedures, and risks are given to the subject and written documentation of informed consent is required prior to starting intervention/administering study product. Consent forms will be IRB-approved, and the subject will be asked to read and review the document. Upon reviewing

the document, the investigator will explain the research study to the subject and answer any questions that may arise. The subjects will sign the informed consent document prior to any procedures being done specifically for the study. The subjects should have the opportunity to discuss the study with their surrogates or think about it prior to agreeing to participate. The subjects may withdraw consent at any time throughout the course of the trial. A copy of the informed consent document will be given to the subjects for their records. The rights and welfare of the subjects will be protected by emphasizing to them that the quality of their medical care will not be adversely affected if they decline to participate in this study.

Privacy/Confidentiality Issues

All samples will be handled and stored by Dr. Morris Groves and the Dr. Mark Emmett laboratory. Patient identifiers (name, address, etc.) will be removed from the study samples and labeled only with a unique study number and a date. The study number will be used to identify a patient, but it will only be accessed by Dr. Morris Groves and his staff. Analysis by Dr. Mark Emmett laboratory will be blind to patient information but not the results of the 2HG analysis. All clinical data will be kept by Dr. Groves in computer files. No data that could be used to identify a patient will be shared with persons not involved in the study. No confidential patient information will be published or discussed in a way that violates patient privacy rights.

Subject confidentiality is strictly held in trust by the participating investigators, their staff, and the sponsor(s) and their agents. This confidentiality is extended to cover testing of biological samples and genetic tests in addition to the clinical information relating to participating subjects.

The study protocol, documentation, data, and all other information generated will be held in strict confidence. No information concerning the study or the data will be released to any unauthorized third party without prior written approval of the Principal Investigator. All patient data will be stored in a password sensitive server and at the treating facility (Texas Oncology). Research data will also be stored in secured storage disks/servers at UTMB and Texas Oncology.

Individuals authorized to view study records will be identified to the study subject on the informed consent but may include a study monitor or other authorized representatives of the sponsor or funding agency or federal or local agencies that regulate research including representatives from the Food and Drug Administration, Office of Human Research Protections, or the Institutional Review Board. Study records may also be made available for internal compliance reviews and quality assurance representatives.

These individuals may inspect all documents and records required to be maintained by the investigator, including but not limited to, medical records (office, clinic, or hospital) and pharmacy records for the subjects in this study. The clinical study site will permit access to such records.

9.0 Record Retention

Protected health information (PHI) is covered under the Health Insurance Portability Accountability Act (HIPAA), consent forms that include the HIPAA Authorization are to be retained for a minimum of 6 years from the date of the authorization.
Research records will be maintained in accordance with the current version of the Texas Health Records Table 17-III Record Retention Schedule, Human Subject Research Records and Documents.

10.0 References

1. Parsons DW, Jones S, Zhang X, et al. An Integrated Genomic Analysis of Human Glioblastoma Multiforme. Science (80-). 2008;321(5897).
2. Yan H, Parsons DW, Jin G, et al. IDH1 and IDH2 Mutations in Gliomas. N Engl J Med. 2009;360(8):765-773. doi:10.1056/NEJMoa0808710.
3. Ward PS, Patel J, Wise DR, et al. The common feature of leukemia-associated IDH1 and IDH2 mutations is a neomorphic enzyme activity converting alpha-ketoglutarate to 2-hydroxyglutarate. Cancer Cell. 2010;17(3):225-234. doi:10.1016/j.ccr.2010.01.020.
4. Borger DR, Tanabe KK, Fan KC, et al. Frequent mutation of isocitrate dehydrogenase (IDH)1 and IDH2 in cholangiocarcinoma identified through broad-based tumor genotyping. Oncologist. 2012;17(1):72-79. doi:10.1634/theoncologist.2011-0386.
5. Amary MF, Bacsi K, Maggiani F, et al. IDH1 and IDH2 mutations are frequent events in central chondrosarcoma and central and periosteal chondromas but not in other mesenchymal tumours. J Pathol. 2011;224(3):334-343. doi:10.1002/path.2913.
6. Vander Heiden MG, Cantley LC, Thompson CB. Understanding the Warburg effect: the metabolic requirements of cell proliferation. Science. 2009;324(5930):1029-1033. doi:10.1126/science.1160809.
7. Dang L, White DW, Gross S, et al. Cancer-associated IDH1 mutations produce 2-hydroxyglutarate. Nature. 2009;462(7274):739-744. doi:10.1038/nature08617.
8. Figueroa ME, Abdel-Wahab O, Lu C, et al. Leukemic IDH1 and IDH2 Mutations Result in a Hypermethylation Phenotype, Disrupt TET2 Function, and Impair Hematopoietic Differentiation. Cancer Cell. 2010;18(6):553-567. doi:10.1016/j.ccr.2010.11.015.
9. Losman JA, Kaelin WG. What a difference a hydroxyl makes: Mutant IDH, (R)-2-hydroxyglutarate, and cancer. Genes Dev. 2013;27(8):836-852. doi:10.1101/gad.217406.113.
10. Capper D, Simon M, Langhans C-D, et al. 2-Hydroxyglutarate concentration in serum from patients with gliomas does not correlate with IDH1/2 mutation status or tumor size. Int J Cancer. 2012;131(3):766-768. doi:10.1002/ijc.26425.
11. Fathi AT, Nahed B V, Wander SA, et al. Elevation of Urinary 2-Hydroxyglutarate in IDH-Mutant Glioma. Oncologist. 2016;21(2):214-219. doi:10.1634/theoncologist.2015-0342.
12. Lombardi G, Corona G, Bellu L, et al. Diagnostic value of plasma and urinary 2-hydroxyglutarate to identify patients with isocitrate dehydrogenase-mutated glioma. Oncologist. 2015;20(5):562-567. doi:10.1634/theoncologist.2014-0266.
13. DiNardo CD, Propert KJ, Loren AW, et al. Serum 2-hydroxyglutarate levels predict isocitrate dehydrogenase mutations and clinical outcome in acute myeloid leukemia. Blood. 2013;121(24).
14. Wang J-H, Chen W-L, Li J-M, et al. Prognostic significance of 2-hydroxyglutarate levels in acute myeloid leukemia in China. Proc Natl Acad Sci U S A. 2013;110(42):17017-17022. doi:10.1073/pnas.1315558110.
15. Lombardi G, Della Puppa A, Zagonel V. Urine 2-Hydroxyglutarate in Glioma. Oncologist. 2016;21(8):1026. doi:10.1634/theoncologist.2016-0123.

16. Kalinina J, Ahn J, Devi NS, et al. Selective detection of the D-enantiomer of 2-Hydroxyglutarate in the CSF of glioma patients with mutated Isocitrate Dehydrogenase. Clin Cancer Res. 2016.
17. Borger DR, Goyal L, Yau T, et al. Circulating Oncometabolite 2-Hydroxyglutarate Is a Potential Surrogate Biomarker in Patients with Isocitrate Dehydrogenase-Mutant Intrahepatic Cholangiocarcinoma. Clin Cancer Res. 2014;20(7).
18. Janin M, Mylonas E, Saada V, et al. Serum 2-Hydroxyglutarate Production in IDH1- and IDH2-Mutated De Novo Acute Myeloid Leukemia: A Study by the Acute Leukemia French Association Group. J Clin Oncol. 2014;32(4):297-305. doi:10.1200/JCO.2013.50.2047.
19. Stein EM, Altman JK, Collins R, et al. AG-221, an Oral, Selective, First-in-Class, Potent Inhibitor of the IDH2 Mutant Metabolic Enzyme, Induces Durable Remissions in a Phase I Study in Patients with IDH2 Mutation Positive Advanced Hematologic Malignancies. Blood. 2014;124(21).
20. Lai A, Kharbanda S, Pope WB, et al. Evidence for sequenced molecular evolution of IDH1 mutant glioblastoma from a distinct cell of origin. J Clin Oncol. 2011;29(34):4482-4490. doi:10.1200/JCO.2010.33.8715.
21. Lu W, Kimball E, Rabinowitz JD. A high-performance liquid chromatography-tandem mass spectrometry method for quantitation of nitrogen-containing intracellular metabolites. J Am Soc Mass Spectrom. 2006;17(1):37-50. doi:10.1016/j.jasms.2005.09.001.

References

[1] D. Hanahan and R. A. Weinberg, “Hallmarks of cancer: the next generation.,” *Cell*, vol. 144, no. 5, pp. 646–74, Mar. 2011.

[2] O. Warburg, “Uber den Stoffwechsel der Carcinomzelle,” *Naturwissenschaften*, vol. 12, no. 50, pp. 1131–1137, Dec. 1924.

[3] H. Yan *et al.*, “*IDH1* and *IDH2* Mutations in Gliomas,” *N. Engl. J. Med.*, vol. 360, no. 8, pp. 765–773, Feb. 2009.

[4] E. R. Mardis *et al.*, “Recurring Mutations Found by Sequencing an Acute Myeloid Leukemia Genome,” *N. Engl. J. Med.*, vol. 361, no. 11, pp. 1058–1066, Sep. 2009.

[5] D. R. Borger *et al.*, “Frequent mutation of isocitrate dehydrogenase (IDH)1 and IDH2 in cholangiocarcinoma identified through broad-based tumor genotyping.,” *Oncologist*, vol. 17, no. 1, pp. 72–9, 2012.

[6] M. F. Amary *et al.*, “IDH1 and IDH2 mutations are frequent events in central chondrosarcoma and central and periosteal chondromas but not in other mesenchymal tumours.,” *J. Pathol.*, vol. 224, no. 3, pp. 334–43, Jul. 2011.

[7] L. Dang *et al.*, “Cancer-associated IDH1 mutations produce 2-hydroxyglutarate,” *Nature*, vol. 462, no. 7274, pp. 739–744, Dec. 2009.

[8] P. Koivunen *et al.*, “Transformation by the (R)-enantiomer of 2-hydroxyglutarate linked to EGLN activation.,” *Nature*, vol. 483, no. 7390, pp. 484–8, Mar. 2012.

[9] H. Sharma, “Development of Novel Therapeutics Targeting Isocitrate Dehydrogenase Mutations in Cancer,” *Curr. Top. Med. Chem.*, vol. 18, no. 6, pp. 505–524, Jun. 2018.

[10] K. E. Yen, M. A. Bittinger, S. M. Su, and V. R. Fantin, “Cancer-associated IDH mutations: biomarker and therapeutic opportunities,” *Oncogene*, vol. 29, no. 49, pp. 6409–6417, Dec. 2010.

[11] J. A. Losman and W. G. Kaelin, “What a difference a hydroxyl makes: Mutant IDH, (R)-2-hydroxyglutarate, and cancer,” *Genes Dev.*, vol. 27, no. 8, pp. 836–852, Apr. 2013.

[12] E. E. Kaufman, T. Nelson, H. M. Fales, and D. M. Levin, “Isolation and characterization of a hydroxyacid-oxoacid transhydrogenase from rat kidney mitochondria.,” *J. Biol. Chem.*, vol. 263, no. 32, pp. 16872–9, Nov. 1988.

[13] Y. Achouri, G. Noël, D. Vertommen, M. H. Rider, M. Veiga-Da-Cunha, and E. Van Schaftingen, “Identification of a dehydrogenase acting on D-2-hydroxyglutarate.,” *Biochem. J.*, vol. 381, no. Pt 1, pp. 35–42, Jul. 2004.

[14] P. S. Ward *et al.*, “The common feature of leukemia-associated IDH1 and IDH2 mutations is a neomorphic enzyme activity converting alpha-ketoglutarate to 2-hydroxyglutarate.,” *Cancer Cell*, vol. 17, no. 3, pp. 225–34, Mar. 2010.

[15] M. Janin *et al.*, “Serum 2-Hydroxyglutarate Production in IDH1- and IDH2-Mutated De Novo Acute Myeloid Leukemia: A Study by the Acute Leukemia French Association

Group," *J. Clin. Oncol.*, vol. 32, no. 4, pp. 297–305, Feb. 2014.

[16] A. M. Intlekofer *et al.*, "L-2-Hydroxyglutarate production arises from noncanonical enzyme function at acidic pH.," *Nat. Chem. Biol.*, vol. 13, no. 5, pp. 494–500, 2017.

[17] P.-N. Bories *et al.*, "Establishing assay-specific 97.5th percentile upper reference limit for serum D-2-hydroxyglutarate for the management of patients with acute myeloid leukemia," *Clin. Chem. Lab. Med.*, vol. 0, no. 0, pp. e57–e59, Sep. 2018.

[18] E. A. Struys, "2-Hydroxyglutarate is not a metabolite; D-2-hydroxyglutarate and L-2-hydroxyglutarate are!," *Proc. Natl. Acad. Sci. U. S. A.*, vol. 110, no. 51, p. E4939, Dec. 2013.

[19] P. A. Tyrakis *et al.*, "S-2-hydroxyglutarate regulates CD8+ T-lymphocyte fate," *Nature*, vol. 540, no. 7632, pp. 236–241, Oct. 2016.

[20] A. J. Worth *et al.*, "Rotenone Stereospecifically Increases (*S*)-2-Hydroxyglutarate in SH-SY5Y Neuronal Cells," *Chem. Res. Toxicol.*, vol. 28, no. 5, pp. 948–954, May 2015.

[21] M. Kranendijk, E. A. Struys, G. S. Salomons, M. S. Van der Knaap, and C. Jakobs, "Progress in understanding 2-hydroxyglutaric acidurias," *J. Inherit. Metab. Dis.*, vol. 35, no. 4, pp. 571–587, Jul. 2012.

[22] A. Intlekofer *et al.*, "Hypoxia Induces Production of L-2-Hydroxyglutarate," *Cell Metab.*, vol. 22, no. 2, pp. 304–311, Aug. 2015.

[23] S. M. Nadtochiy, X. Schafer, D. Fu, K. Nehrke, J. Munger, and P. S. Brookes, "Acidic pH Is a Metabolic Switch for 2-Hydroxyglutarate Generation and Signaling.," *J. Biol. Chem.*, vol. 291, no. 38, pp. 20188–97, Sep. 2016.

[24] J.-A. Losman *et al.*, "(R)-2-hydroxyglutarate is sufficient to promote leukemogenesis and its effects are reversible.," *Science*, vol. 339, no. 6127, pp. 1621–5, Mar. 2013.

[25] C. Lu *et al.*, "IDH mutation impairs histone demethylation and results in a block to cell differentiation.," *Nature*, vol. 483, no. 7390, pp. 474–8, Mar. 2012.

[26] D. Rohle *et al.*, "An inhibitor of mutant IDH1 delays growth and promotes differentiation of glioma cells.," *Science*, vol. 340, no. 6132, pp. 626–30, May 2013.

[27] M. Heuser, M. M. Araujo Cruz, R. Goparaju, and A. Chaturvedi, "Enigmas of IDH mutations in hematology/oncology.," *Exp. Hematol.*, vol. 43, no. 8, pp. 685–97, Aug. 2015.

[28] O. Clark, K. Yen, and I. K. Mellinghoff, "Molecular Pathways: Isocitrate Dehydrogenase Mutations in Cancer," *Clin. Cancer Res.*, vol. 22, no. 8, 2016.

[29] M. E. Figueroa *et al.*, "Leukemic IDH1 and IDH2 Mutations Result in a Hypermethylation Phenotype, Disrupt TET2 Function, and Impair Hematopoietic Differentiation," *Cancer Cell*, vol. 18, no. 6, pp. 553–567, 2010.

[30] M. Sasaki *et al.*, "D-2-hydroxyglutarate produced by mutant IDH1 perturbs collagen maturation and basement membrane function.," *Genes Dev.*, vol. 26, no. 18, pp. 2038–49, Sep. 2012.

[31] L. G. Richardson, B. D. Choi, and W. T. Curry, "(R)-2-hydroxyglutarate drives immune quiescence in the tumor microenvironment of IDH-mutant gliomas," *Transl. Cancer Res.*,

vol. 8, no. 2, pp. S167–S170, 2019.

[32] P. Wang *et al.*, “Oncometabolite D-2-Hydroxyglutarate Inhibits ALKBH DNA Repair Enzymes and Sensitizes IDH Mutant Cells to Alkylating Agents,” *Cell Rep.*, vol. 13, no. 11, pp. 2353–2361, Dec. 2015.

[33] D. Ye, K.-L. Guan, and Y. Xiong, “Metabolism, Activity, and Targeting of D- and L-2-Hydroxyglutarates.,” *Trends in cancer*, vol. 4, no. 2, pp. 151–165, Feb. 2018.

[34] W. Oldham and J. Loscalzo, “Quantification of 2-Hydroxyglutarate Enantiomers by Liquid Chromatography-mass Spectrometry,” *BIO-PROTOCOL*, vol. 6, no. 16, 2016.

[35] J. Delahousse *et al.*, “Circulating oncometabolite D-2-hydroxyglutarate enantiomer is a surrogate marker of isocitrate dehydrogenase–mutated intrahepatic cholangiocarcinomas,” *Eur. J. Cancer*, vol. 90, pp. 83–91, Feb. 2018.

[36] J. P. Kamerling, G. J. Gerwig, and J. F. Vliegenthart, “Determination of the configurations of lactic and glyceric acids from human serum and urine by capillary gas-liquid chromatography.,” *J. Chromatogr.*, vol. 143, no. 2, pp. 117–23, Mar. 1977.

[37] J. P. Kamerling *et al.*, “Determination of the absolute configuration of some biologically important urinary 2-hydroxydicarboxylic acids by capillary gas—liquid chromatography,” *J. Chromatogr. B Biomed. Sci. Appl.*, vol. 222, no. 2, pp. 276–283, Feb. 1981.

[38] R. A. Chalmers *et al.*, “D-2-hydroxyglutaric aciduria: Case report and biochemical studies,” *J. Inherit. Metab. Dis.*, vol. 3, no. 1, pp. 11–15, Dec. 1980.

[39] E. A. Struys, E. E. W. Jansen, N. M. Verhoeven, and C. Jakobs, “Measurement of urinary D- and L-2-hydroxyglutarate enantiomers by stable-isotope-dilution liquid chromatography-tandem mass spectrometry after derivatization with diacetyl-L-tartaric anhydride.,” *Clin. Chem.*, vol. 50, no. 8, pp. 1391–5, Aug. 2004.

[40] Q.-Y. Cheng *et al.*, “Sensitive Determination of Onco-metabolites of D- and L-2-hydroxyglutarate Enantiomers by Chiral Derivatization Combined with Liquid Chromatography/Mass Spectrometry Analysis,” *Sci. Rep.*, vol. 5, no. 15217, 2015.

[41] J. Kalinina *et al.*, “Selective detection of the D-enantiomer of 2-Hydroxyglutarate in the CSF of glioma patients with mutated Isocitrate Dehydrogenase,” *Clin. Cancer Res.*, 2016.

[42] P. M. Jones, R. Boriack, E. A. Struys, and D. Rakheja, “Measurement of Oncometabolites d-2-Hydroxyglutaric Acid and l-2-Hydroxyglutaric Acid,” Humana Press, New York, NY, 2017, pp. 219–234.

[43] M. S. Rashed, M. AlAmoudi, and H. Y. Aboul-Enein, “Chiral liquid chromatography tandem mass spectrometry in the determination of the configuration of 2-hydroxyglutaric acid in urine,” *Biomed. Chromatogr.*, vol. 14, no. 5, pp. 317–320, Aug. 2000.

[44] C. Calderón, J. Horak, and M. Lämmerhofer, “Chiral separation of 2-hydroxyglutaric acid on cinchonan carbamate based weak chiral anion exchangers by high-performance liquid chromatography,” *J. Chromatogr. A*, vol. 1467, pp. 239–245, Oct. 2016.

[45] C. Calderón and M. Lämmerhofer, “Chiral separation of short chain aliphatic hydroxycarboxylic acids on cinchonan carbamate-based weak chiral anion exchangers and zwitterionic chiral ion exchangers,” *J. Chromatogr. A*, vol. 1487, pp. 194–200, Mar. 2017.

[46] R. A. Patil, C. A. Weatherly, and D. W. Armstrong, “Chiral Gas Chromatography,” in *Chiral Analysis*, 2nd ed., Elsevier, 2018, pp. 468–505.

[47] A. Kaunzinger, A. Rechner, T. Beck, A. Mosandl, A. C. Sewell, and H. Böhles, “Chiral compounds as indicators of inherited metabolic disease. Simultaneous stereodifferentiation of lactic-, 2-hydroxyglutaric- and glyceric acid by enantioselective cGC.,” *Enantiomer*, vol. 1, no. 3, pp. 177–82, 1996.

[48] H. J. Chaves Das Neves, P. Noronha, and H. Rufino, “A New Method for the Chiral HRGC Assay of L-2-Hydroxyglutaric Acid in Urine.”

[49] J. Balss *et al.*, “Enzymatic assay for quantitative analysis of (d)-2-hydroxyglutarate,” *Acta Neuropathol.*, vol. 124, no. 6, pp. 883–891, Dec. 2012.

[50] D. Bal and A. Gryff-Keller, “1H and13C NMR study of 2-hydroxyglutaric acid and its lactone,” *Magn. Reson. Chem.*, vol. 40, no. 8, pp. 533–536, Aug. 2002.

[51] C. Choi *et al.*, “Prospective Longitudinal Analysis of 2-Hydroxyglutarate Magnetic Resonance Spectroscopy Identifies Broad Clinical Utility for the Management of Patients With IDH-Mutant Glioma.,” *J. Clin. Oncol.*, vol. 34, no. 33, pp. 4030–4039, Nov. 2016.

[52] M. I. de la Fuente *et al.*, “Integration of 2-hydroxyglutarate-proton magnetic resonance spectroscopy into clinical practice for disease monitoring in isocitrate dehydrogenase-mutant glioma,” *Neuro. Oncol.*, vol. 18, no. 2, pp. 283–290, Feb. 2016.

[53] D. Bal and A. Gryff-Keller, “1H and13C NMR study of 2-hydroxyglutaric acid and its lactone,” *Magn. Reson. Chem.*, vol. 40, no. 8, pp. 533–536, Aug. 2002.

[54] R. Gómez-Bombarelli, E. Calle, and J. Casado, “Mechanisms of Lactone Hydrolysis in Acidic Conditions,” *J. Org. Chem.*, vol. 78, no. 14, pp. 6880–6889, Jul. 2013.

[55] R. Gómez-Bombarelli, E. Calle, and J. Casado, “Mechanisms of Lactone Hydrolysis in Neutral and Alkaline Conditions,” *J. Org. Chem.*, vol. 78, no. 14, pp. 6868–6879, Jul. 2013.

[56] K. Gilmore, R. K. Mohamed, and I. V Alabugin, “The Baldwin rules: revised and extended,” *WIREs Comput Mol Sci*, vol. 6, pp. 487–514, 2016.

[57] M. Duran, J. P. Kamerling, H. D. Bakker, A. H. van Gennip, and S. K. Wadman, “L-2-Hydroxyglutaric aciduria: an inborn error of metabolism?,” *J. Inherit. Metab. Dis.*, vol. 3, no. 4, pp. 109–12, 1980.

[58] E. Fernández-Galán *et al.*, “Validation of a routine gas chromatography mass spectrometry method for 2-hydroxyglutarate quantification in human serum as a screening tool for detection of idh mutations,” *J. Chromatogr. B*, vol. 1083, pp. 28–34, Apr. 2018.

[59] J. Han *et al.*, “Elevated d-2-hydroxyglutarate during colitis drives progression to colorectal cancer.,” *Proc. Natl. Acad. Sci. U. S. A.*, vol. 115, no. 5, pp. 1057–1062, Jan. 2018.

[60] K. M. Gibson *et al.*, “Stable-Isotope Dilution Analysis of D- and L-2-Hydroxyglutaric Acid: Application to the Detection and Prenatal Diagnosis of D- and L-2-Hydroxyglutaric Acidemias,” *Pediatr. Res.*, vol. 34, no. 3, pp. 277–280, Sep. 1993.

[61] S. K. Strain, M. D. Groves, and M. R. Emmett, “Differentiation of 2-hydroxyglutarate enantiomers and its lactones by gas chromatography/electron ionization tandem mass

spectrometry," *Rapid Commun. Mass Spectrom.*, vol. 33, no. 17, pp. 1401–1409, Sep. 2019.

[62] S. K. Strain, M. D. Groves, K. L. Olino, and M. R. Emmett, "Measurement of 2-hydroxyglutarate enantiomers in serum by chiral gas chromatography-tandem mass spectrometry and its application as a biomarker for IDH mutant gliomas," *Clin. Mass Spectrom.*, vol. 15, pp. 16–24, Jan. 2020.

[63] F. and D. A. FDA, "Bioanalytical method validation: Guidance for Industry," 2018.

[64] K. Zhang, C.-D. Liao, S. Prakash, M. Conway, and H.-F. Cheng, "Interlaboratory Validation of a Stable Isotope Dilution and Liquid Chromatography Tandem Mass Spectrometry Method for the Determination of Aflatoxins in Milk, Milk-Based Infant Formula, and Feed," *J. AOAC Int.*, vol. 101, no. 3, pp. 677–685, May 2018.

[65] R. J. Ouellette, J. D. Rawn, R. J. Ouellette, and J. D. Rawn, "Introduction to Organic Reaction Mechanisms," in *Organic Chemistry*, 2nd ed., Academic Press, 2018, pp. 51–86.

[66] F. W. McLafferty and F. Turecek, *Interpretation of mass spectra*, 4th ed. University Science Books, 1993.

[67] D. A. Volmer, "Prerequisites for supplying complementary high-resolution mass spectrometry data in RCM publications," *Rapid Commun. Mass Spectrom.*, vol. 24, no. 24, pp. 3499–3500, Dec. 2010.

[68] J. Rosas *et al.*, "Alternative Mass Spectrometry Techniques for the Validation of Fragmentation Pattern of Capsaicin and Dihydrocapsaicin," *Rapid Commun. Mass Spectrom.*, Jan. 2019.

[69] J. Assaf, A. S. Kollmeier, C. Müller, and M. K. Parr, "Reconsidering mass spectrometric fragmentation in electron ionization mass spectrometry - new insights from recent instrumentation and isotopic labelling exemplified by ketoprofen and related compounds," *Rapid Commun. Mass Spectrom.*, vol. 33, no. 2, pp. 215–228, Jan. 2019.

[70] J. P. Kamerling, G. J. Gerwig, and J. F. Vliegenthart, "Determination of the configurations of lactic and glyceric acids from human serum and urine by capillary gas-liquid chromatography.," *J. Chromatogr.*, vol. 143, no. 2, pp. 117–23, Mar. 1977.

[71] J. P. Kamerling *et al.*, "Determination of the absolute configuration of some biologically important urinary 2-hydroxydicarboxylic acids by capillary gas—liquid chromatography," *J. Chromatogr. B Biomed. Sci. Appl.*, vol. 222, no. 2, pp. 276–283, Feb. 1981.

[72] F. Sahm *et al.*, "Detection of 2-Hydroxyglutarate in Formalin-Fixed Paraffin-Embedded Glioma Specimens by Gas Chromatography/Mass Spectrometry," *Brain Pathol.*, vol. 22, no. 1, pp. 26–31, Jan. 2012.

[73] R. Zenobi, "Ionization Methods in Mass Spectrometry," *Anal. Chem.*, vol. 87, no. 7, pp. 3543–3543, Apr. 2015.

[74] K. A. Schug *et al.*, "Vacuum ultraviolet detector for gas chromatography.," *Anal. Chem.*, vol. 86, no. 16, pp. 8329–35, Aug. 2014.

[75] B. A. Wallace *et al.*, "Protein characterisation by synchrotron radiation circular dichroism spectroscopy," *Q. Rev. Biophys.*, vol. 42, no. 04, pp. 317–370, Nov. 2009.

[76] D. Calloway, “Beer-Lambert Law,” *J. Chem. Educ.*, vol. 74, no. 7, p. 744, Jul. 1997.

[77] D. S. Wishart *et al.*, “HMDB 4.0: the human metabolome database for 2018,” *Nucleic Acids Res.*, vol. 46, no. D1, pp. D608–D617, Jan. 2018.

[78] K. M. Gibson *et al.*, “Stable-Isotope Dilution Analysis of D- and L-2-Hydroxyglutaric Acid: Application to the Detection and Prenatal Diagnosis of D- and L-2-Hydroxyglutaric Acidemias,” *Pediatr. Res.*, vol. 34, no. 3, pp. 277–280, Sep. 1993.

[79] G. F. Hoffmann, W. Meier-Augenstein, S. Stöckler, R. Surtees, D. Rating, and W. L. Nyhan, “Physiology and pathophysiology of organic acids in cerebrospinal fluid.,” *J. Inherit. Metab. Dis.*, vol. 16, no. 4, pp. 648–69, 1993.

[80] C. D. DiNardo *et al.*, “Serum 2-hydroxyglutarate levels predict isocitrate dehydrogenase mutations and clinical outcome in acute myeloid leukemia,” *Blood*, vol. 121, no. 24, 2013.

[81] J.-H. Wang *et al.*, “Prognostic significance of 2-hydroxyglutarate levels in acute myeloid leukemia in China.,” *Proc. Natl. Acad. Sci. U. S. A.*, vol. 110, no. 42, pp. 17017–22, Oct. 2013.

[82] P. M. Jones, R. Boriack, E. A. Struys, and D. Rakheja, “Measurement of Oncometabolites d-2-Hydroxyglutaric Acid and l-2-Hydroxyglutaric Acid,” Humana Press, New York, NY, 2017, pp. 219–234.

[83] H. Churchill, H. Naina, R. Boriack, D. Rakheja, and W. Chen, “Discordant intracellular and plasma D-2-hydroxyglutarate levels in a patient with IDH2 mutated angioimmunoblastic T-cell lymphoma.,” *Int. J. Clin. Exp. Pathol.*, vol. 8, no. 9, pp. 11753–9, 2015.

[84] D. Rakheja, R. L. Boriack, M. Mitui, S. Khokhar, S. A. Holt, and P. Kapur, “Papillary thyroid carcinoma shows elevated levels of 2-hydroxyglutarate,” *Tumor Biol.*, vol. 32, no. 2, pp. 325–333, Apr. 2011.

[85] J. O. Wobbrock, L. Findlater, D. Gergle, and J. J. Higgins, “The aligned rank transform for nonparametric factorial analyses using only anova procedures,” in *Proceedings of the 2011 annual conference on Human factors in computing systems - CHI ’11*, 2011, p. 143.

[86] C. Franceschi and J. Campisi, “Chronic Inflammation (Inflammaging) and Its Potential Contribution to Age-Associated Diseases,” *Journals Gerontol. Ser. A Biol. Sci. Med. Sci.*, vol. 69, no. Suppl 1, pp. S4–S9, Jun. 2014.

[87] D. Senyilmaz and A. A. Teleman, “Chicken or the egg: Warburg effect and mitochondrial dysfunction.,” *F1000Prime Rep.*, vol. 7, p. 41, 2015.

[88] A. L. Cohen, S. L. Holmen, and H. Colman, “IDH1 and IDH2 Mutations in Gliomas,” *Curr. Neurol. Neurosci. Rep.*, vol. 13, no. 5, p. 345, May 2013.

[89] F. B. Mesfin and M. A. Al-Dhahir, *Cancer, Brain Gliomas*. StatPearls Publishing, 2019.

[90] Q. T. Ostrom *et al.*, “CBTRUS statistical report: primary brain and central nervous system tumors diagnosed in the United States in 2007-2011.,” *Neuro. Oncol.*, vol. 16 Suppl 4, no. Suppl 4, pp. iv1-63, Oct. 2014.

[91] D. N. Louis *et al.*, “The 2016 World Health Organization Classification of Tumors of the Central Nervous System: a summary,” *Acta Neuropathol.*, vol. 131, no. 6, pp. 803–820, Jun. 2016.

[92] J. T. Grier and T. Batchelor, “Low-grade gliomas in adults.,” *Oncologist*, vol. 11, no. 6, pp. 681–93, Jun. 2006.

[93] A. Omuro *et al.*, “Glioblastoma and Other Malignant Gliomas,” *JAMA*, vol. 310, no. 17, p. 1842, Nov. 2013.

[94] M. S. Walid, “Prognostic factors for long-term survival after glioblastoma.,” *Perm. J.*, vol. 12, no. 4, pp. 45–8, 2008.

[95] D. W. Parsons *et al.*, “An Integrated Genomic Analysis of Human Glioblastoma Multiforme,” *Science (80-.).*, vol. 321, no. 5897, 2008.

[96] “Glioblastoma and Malignant Astrocytoma.” American Brain Tumor Association, Chicago, 2016.

[97] E. M. Stein *et al.*, “AG-221, an Oral, Selective, First-in-Class, Potent Inhibitor of the IDH2 Mutant Metabolic Enzyme, Induces Durable Remissions in a Phase I Study in Patients with IDH2 Mutation Positive Advanced Hematologic Malignancies,” *Blood*, vol. 124, no. 21, 2014.

[98] E. M. Stein *et al.*, “Safety and Efficacy of AG-221, a Potent Inhibitor of Mutant IDH2 That Promotes Differentiation of Myeloid Cells in Patients with Advanced Hematologic Malignancies: Results of a Phase 1/2 Trial,” *Blood*, vol. 126, no. 23, 2015.

[99] M. S. Waitkus, B. H. Diplas, and H. Yan, “Biological Role and Therapeutic Potential of IDH Mutations in Cancer,” *Cancer Cell*, vol. 34, no. 2, pp. 186–195, Aug. 2018.

[100] D. Capper *et al.*, “2-Hydroxyglutarate concentration in serum from patients with gliomas does not correlate with IDH1/2 mutation status or tumor size,” *Int. J. Cancer*, vol. 131, no. 3, pp. 766–768, Aug. 2012.

[101] A. T. Fathi *et al.*, “Elevation of Urinary 2-Hydroxyglutarate in IDH-Mutant Glioma.,” *Oncologist*, vol. 21, no. 2, pp. 214–9, Feb. 2016.

[102] G. Lombardi *et al.*, “Diagnostic value of plasma and urinary 2-hydroxyglutarate to identify patients with isocitrate dehydrogenase-mutated glioma.,” *Oncologist*, vol. 20, no. 5, pp. 562–7, May 2015.

[103] D. R. Borger *et al.*, “Circulating Oncometabolite 2-Hydroxyglutarate Is a Potential Surrogate Biomarker in Patients with Isocitrate Dehydrogenase-Mutant Intrahepatic Cholangiocarcinoma,” *Clin. Cancer Res.*, vol. 20, no. 7, 2014.

[104] E. A. Struys, “2-Hydroxyglutarate is not a metabolite; D-2-hydroxyglutarate and L-2-hydroxyglutarate are!,” *PNAS*, vol. 110, no. 51, p. E4939, Dec. 2013.

[105] G. Lombardi, A. Della Puppa, and V. Zagonel, “Urine 2-Hydroxyglutarate in Glioma.,” *Oncologist*, vol. 21, no. 8, p. 1026, Aug. 2016.

[106] A. Kumps, P. Duez, and Y. Mardens, “Metabolic, nutritional, iatrogenic, and artifactual sources of urinary organic acids: a comprehensive table.,” *Clin. Chem.*, vol. 48, no. 5, pp. 708–17, May 2002.

[107] D. Rakheja, R. L. Boriack, M. Mitui, S. Khokhar, S. A. Holt, and P. Kapur, “Papillary thyroid carcinoma shows elevated levels of 2-hydroxyglutarate,” *Tumor Biol.*, vol. 32, no. 2, pp. 325–333, Apr. 2011.

[108] E.-H. Shim *et al.*, “L-2-Hydroxyglutarate: An Epigenetic Modifier and Putative Oncometabolite in Renal Cancer,” *Cancer Discov.*, vol. 4, no. 11, pp. 1290–1298, Nov. 2014.

[109] A. Terunuma *et al.*, “MYC-driven accumulation of 2-hydroxyglutarate is associated with breast cancer prognosis,” *J. Clin. Invest.*, vol. 124, no. 1, pp. 398–412, Jan. 2014.

[110] H. Colvin *et al.*, “Oncometabolite D-2-Hydroxyglurate Directly Induces Epithelial-Mesenchymal Transition and is Associated with Distant Metastasis in Colorectal Cancer,” *Sci. Rep.*, vol. 6, no. 1, p. 36289, Dec. 2016.

[111] S. M. Nadtochiy, W. Urciuoli, J. Zhang, X. Schafer, J. Munger, and P. S. Brookes, “Metabolomic profiling of the heart during acute ischemic preconditioning reveals a role for SIRT1 in rapid cardioprotective metabolic adaptation,” *J. Mol. Cell. Cardiol.*, vol. 88, pp. 64–72, Nov. 2015.

[112] E. Ansó *et al.*, “The mitochondrial respiratory chain is essential for haematopoietic stem cell function,” *Nat. Cell Biol.*, vol. 19, no. 6, pp. 614–625, Jun. 2017.

[113] D. Ye, K.-L. Guan, and Y. Xiong, “Metabolism, Activity, and Targeting of D- and L-2-Hydroxyglutarates.,” *Trends in cancer*, vol. 4, no. 2, pp. 151–165, Feb. 2018.

[114] M. G. Vander Heiden, L. C. Cantley, and C. B. Thompson, “Understanding the Warburg effect: the metabolic requirements of cell proliferation.,” *Science*, vol. 324, no. 5930, pp. 1029–33, May 2009.

[115] D. Capper *et al.*, “2-Hydroxyglutarate concentration in serum from patients with gliomas does not correlate with IDH1/2 mutation status or tumor size,” *Int. J. Cancer*, vol. 131, no. 3, pp. 766–768, Aug. 2012.

[116] A. Lai *et al.*, “Evidence for sequenced molecular evolution of IDH1 mutant glioblastoma from a distinct cell of origin.,” *J. Clin. Oncol.*, vol. 29, no. 34, pp. 4482–90, Dec. 2011.

[117] W. Lu, E. Kimball, and J. D. Rabinowitz, “A high-performance liquid chromatography-tandem mass spectrometry method for quantitation of nitrogen-containing intracellular metabolites,” *J. Am. Soc. Mass Spectrom.*, vol. 17, no. 1, pp. 37–50, Jan. 2006.

Vita

Shinji K. Strain was born November 10, 1988 in Okinawa, Japan to William Gray and Takako Strain. Shinji grew up in Dickinson, TX and attended The University of Texas at Austin where he earned a Bachelor's Degree in Physics with Special Honors. Shinji then did two years of post-baccalaureate research and graduate studies at Rice University in the Bioengineering Dept. where he was supported by a T32 Nanobiology Training Grant. Shinji then joined the M.D.-Ph.D. program at The University of Texas Medical Branch (UTMB). During his doctoral work at UTMB, he published 2 abstracts, 2 book chapters, submitted 2 papers, 1 patent, and presented his work at numerous national conferences. He was supported by a TL1 grant from the UTMB Institute for Translational Sciences and received several awards including but not limited to endowment scholarships, teaching awards, and several oral and poster presentation awards. Shinji will be returning to medical school after completion of his Ph.D. and will be pursuing a career as a surgeon-scientist.

Permanent address: 11030 31st Ave N Texas City, TX 77591

This dissertation was typed by Shinji Kenneth Strain